Link-directionalities

in Carrier Sense Wireless Networks



Ping Chung Ng

St. Catherine's College

A thesis is submitted for the degree of
Doctor of Philosophy

September 2008

Department of Engineering Science

University of Oxford

Acknowledgements

I would like to express my sincere gratitude to Professor David J. Edwards for guiding me throughout my D.Phil. studies. I deeply appreciate the advices and academic freedom he gave me during my studies at Oxford.

Thanks also to Professor Soung Cheng Liew at the Chinese University of Hong Kong for assisting greatly in the work carried out to date. Special appreciation to my dad Bor, mum Celina, grandparents, uncle Victor, uncle Tony, aunt Sanie, uncle Bill, sister Joyce and to the rest of my family for their encouragement, continuous support and concern. I would also like to thank St. Catherine's College, Institution of Engineering and Technology, and Royal Academy of Engineering for their financial support to present my papers in international conferences.

This project is fully funded by the Croucher Foundation, Hong Kong. My sincere thanks to Mr. Noel Croucher.

Publications

Journal Papers

1. P. C. Ng, D. Edwards, S. C. Liew, "Eliminating Interference in WLANs by Colouring Link-directional Interference Graphs", *ACM Wireless Networks*, under 1st review, Nov. 2007

2. P. C. Ng, D. Edwards, S. C. Liew, "Scaling Capacity by Two Channels in IEEE802.11 Ad-hoc Networks with a SIR Comparison Algorithm", *IEEE Transactions on Wireless Communications*, revised manuscript under 2nd review, August 2007

A Pending US Patent

P. C. Ng, "Channel Assignments in Carrier Sense Wireless Networks," U.S. PTO 11/710634, U.S.A.

Conference Papers

3. P. C. Ng, D. Edwards, S. C. Liew, "Colouring Link-directional Interference Graphs in Wireless Ad Hoc Networks", *IEEE GlobeCom'07*, Washington DC, USA, Nov. 2007

4. P. C. Ng, D. Edwards, S. C. Liew, "Eliminating Inter-BSS Co-channel Interference by MC-CDMA in WLANs", *IEEE WCNC'07*, Hong Kong, March 2007

5. P. C. Ng, D. Edwards, S. C. Liew, "Doubling Capacity by a Link-directionality-based Dual Channel MAC Protocol for IEEE 802.11 Ad-hoc Networks", *IEEE GlobeCom'06*, San Francisco, USA, Nov. 2006.

6. P. C. Ng, D. Edwards, S. C. Liew, "A Link-directionality-based Dual Channel MAC Protocol with a Power Exchange Algorithm for IEEE 802.11 Ad-hoc Networks", *IEEE PIMRC'06*, Helsinki, Finland, Sept. 2006.

Other Publications

Two Best Paper Awards

1. P. C. Ng, S. C. Liew, "Offered Load control in IEEE 802.11 Multi-hop Ad-hoc Networks," *The 1st IEEE International Conference on Mobile Ad-hoc and Sensor System (MASS'04)*, Florida, U.S.A, Oct 2004.

2. P. C. Ng, S. C. Liew, "Re-routing Instability in IEEE 802.11 Multi-hop Ad-hoc Networks," *The 4th IEEE International Workshop on Wireless Local Network (WLN'04 in LCN'04)*, Florida, U.S.A., Nov 2004.

Journals

3. P. C. Ng, S. C. Liew, "Throughput Analysis of IEEE 802.11 Multi-hop Ad hoc Networks," *IEEE/ACM Transaction on Networking (TON)*, Vol. 15, No. 2, pp. 309-322, April 2006.

4. P. C. Ng, S. C. Liew, "Re-routing Instability in IEEE 802.11 Multi-hop Ad-hoc Networks," *OCP Ad-hoc & Sensor Wireless Networks, An International Journal*, Vol.1, pp.1-25, Aug. 2005Aug. 2005

Conference Papers

5. P. C. Ng, S. C. Liew, K. C. Sha, and W. T. To, "Experimental Study of Hidden-node Problem in IEEE 802.11 Wireless Networks," *ACM Sigcomm'05,* Philadelphia, U.S.A., Aug 2005.

6. P. C. Ng and S. C. Liew, "Voice over Wireless LAN via IEEE 802.16 Wireless MAN and IEEE 802.11 Wireless Distribution System," *IEEE WirelessCom'05*, Hawaii, U.S.A., July 2005.

7. P. C. Ng, S. C. Liew, L. B. Jiang, "Achieving Scalable Performance in Large-Scale IEEE 802.11 Wireless Networks," *IEEE WCNC*, New Orleans, U.S.A., Mar. 2005

8. P. C. Ng, S. C. Liew, L. B. Jiang, "A Performance Evaluation Framework for IEEE 802.11 Ad-hoc Networks," *ACM PE-WASUN' 04,* Venice, Italy, Oct. 2004

9. P. C. Ng, S. C. Liew, W. Wang, "Voice over WLAN via Wireless Distribution System," *IEEE VTC'04 Fall*, Los Angeles, U.S.A., Sept. 2004.

Link-directionalities in Carrier Sense Wireless Networks

Ping Chung Ng
St. Catherine's College
Doctor of Philosophy
Hilary, 2008

In this thesis, research is described which leads to the proposal of a link-directionality-based dual channel MAC (Medium Access Control) protocol (DCP) for carrier sense wireless ad hoc networks. It attempts to double the capacities of such networks using an industrial standard (the single-channel IEEE 802.11 protocol) as a benchmark. Simulations show that the proposed scheme can increase the capacities to more than 1.7 times of the single-channel IEEE 802.11 protocol in large-scale random network topologies. The algorithm, however, requires extra radio spectrum resource which could be costly.

In addition to DCP, a signal-to-interference ratio comparison algorithm (SCA) is proposed to further release the protocol constraints imposed by the virtual carrier-sensing mechanism. Interestingly, while the capacity of the pure DCP decreases when link lengths are short, the capacity of the pure SCA increases when link lengths are short. The two algorithms compensate for the downside of each other to bring about a more uniform capacity improvement. Simulations show that the integrated scheme can further increase the network throughputs to more than 2.13 times in random topologies.

This thesis also clarifies inter-link interference in wireless ad-hoc networks by using link-directional interference graphs (l-graph). By colouring the l-graphs, independent data streams obtained by Multi-Carrier Code Division Multiple Access (MC-CDMA) are assigned for

transmitting up-link and down-link traffic separately in order to eliminate the hidden-node and exposed-node problems in wireless local area networks (WLAN).

Finally, a generic approach for capacity analysis is proposed to show that the concept of link-directionality can also be adopted with other network models, protocols and parameter settings. However, in certain scenarios where links are densely packed together, the advantage of using link-directionality could be diminished. Therefore, the proposed generic approach for capacity analysis allows one to determine whether channel allocations according to link-directionalities should be applied to a given network.

Abbreviations

ACK	Acknowledgement
AODV	Ad-hoc On-demand Distance Vector
AP	Access Point
ARQ p-graph	Automatic Repeat-request Physical Interference Graph
BER	Bit Error Rate
BSS	Basic Service Set
CPThreshold	SIR (signal-to-interference ratio) Capture Threshold
CSMA/CA	Carrier Sense Multiple Access with Collision Avoidance
CTS	Clear-to-send
CW	Contention Window
DAA	Digital Adaptive Array
DCF	IEEE 802.11 Distributed Co-ordination Function
DCP	Link-directionality-based Dual Channel MAC Protocol
DCPwSCA	DCP with Signal-to-Interference Ratio Comparison Algorithm
DIFS	Distributed Interframe Space
DQPSK	Differential Quadrature Phase-shift Keying
DSDV	Destination Sequenced Distance Vector
DSR	Dynamic Source Routing
DSSS	Direct-Sequence Spread Spectrum
FDMA	Frequency Division Multiple Access
InRange	Interference Range
l-graph	Link-directional Interference Graph
MAC	Medium Access Control
MC-CDMA	Multi-carrier Code Division Multiple Access
MIMO	Multiple Input Multiple Output
NAV	Network Allocation Vector
OFDM	Orthogonal Frequency-Division Multiplexing
PInRange	Physical Interference Range
PCSRange	Physical Carrier Sensing Range
p-graph	Physical interference Graph
QoS	Quality-of-service
QPSK	Quadrature Phase-shift Keying
RTS	Request-to-send
SCA	SIR (Signal-to-Interference Ratio) Comparison Algorithm
SF	Spreading Factor
SIFS	Short Interframe Space
SimTable	Simultaneous Transmission Table
SIR	Signal-to-Interference Ratio

SNR	Signal-to-Noise Ratio
SSThreshold	Signal Strength Threshold
TCP	Transport Control Protocol
TDMA	Time Division Multiple Access
TxRange	Transmission Range
UDP	User Datagram Protocol
UWB	Ultra Wide Band
VCSRange	Virtual Carrier-sensing Range
WLAN	Wireless Local Area Network

( ) *Brackets for Conditions:*

There are brackets used in this thesis to represent conditions. The conditions within the brackets notice the scenario when the symbols swap their roles.

e.g. “Node A1 (B1) transmits packets to node A2 (B2)” *represents*
“Node A1 transmits packets to node A2” and “Node B1 transmits packets to node B2”

Contents

1. Introduction 1
1.1. Overview of the IEEE 802.11 Protocol 7
1.1.1. IEEE 802.11 DCF RTS/CTS access mode 10
1.1.2. An Overview of Multi-channel Schemes 11
1.2. Other Performance Enhancement Schemes 13
1.3. Interference in Carrier Sense Wireless Networks 20
1.4. Outline of Thesis 23
2. Link-directionality-based Dual Channel MAC Protocol (DCP) for Ad-hoc Networks 27
2.1. The Proposed New MAC Protocol 31
2.1.1. Basic Concept 32
2.1.2. Algorithms of the Protocol 33
2.1.3. Assigning Channels in Various Topologies 37
2.2. Handling Collisions 44
2.2.1. Contention Window Collisions 44
2.2.2. Hidden-node Problem 45
2.3. Simulation Results 49
2.4. Conclusion 53
3. Further Improving Capacity by Signal-to-interfernce Ratio Comparison Algorithm (SCA) 55
3.1.1. DCP with SIR comparison algorithm (DCPwSCA) 57
3.1.2. Overheads of DCPwSCA 59
3.2. Analysis of Capacity Improvement 60
3.2.1. Optimal Upper Bound on Throughput Capacity of Random Networks 61
3.2.2. Upper Capacity Bound of Original 802.11 Protocol 62
3.2.3. Upper Capacity Bound of DCP 64
3.2.4. Upper Capacity Bound of DCP with SIR Comparison Algorithm (DCPwSCA) 65
3.2.5. Upper Capacity Bound of SIR Comparison Algorithm (SCA) only (without DCP) 66
3.2.6. Comparisons 67
3.3. Simulation Results 70
3.4. Conclusion 71
4. Eliminating Interference in WLANs by Colouring Link-directional Interference Graphs 74
4.1. Physical Interference Graph (P-graph) 75
4.2. ARQ Physical Interference graph (ARQ P-graph) 78
4.3. Link-directional Interference graph (l-graph) 80
4.3.1. An example in a Lattice Topology 86
4.3.2. Simulation Results 88
4.4 A Generic Approach for Capacity Analysis 89
4.5 Insights in WLAN Channel Allocations 102
4.5.1. Capacity Limitations in WLAN 104
4.5.2. Proposed Solution 109
4.5.3. Hardware and MAC Requirements 111
4.5.4. Why Not Assign One Data Stream to One BSS 115
4.6. Conclusion 117
5. Conclusion & Future Work 119
5.1. Conclusion 119
5.2. Future Work 122
Appendix A. Verification of NS-2 Simulator 128
Appendix B. Implementations of Algorithms in NS-2 Simulator 130
Biblography 135

1. Introduction

On 17th June 1946, the first mobile communications system was deployed in St. Louis, U.S.A [1] by the Bell System to cover over a metropolitan area. Its usage, however, was not common due to the limited channel resource which could only support a small number of users. High transmission powers were also required at user terminals for long-range communications with base stations. It made the batteries and equipments of mobile users heavy and bulky to carry. Only the introduction of cellular mobile communications systems in the late 1970s made the deployment of mobile communications systems widespread [2]. Mobile terminals used lower transmission powers to allow radio frequency reuse in other cells to increase the overall network capacity. Since then, wireless networks have been deployed to facilitate communications in daily life. They provide voice and data network services for mobile users such as wireless telephony or wireless Internet access for laptop computers. This chapter outlines the development of wireless networks. Figure 1.1 separates wireless networks into two major groups according to their origins: 1) voice communications; and 2) data communications. The boundary between voice and data wireless networks, however, may become less clear in the future. Forthcoming wireless access protocols may support various types of technologies and standards in a mobile handset.

Voice communications

Voice communications are provided by cellular mobile telephone systems which have evolved from the first (1G), to the second (2G) [3][4], and then to the third generation (3G). The first generation network (1G) in the 1980s used frequency division multiple access (FDMA) system to provide voice services at data rate of 8-10kbps. Instead of analog radio signal, in the 1990s, the second generation network (2G) used digital signal. It includes the widely deployed Global System for Mobile Communications (GSM) which is based on time division multiple access (TDMA) [3].

2G networks can support some limited data communications such as short messaging service (SMS) or wireless application protocol (WAP) for Internet access. Although telephony is still the major application, the third generation network (3G) provides much high data rates for a wider range of data services such as music downloading, video telephony or multimedia messaging service (MMS). With High-Speed Downlink Packet Access (HSDPA) and High-Speed Uplink Packet Access (HSUPA), a 3.75G mobile telephony protocol, mobile devices can support up to 14.4 Mbps for downlink and 5.76 Mbps for uplink [5]. Besides making a phone call, sending emails, browsing web pages or even watching videos can now be done via a mobile handset. The fourth-generation mobile network (4G) may further integrate different wireless access protocols in a mobile device to support both voice and high-speed data communications. Therefore, the boundary between voice and data wireless networks will become less clear in the future.

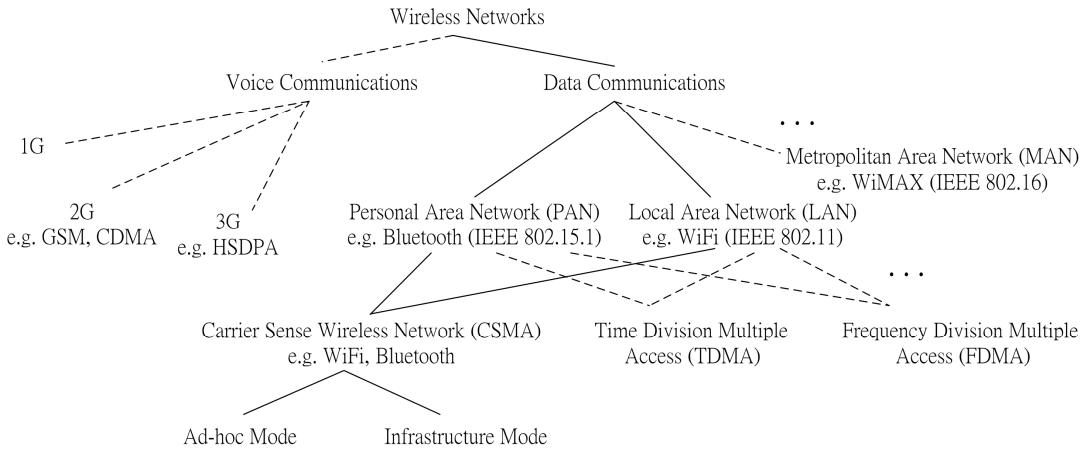


Figure 1.1. Classifications of wireless networks into voice and data communications

Data communications

Since the 1990s, Internet applications, for example, the World Wide Web (WWW) [6], emails or instant messaging, have changed the way of personal data communications. A few years ago, these services could be easily accessed by wired networks (e.g. Asymmetric Digital Subscriber Line

(ADSL)) but were much less accessible via wireless due to the limited data transmission rate and high data service charges of wireless networks. The recent wide deployment of wireless local area networks (Wireless LAN) has changed the situation to allow laptops or personal digital assistants (PDA) to access the Internet, for example, in university campuses, cafés, or shopping malls. At the same time, the expanding growth of Internet applications such as video streaming, video conferencing or peer-to-peer file sharing, increases the demand for wireless network capacities.

Carrier sense wireless networks

Data communications can be provided by several wireless access schemes, for example, carrier sense multiple access (CSMA), time division multiple access (TDMA) or frequency division multiple access (FDMA) [7]. Among them, CSMA is the most popular technology due to its distributive feature. A wireless terminal decides if it should transmit data or not based on its local environment. The terminal transceiver can sense wireless transmissions within a range called the carrier-sensing range. It can transmit data when the channel is sensed as “idle”, otherwise, it will defer the transmission after the currently sensing communications. As shown in Fig. 1.2, within this range, only one wireless station can transmit at one time so as to prevent collisions. If two wireless links are packed closely together, simultaneous transmissions will be disallowed by the radio protocol. Both the widely deployed wireless local area networks (WLAN IEEE 802.11) and wireless Bluetooth (IEEE 802.15.1) systems use carrier sense multiple access (CSMA).

Carrier sense wireless networks can be set up in two modes: 1) ad-hoc mode; and 2) infrastructure mode. The infrastructure mode is distinguished from the ad-hoc mode by the use of access points. In ad-hoc mode, two wireless stations can communicate directly with each other. However, in infrastructure mode, a wireless station is associated with an access point and all traffic must be sent to or received from the access point.

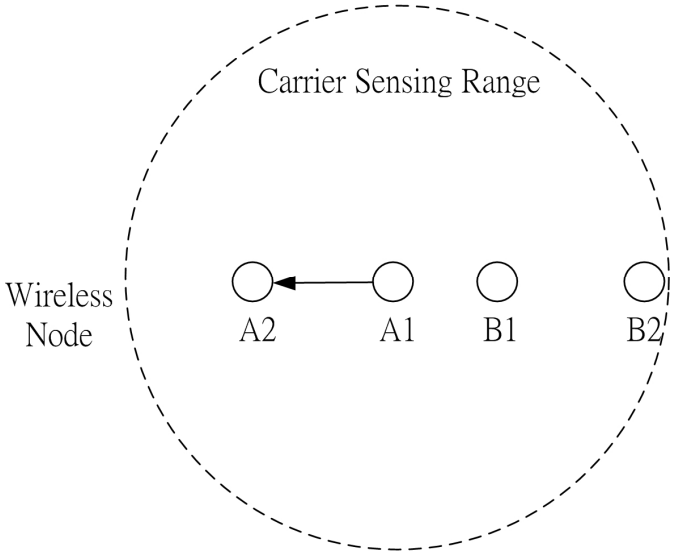


Figure 1.2. Only one transmission is allowed at one time within a carrier-sensing range

The origin of ad-hoc networks came from the infrastructureless wireless network in the 1970s with the attempt to connect wireless terminals on a battlefield [7]. During the 1970s, the Aloha project at the University of Hawaii interconnects terminals at campuses located on different islands to the host computer on the main campus [8]. A radio transceiver is attached to the terminal and sends packets as soon as they become available [9]. This single-hop project later led to the development of the multi-hop multiple access packet radio network (PRNET) [10]. The most attractive features of PRNET is its rapid self-initializing and self-organizing deployment. Wireless terminals can discover their radio connectivity to neighbour nodes and then establish their transmission routes to destinations.

Ad-hoc mode

For the first mode (ad-hoc mode), a wireless ad-hoc network is a self-configuring peer-to-peer network of mobile nodes connected by wireless links. It provides quick and easy networking in

circumstances that require temporary network services or when cabling is difficult, for example, in open area conversations, environmental information gathering, disaster rescues or military usages.

A potential application of wireless ad-hoc networks is to construct temporary communications networks in the aftermath of disasters like Tsunamis (e.g. South East Asia, December 2004) or hurricanes (e.g. Florida, summer 2005). In these scenarios, most of the networking infrastructure was destroyed and it was costly and time-consuming to repair the cabling networks. Instead, wireless stations can be deployed easily, particularly with ad-hoc networks which do not necessarily require network planning before deployment. In ad-hoc networks, a wireless station can be placed anywhere within the communications distance of another station so that they are connected and can rely on each other for forwarding data between rescue centers and remote areas [11]. This can ease the difficulties involved in disaster rescues and reconstructions.

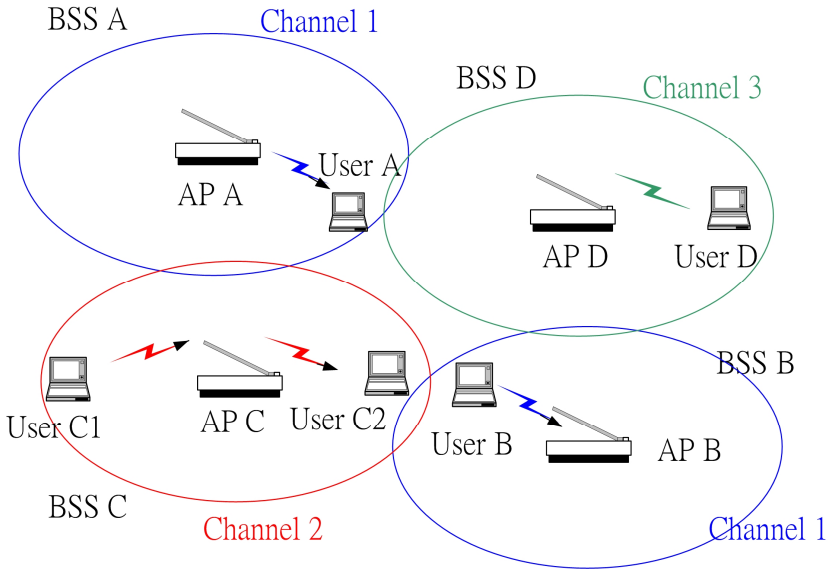


Figure 1.3. A carrier sense wireless network with the infrastructure mode

Infrastructure mode

For the second mode (infrastructure mode), all wireless terminals must associate with an access point and use it as a relay for communications. Figure 1.3 shows an example. There are two wireless

users, C1 and C2, associated with access point C. When C1 transmits a packet to C2, it must first transmit the packet to access point C and then access point C will forward the packet to C2 even though C1 and C2 are within the communications range of each other. This infrastructure mode wireless network has been widely deployed, for example, in campuses, cafés, or convention centers. This allows wireless Internet access with the use of the WiFi (IEEE 802.11 Wireless LAN) standard.

Problem: Capacity limitation of carrier senses wireless networks

One of the major problems of carrier sense wireless network is the limited capacity. As shown in Fig. 1.2, when node A1 is transmitting data to node A2, node B1 cannot send data to node B2 in order to avoid signal interference and packet collision at node A2. Therefore, only one transmission is allowed at one time within a carrier-sensing range. This severely limits the network capacity, particularly when the carrier sensing range is large. There are many capacity enhancement schemes proposed in the literature (see sub-section 1.2 for details). One of the approaches is to use additional radio spectrum resource. For example, in Fig. 1.2, another independent wireless channel can be assigned to link B for simultaneous transmissions with link A. This doubles the network capacity by using two wireless channels.

When a given wireless network uses more radio bandwidth, it should be expected to achieve a correspondingly higher network capacity. If an ad-hoc network achieves capacity C by using a single channel, the targeted capacity by using n channels should therefore be $n \cdot C$. However, most of the multi-channel protocols proposed in the literature simply compare their performances with the single-channel scheme, without considering the additional channel resources used. In fact, most of them (e.g., [12] [13]) only appear to be able to achieve less than 60% of the expected targeted capacities $n \cdot C$. This inefficiency can be attributed to three reasons: i) an additional control channel is used to allocate transmission channels; ii) the overheads incurred by the information added to the packet headers; and iii) the transmissions of RTS/DATA (Request-to-send / Data packets) and the

reception of CTS/ACK (Clear-to-send / Acknowledgment packets) by a node (or terminal) are assigned to the same channel which limit the potential for simultaneous transmissions (details will be explained in Chapter 2.1).

In this thesis, research is presented which attempts to achieve the targeted capacity $2 \cdot C$ by a dual-channel system in carrier sense ad-hoc networks. The single-channel IEEE 802.11 protocol is used as a benchmark. The proposed protocol presented does not require the attributes cited as i) and ii) above. Instead, it is proposed to transmit RTS/DATA and CTS/ACK of a link in separate channels to *scale* the capacity better. In addition, the protocol is integrated with an SIR (Signal-to-Interference Ratio) comparison algorithm (SCA) to further increase the network capacity. Finally, a novel link-directional interference graph (l-graph) is proposed. Colouring the l-graphs can provide insights in allocating channels to eliminate the hidden-node and exposed-node interference in Wireless LANs.

This chapter serves as an introduction of the thesis. Firstly, it begins with an overview of the IEEE 802.11 protocol and multi-channel protocols proposed in the literature. Secondly, it reviews other performance enhancement approaches and outlines the integration of two of the proposed algorithms which can compensate for the downside of each other. Thirdly, it introduces the interference graph, the hidden-node, and exposed-node problems.

1.1. Overview of the IEEE 802.11 Protocol

The IEEE 802.11 standard working group was formed in 1987 to develop a global standard for radio networks operating in the 2.4GHz frequency band [14]. It provides specifications of the physical layer (PHY) and media-access-control (MAC) layer. The original standard uses direct-sequence spread spectrum or frequency-hopping spread spectrum to provide a 2Mbps data rate. IEEE 802.11b was standardized in 1999 to increase the data rate up to 11Mbps. In 2003, IEEE 802.11g was approved to provide data rates of up to 54Mbps in 2.4GHz frequency band. Another

amendment of the 802.11 family, IEEE 802.11a, with a data rate of up to 54Mbps operates in the 5GHz frequency band which is unlicensed in the United States but not in most other countries [15]. There are other task groups of the IEEE 802.11 standard family [16]. Table I outlines some of them. IEEE 802.11e provides quality of service (QoS) for multi-media applications; 802.11i enhances security; 802.11n uses multiple-input-multiple-output (MIMO) to further increase the achievable data rate.

Table I. Projects and tasks of the IEEE 802.11 standard [16]

Project	Task
802.11a	5GHz for 54Mbps
802.11b	2.4GHz for 11Mbps
802.11d	Regulatory Domains
802.11g	2.4GHz for 54Mbps
802.11i	Enhanced Security
802.11h	Spectrum Management
802.11f	Inter-access-point Protocol
802.11e	MAC enhancements for Quality of Service
802.11n	High Throughput (MIMO)
802.11p	Wireless Access Vehicular Environment
802.11s	Mesh Networking

The MAC protocol of the IEEE 802.11 Distributed Co-ordination Function (DCF) [17] is based on Carrier Sense Multiple Access with Collision Avoidance (CSMA/CA). CSMA/CA was developed to prevent collisions by sensing the wireless channel. When an on-going transmission is detected by a wireless terminal, it defers its transmissions after the sensed signal. The message duration is added into the packet header as network allocation vector (NAV) [14]. It notices other neighbour nodes to back-off for the duration of the message transmission. After receiving a message successfully, the receiver replies an acknowledgement packet (ACK) to the sender for confirmation. Inter-frame space (IFS) is used to provide priorities. When the channel media is free, a procedure with shorter

IFS is given a higher priority. Figure 1.4 shows an example in which short inter-frame space (SIFS) is smaller than the distributed inter-frame space (DIFS). This gives the acknowledgement packet (ACK) a higher priority than a data packet. The physical layer measures the energy level at the antenna. If the received signal strength is lower than a specified threshold, the channel is declared as clear and the MAC layer is signaled to allow data transmission.

Since the IEEE 802.11 industrial standard is the most widely adopted MAC (Medium Access Control) protocol used in carrier sense wireless networks, this research uses it as the benchmark. The proposed concept of link-directionality will also be implemented on top of the IEEE 802.11 standard. There are two access modes for the IEEE 802.11 DCF: 1) basic access mode and 2) RTS/CTS access mode. The basic access mode is a two-way handshaking mechanism. An acknowledgement (ACK) is returned by the destination after successfully receiving the DATA packet from the data source. RTS/CTS access mode, on the other hand, is a four way hand-shaking mechanism. Before sending the DATA and ACK, the source transmits a Request-To-Send (RTS) short frame. On reception the destination returns a Clear-To-Send (CTS) frame. The RTS/CTS mechanism reduces the duration of a collision in which the transmitted packet is corrupted or the sent data cannot be successfully extracted by the receiver node, and is particularly designed for the hidden-node problem [18]. The basic access mode is more suitable for Wireless Local Area Network (WLAN) scenarios which use access points (AP) as connection hubs for mobile users. The RTS/CTS access mode, on the other hand, is more appropriate for ad-hoc networks. Since wireless nodes are widely dispersed in ad-hoc networks, a source node may not detect all the transmissions sensed by a destination node. The RTS/CTS mechanism allows the destination node to notify the neighbours its forthcoming reception of signal by sending the CTS frame. This can reduce the chance of collision in ad-hoc networks. Thus, in this thesis, the use of RTS/CTS access mode is assumed in Chapters 2 and 3 for ad-hoc networks.

1.1.1. IEEE 802.11 DCF RTS/CTS access mode

Figure 1.4 shows the details of the protocol. Consider a link with two wireless nodes, source A and destination B. When source A has a packet to send to destination B, it first monitors the channel activity. If the channel is idle for a period of time, distributed interframe space (DIFS) [19] as shown in Fig. 1.4, source A starts counting down its contention window. This backoff time counter is decremented as long as the channel is sensed idle. It stops when a transmission is detected on the channel and resumes when the channel is sensed idle again for a DIFS time [19]. Source A transmits a RTS frame to B when the time counter reaches zero. After receiving the RTS successfully, destination B waits for a period of time, short interframe space (SIFS), and replies a CTS frame back to A. Source A can then begin its DATA packet transmission. If destination B can successfully receive the DATA packet, it will send an acknowledgement (ACK) back to source A. Otherwise, source A will time out and double its contention window size for retransmission.

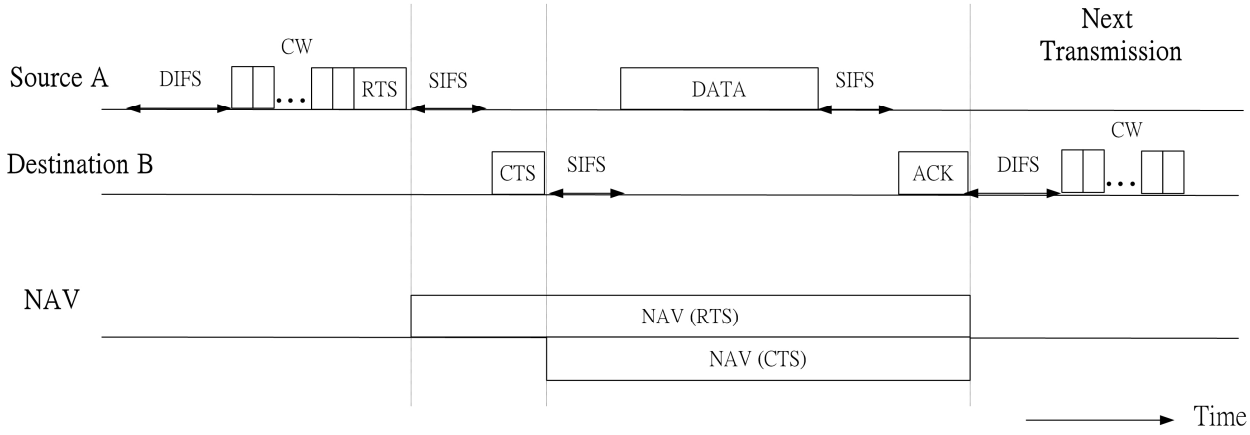


Figure 1.4. IEEE 802.11 DCF RTS/CTS Access Mechanism [17]

The RTS and CTS frames contain the information of the lengths of packets to be transmitted. This information can be decoded by any nearby listening station which then updates its network allocation vector (NAV). The NAV is set to the period of time in which the channel will remain busy due to this transmission. Thus, nearby stations can defer their transmissions after receiving either the

RTS or CTS frame to avoid collisions.

1.1.2. An Overview of Multi-channel Schemes

To increase the network capacity, one of the approaches is to use additional radio spectrum resource. There are many proposed multi-channel protocols for 802.11 ad-hoc networks in the literature. Reference [20] compared these protocols and classified them into four categories: 1) dedicated control channel, 2) split phase, 3) common hopping, and 4) multiple rendezvous. The proposed protocol does not belong to these categories. Instead, the proposed scheme assigns transmission channels based on link-directionalities.

1) Dedicated control channel

References [21][22] proposed the use of a control channel to exchange RTS/CTS packets which contain the channel information (see Fig. 1.5). Then, nodes use the agreed data channels to send DATA and ACK packets. These protocols require a separate control channel which does not carry data packets. This significantly increases the overheads incurred by the protocol. For example, if three channels are used, the targeted capacity would be $3 \cdot C$. One of the three channels, however, is assigned as the control channel and this wastes one-third of the data transmission capacity.

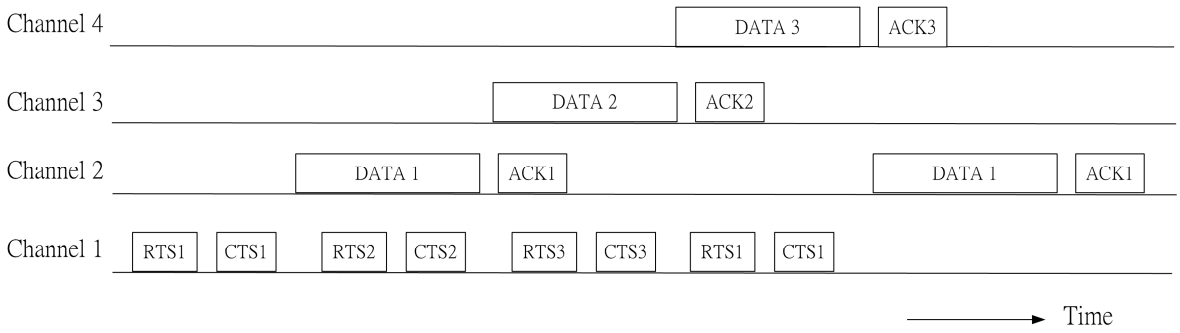


Figure 1.5. Using a dedicated control channel to allocate transmission channels for links

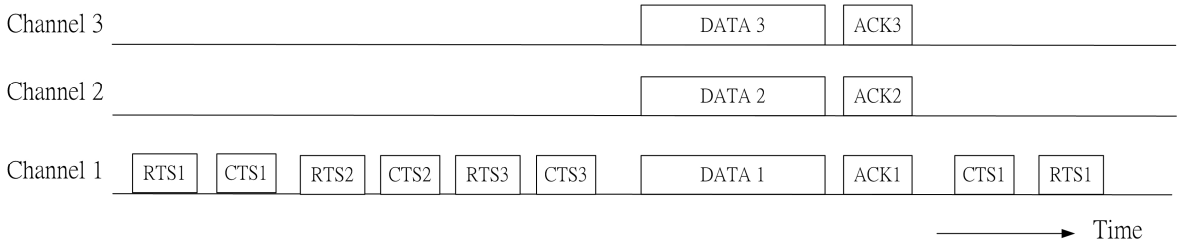


Figure 1.6. Splitting the transmission time into control phase and data phase

2) Split phase

References [23][24] proposed the split of the transmission time into two phases: i) control phase and ii) data phase (see Fig. 1.6). During the control phase, all nodes switch to the control channel and allocate the transmission channels for the next data phase. These protocols require synchronization between nodes which is difficult to achieve in distributed ad-hoc networks. In addition, during the control phase, no data can be transmitted in other data channels. This, again, wastes the communications resource.

3) Common hopping

Another approach is to use frequency hopping [25]. Nodes use pre-assigned hopping patterns to switch channels for transmitting RTS/CTS packets until agreements are made between nodes. Then, as shown in Fig. 1.7, they will use the agreed channels for data transmissions. As mentioned in [20], these protocols may incur significant overheads due to the frequent channel switching.

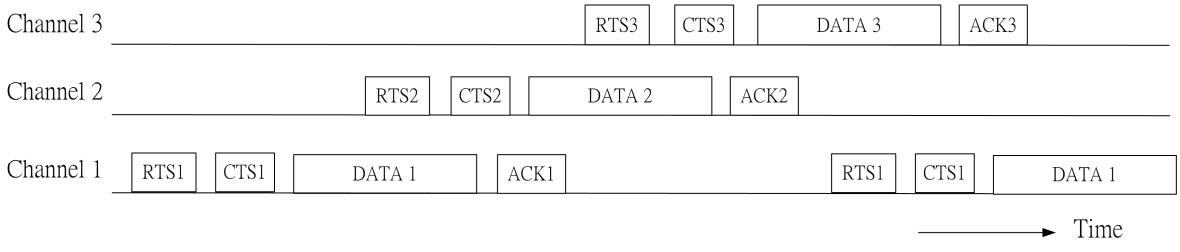


Figure 1.7. Switching channels for RTS/CTS transmissions until agreements are made

The above protocols, however, require i) a dedicated control channel, ii) synchronizations between

distributed nodes, or iii) the channel hopping of radio transceivers. These can induce significant overheads which in turn reduce the achievable network capacity.

Recent Research with Multi-channel Schemes

In recent years, there has been further research on multi-channel schemes. Many of them [26][27][28] tried to further increase the network capacity based on the scheme described above. Reference [26] used a split-phase approach with two phases: a) channel negotiation; and b) data transmissions. The proposed protocol can adjust the size of negotiation interval according to the observed network traffic condition. This minimizes the airtime used for channel allocations which in turn allows more data transmissions. In reference [27], the dedicated control channel scheme and the split-phase approach are combined. The protocol uses two transceivers to carry out channel negotiations on two channels. It saves half of the time for channel allocations and thus leaves more time for data transmissions. Reference [28] is a dedicated control channel scheme which selects a free data channel for each transmission according to the time interval of exchanging the CTS control signal packets. It uses control channel bandwidth more efficiently to reduce the chance of shared channel congestion, especially in heavily congested networks.

In reference [29], time offsets between channels were introduced for asynchronous multi-channel environments. Nodes that have no tasks involved in the current channel can switch to some other channels for more data transmission trials, thereby enhancing the total throughput. Finally, reference [30] suggested using multiple network interface cards at a node for simultaneous communications. However, the required frequency filtration in transceiver design may be difficult to implement.

1.2. Other Performance Enhancement Schemes

Besides the multi-channel approach, there are other performance enhancement schemes which have been proposed in the literature. They include: 1) Power Control [31][32]; 2) Multiple Input

Multiple Output [33][34]; 3) Directional Antenna [35][36]; 4) Routing [7][37]; 5) Offered Load Control [38][39]; and 6) Cross-layer Solution [40][41]. Extensive research has been carried out in these areas and this is detailed below. This thesis, however, focuses on a novel approach. The well-defined medium access control (MAC) protocol (i.e. IEEE 802.11 standard) facilitates the implementation of the proposed schemes. The approach for assigning channels to links according to their link-directionalities could be an attractive approach for future carrier sense wireless networks and it is believed that the proposed scheme can be adopted and implemented with current standards and technologies.

1.2.1. Power Control

Reference [31] studied the impact of transmission power control on network capacity and power saving in wireless ad-hoc networks. It suggested limiting the transmit power of links so as to construct a minimum spanning tree for the connectivity of nodes. The paper demonstrated that a variable-range transmission approach can outperform a common-range transmission approach in terms of power savings and increased capacity. In addition, there is an optimum setting for transmission range, not necessarily the minimum power, which can maximize the capacity of a multi-hop network in the presence of node mobility. This inspires the need to re-design routing protocols (e.g., [32][42]) for ad-hoc networks with power control to exploit the potential for capacity improvement.

Researchers [43][44][45] attempted to minimize the transmit power to save energy for wireless nodes. However, reference [46] showed that some proposed power control schemes [47][48] in the literature may actually increase collisions and degrades network throughputs which can in turn result in more energy consumption. The paper proposed to periodically increase the transmit power during data transmissions so that nearby nodes can sense the transmissions and avoid collisions.

Reference [49] examined a cross-layer approach of joint link scheduling and power control with

the aim to improve network throughput. Most of the previous work (e.g. [50][51]) on this cross-layer approach focuses on minimizing the power consumption. These schemes are useful for wireless sensor networks [52][53] in which network lifetime is the primary concern. However, they may not be the appropriate solution for emerging multi-hop networks such as wireless mesh networks [54][55], in which network throughput is the major issue. This paper suggested scheduling the transmissions in a way to maximize channel spatial reuse. Reference [49] also defined a new parameter called the demand satisfaction factor to achieve a good tradeoff between throughput and fairness.

1.2.2. MIMO (Multiple Input Multiple Output)

Multiple Input Multiple Output (MIMO) technology uses digital adaptive array antennas at both the transmitter and receiver ends of a communication link. The performance enhancements are achieved due to 1) spatial multiplexing, 2) antenna diversity, 3) beamforming, and 4) diversity gain.

1) Spatial Multiplexing

Wireless terminals with N transmitter antennas and M receiver antennas (where N and M are integer) send multiple independent data streams simultaneously. The receiver can separate these streams to achieve high spectral efficiencies which in turn increase the link capacity. This is referred to as spatial multiplexing [34][56][57][58]. To optimize the performance enhancement, reference [33] proposed a new medium access control (MAC) protocol to take into account the scheduling and fairness of theses MIMO links.

2) Antenna Diversity

Similar data signals are transmitted from multiple antennas. The receiver combines and selects signals from the antennas to improve the signal-to-noise ratio (SNR). If one of the antennas faces noise, fading or interference, the receiver can switch to other antennas for receptions [59].

3) Beamforming

Beamforming can be used to control the directionality of the radiation pattern of an antenna [60]. When a beamforming antenna receives a signal, it increases the sensitivity in the direction of the receiving signal and decreases the sensitivity in the direction of interference and noise. This increases the signal-to-noise ratio (SNR) of the reception.

4) Diversity Gain

Diversity techniques transmit signals over multiple independently fading paths in time, frequency or space [60]. The receiver combines the multiple arriving signals to reconstruct the message. This reduces the amplitude variations of the signal. Space-time coding allows transmitter to extract spatial diversity gain without channel knowledge [61].

The IEEE 802.11n standard adopts MIMO technology to increase the network capacity of Wireless LANs. An IEEE 802.11n wireless router [62] can increase the link data rate to up to 12 times faster than that of the IEEE 802.11g, which has a 54Mbps link data rate. However, reference [63] pointed out that a theoretical throughput limit exists due to protocol overheads and limitations of physical implementations. Thus, simply increasing the link data rate may not help a lot. It showed that an IEEE 802.11a link with payload size of 1500bytes can only achieve a maximum of 75Mbps. Reference [64], therefore, proposed an efficient MAC protocol with strategies such as packing, concatenation, or multiple frame transmission, to overcome the overheads and improve the capacity.

Reference [65] considered the power management in MIMO ad-hoc networks. If bad channel conditions occur in some communications links, they may result in very low data transmission rates even though their transmit powers are high. It is not energy efficient. There has been a growing interest in applying game theory to study power control and rate control for wireless data networks [66][67]. In reference [65], the power allocation in each link is built into a non-cooperative game where a utility function is identified and maximized. A mechanism for shutting down inefficient

links was thus proposed to achieve higher capacity and better energy efficiency.

1.2.3. Directional Antenna

A directional antenna provides a higher gain for greater transmission range by beam-forming toward a desired direction [35]. It can also selectively receive signals from a certain desired direction to avoid unwanted interference. Thus, two links in a vicinity could communicate simultaneously which in turn can increase the network capacity. The original IEEE 802.11 MAC protocol, however, is not designed for nodes with directional antennas. Therefore, extensive research has been carried out to proposed new MAC schemes (e.g. [36][68][69][70]) for networks using directional antennas. Reference [35] proposed the use of multi-hop request-to-send (RTS) packets to establish links between distant nodes while reference [71] adopted several new mechanisms in its protocol such as directional power-controlled MAC, neighbour discovery with beam-forming, link characterization, or proactive routing and forwarding. They both perform better than the IEEE 802.11 in term of throughput and delay, although the performance enhancements also depend on the network topology and flow patterns.

Reference [72] proposed a load-sensitive routing protocol for ad-hoc networks using directional antennas. It utilizes the aggregate queue size of all nodes in a path as the load metric for choosing routes. It outperforms the widely used hop count routing metric in term of end-to-end delay and throughput. Reference [73] extended the use of directional antennas for multicast communications in ad-hoc networks. An online routing algorithm was proposed with the aim of reducing the power consumption so as to maximize the network lifetime. In reference [74], a directional antenna is also used in multi-channel protocol to increase the spatial reuse in Wireless LANs. This multi-channel scheme can be classified as the split-phase approach which has been described in sub-section 1.1.2.

1.2.4. Routing

Numerous ad-hoc routing protocols have been proposed in the literature. They can be categorized into two approaches: 1) proactive / table-driven; or 2) reactive / on-demand-driven [7]. The proactive approach protocols (e.g., Destination Sequenced Distance Vector (DSDV) [37]), attempt to preserve consistent and up-to-date routing information from each node to every other node in the entire network. Each node maintains its own routing table and propagates route updates throughout the network to notify other nodes of changes in the network topology. In reactive approach protocols (e.g. Ad-hoc On-demand Distance Vector (AODV) [32] and Dynamic Source Routing (DSR) [75]), route discoveries are initiated only when desired by the source nodes. A node keeps using the created route until that route becomes inaccessible or the route is no longer needed [76]. Generally, on-demand routing incurs less overheads than proactive routing, particularly in highly mobile ad-hoc networks which require frequent route discoveries.

Multi-path routing protocols seek multiple paths in a single route discovery attempt. They can be used to balance load by transmitting packets on different paths. Reference [77] proposed a dual-channel routing scheme which uses two routes of maximally disjoint paths with independent channels to distribute traffic. It achieves higher network throughput since dual-channel forwarding can take place concurrently. Similarly, a quality-of-service (QoS) routing algorithm was modified from AODV in [78]. It spreads the traffic flows over the global topology which in turn increases the throughput and decreases the number of packet collisions along the paths.

Reference [79] suggested a route reservation scheme which reserves a multi-hop route from a source node to its destination. This can yield better end-to-end delay performance compared to non-reservation-based routing schemes such as AODV or DSDV. However, this advantage comes at the expense of lower throughput [80] since the scheme stops other traffic flows from using the reserved intermediate nodes.

1.2.5. Offered Load Control

In multi-hop ad-hoc networks, stations may pump more traffic into the networks than can be supported, resulting in high packet-loss rate, instability and unfairness problems [38]. Reference [38] suggested controlling the offered load at the sources can eliminate these problems. In addition, it provides an analysis to estimate the optimal offered load that maximizes the throughput of a multi-hop traffic flow. The analysis is based on the observation that a large-scale 802.11 network with hidden nodes is a network in which the carrier-sensing capability breaks down partially. Its performance is therefore somewhere between a carrier-sensing network and an Aloha network.

In reference [39], the offered load control (end-to-end rate control) was integrated with an opportunistic power scheduling. It models the time-varying wireless channel as a stochastic process and formulates it as an optimization problem. However, a centralized algorithm with global information is needed to obtain the optimal solution for improving system performances. Distributed approaches, which are more suitable for ad-hoc networks, however, are still left open for further research.

1.2.6. Cross-layer Solutions

Various performance enhancement schemes for carrier sense wireless networks have been outlined in above sub-sections. Another approach to improve performances is to integrate some of these schemes together which is generally known as the cross-layer solution. For example, in reference [40], a cross-layer optimization framework was proposed to jointly design the scheduling, power control and adaptive modulation in ad-hoc networks. Specifically, the transmitted power is dynamically adapted according to the packet arrival, quality-of-service requirements, power limits, and channel conditions. The paper showed the proposed cross-layer scheme can achieve significant gains in throughput and power efficiency. Another example was shown in reference [41] which considered the specific characteristics of MIMO physical layer as an integral part of the MAC layer

design process. For the multi-channel approach, references [81][82] integrated it with directional antennas while references [83][84][85] proposed routing protocols to exploit multiple channels to improve network capacity.

There has been extensive research carried out in the areas listed above. This thesis, however, focuses on a novel approach which has not been studied before. The proposed ideas can be implemented based on the well-defined IEEE 802.11 industrial standard. In the next sub-section, the interference, hidden-node, and exposed-node problems of carrier sense wireless networies are introduced.

1.3. Interference in Carrier Sense Wireless Networks

In carrier sense wireless networks, two wireless nodes (e.g., nodes X and Y) can communicate if they are located within the transmission range (TxRange) of each other. A wireless link (e.g. link X-Y) can then be established between these two nodes. However, when a third wireless node (e.g., node Z) placed inside the interference ranges of node X and/or node Y is transmitting, link X-Y can not transmit at the same time. Otherwise, collisions will occur and this will degrade the network capacity. Link interference graphs can then be used to model these interference relationships between links. Link vertices are connected by interference edges if they cannot transmit simultaneously in the same channel. To eliminate interference, colouring algorithms can be applied to interference graphs for assigning orthogonal transmission channels or scheduling transmissions.

Many wireless network protocols in the literature are designed based on the interference graphs, for example, [86] [87] [88]. Reference [86] proposed a distributed algorithm to determine max-min fair share for links according to the interference graphs of ad-hoc networks. The algorithm is then integrated with the IEEE 802.11 protocol to achieve fairness among wireless links. Reference [87] introduced an approach for access points to allocate transmission channels in WLANs based on the

colouring results of interference graphs. Simulations showed that the scheme can achieve higher network throughputs than random channel allocations.

1.3.1. Hidden-node Problem

The hidden-node phenomenon happens when wireless nodes outside the carrier-sensing range of each other are nonetheless close enough to interfere with each other [89]. Consider Fig. 1.8. When node 4 sends a packet to node 5, node 2 senses the channel to be busy while node 1 senses the channel to be idle, since node 4 is inside the carrier-sensing range of node 2 but outside that of node 1. Once node 1 senses the channel as idle, it may count down its back-off contention window until zero and transmit a packet to node 2. If the transmission from node 4 is still in progress, node 2 will continue to sense the channel as busy, and it will not receive the packet from node 1. As a result, node 2 will not return an ACK to node 1. Node 1 may then time out and double the contention window size for retransmission later.

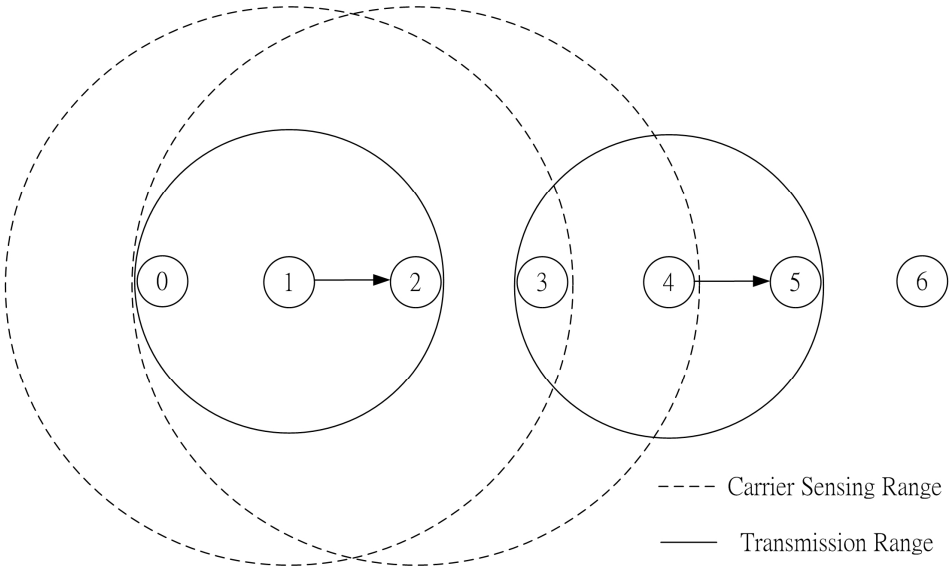


Figure 1.8. Node 4 as a hidden node to node 1

Meanwhile, node 4 transmits the packet successfully and is not aware of the collision at node 2. When transmitting the next packet, node 4 will use the minimum contention window size. The hidden-node scenario favours node 4, and the chance of collision at node 2 can not be reduced even though node 1 backs off before the next retry. The hidden-node problem thus severely increases the chance of collisions. It is also known as the root cause of many performance problems such as throughput degradation, re-routing instability [76], or unfair throughput distribution [89].

Note that the negative effect of a hidden node is much more than that of a contending node within the carrier-sensing range. This is because the carrier-sensing capability in the CSMA/CA protocol breaks down with respect to the hidden node, making collisions much more likely.

The RTS/CTS mechanism in 802.11 was designed with an attempt to solve the hidden node problem. Reference [90] proposed a hidden station detection mechanism. When a node detects a hidden-node, it can trigger the usage of the RTS/CTS mechanism. However, reference [18] argued that when the carrier-sensing range is larger than two times of the transmission range, RTS/CTS is no longer needed.

In reference [89], a hidden-node-free design was studied. Besides the modification of receiver chip set, the solution also requires the carrier-sensing range to be set to more than 3.78 times of the transmission range. This may in turn limit the network capacity by disallowing links which are far enough away to transmit at the same time.

1.3.2. Exposed-node Problem

Figure 1.9 shows an exposed-node scenario. When node A1 is sending data to A2, node B1 can not transmit due to carrier-sensing, even though there is no mutual interference since B1 is outside the interference range of A1. The carrier sensing mechanism only allows one transmission at one time within a carrier-sensing range. Therefore, the larger the carrier-sensing range, the worse is the exposed-node problem and thus the network throughput. Reference [91] reported that the capacity of

IEEE 802.11 is not scalable due to this exposed-node problem.

Comparing with the hidden-node problem, there is much less work on the exposed-node problem in the literature. References [92][93] attempted to remove the hidden-node and exposed-node problems by notifying neighbour nodes with a “Busy Tone”. Reference [91] modified the protocol with an algorithm to selectively disregard the carrier-sensing mechanism in order to remove the exposed-node problem. This scheme allows IEEE 802.11 networks to achieve scalable capacities which commensurate with the seminal theoretical results in [94][95].

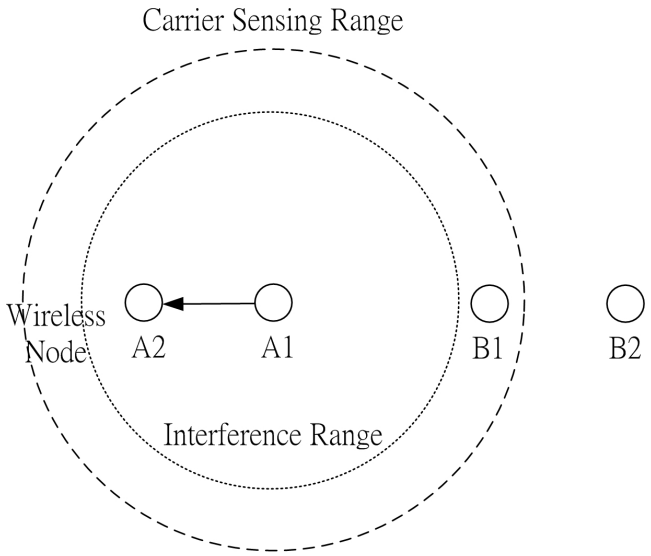


Figure 1.9. Node A1 as an exposed node to node B1

1.4. Outline of Thesis

The capacity of carrier-sense wireless networks is limited by its carrier-sensing mechanism since only one transmission is allowed at one time in a carrier-sensing range. With the increasing data traffic induced by the growing internet applications such as video streaming or peer-to-peer file sharing, it is essential to improve the limited capacity of carrier sense wireless networks. This research therefore proposes two novel algorithms with an attempt to mitigate the problem: 1) a

link-directionality-based dual channel MAC protocol (DCP), and 2) a signal-to-interference ratio comparison algorithm (SCA).

For 1), links in the vicinity of each other are allowed to transmit simultaneously by assigning their transmission and reception channels based on link-directionalities in order to increase capacities. The capacity improvement achieved by DCP, however, decreases when link lengths are short (the transmitter-receiver distance of a link).

For 2), the signal-to-interference (SIR) comparison algorithm inserts SIR information in packet headers so that links in the vicinity of each other can compare their SIRs. This approach reduces the exposed node problem identified in reference [51] to allow more links to transmit simultaneously. The throughput enhancement of the signal-to-interference ratio comparison algorithm (SCA), on the other hand, decreases when the link length increases. Thus the capacity improvement of the link-directionality-based dual channel protocol (DCP) exceeds that of SCA in the case of long transmitter-receiver distances, and vice versa in the case of short transmitter-receiver distances. When combined, these two algorithms compensate for the shortcoming of each other to achieve superior performance in a wide range of situations. This will be demonstrated analytically in sub-section 3.1 by computing the exclusion region [33] of links established by each algorithm.

After receiving a DATA packet, a receiver node in a wireless data network replies an acknowledgement (ACK) packet to a transmitter node. This generates a reverse traffic in the link. In traditional interference graphs, a single link vertex is used to represent both the DATA and acknowledgement (ACK) traffic in opposite directions of a link. Chapter 4 will show that it is insufficient to capture the interference relationships. In fact, some directional traffic can actually transmit simultaneously but some links are prohibited by the traditional interference graphs. Thus, in this thesis, a novel link-directional interference graph (l-graph) is proposed. By colouring l-graphs, wireless protocols can allocate channels or schedule transmissions to improve network capacities. Based on this insight, a solution is proposed to assign orthogonal streams obtained by Multi-carrier

Code Division Multiple Access (MC-CDMA) in wireless local area networks (WLAN) to mitigate inter-BSS (Basic Service Set) co-channel interference caused by the hidden-node and exposed-node problems.

A generic approach for capacity analysis is also proposed to justify the capacity advantage of using link-directionality in a network topology. This approach shows that the concept of link-directionality is not limited to the propagation model, channel model, modulation scheme and medium access control protocol (MAC) protocol assumed in the simulations in this thesis. In fact, the concept of link-directionality can be adopted with other network models, protocols and parameter settings. The achievable network capacity obtained by this approach for a given network can then be compared with the single-channel scheme. This allows one to determine whether channel allocations according to link-directionalities should be applied to the given network.

The rest of this thesis is organized as follows. In Chapter 2, the concept of splitting traffic based on link-directionalities is described. Then it gives the details of the proposed MAC protocol. The protocol overheads and packet collision problems are also considered. Finally, simulations show that the proposed protocol can sufficiently improve the network capacity.

Chapter 3 details the SIR comparison algorithm (SCA). It then analyzes the capacity improvements of DCP, SCA and the integrated protocol (DCP with SCA). Simulations show that DCP with SCA (DCPwSCA) can significantly multiply the network capacities in both lattice and random topologies.

In Chapter 4, the physical interference graph model is reviewed. It then presents the link-directional interference graph to clarify the interference relationships between directional links. A colouring algorithm is therefore applied to the link-directional interference graph in order to schedule transmissions and allocate channels for time division multiple access (TDMA) and frequency division multiple access (FDMA) networks. Moreover, a generic approach for capacity analysis emphasizes the advantage of using link-directionality. An example of this generic approach

is presented. Finally, the insight to assign multi-carrier code division multiple access (MC-CDMA) generated data streams in WLANs is used to mitigate the hidden-node and exposed-node problems.

Chapter 5 concludes the thesis and presents topics for future research.

Novel Contributions

The major contributions of this research are:

- Network throughput enhancements by using link-directionalities for channel allocations in a media-access-control MAC protocol (DCP)
- Throughput enhancements by a signal-to-interference ratio comparison algorithm (SCA)
- Integration of DCP and SCA to increase network throughputs under various link (transmitter-to-receiver) distance scenarios.
- Construction of link-directional interference graphs to analyze the throughput enhancements achieved by using link-directionalities
- Elimination of the hidden-node and exposed-node problems in wireless local area networks by channel allocations according to link-directionalities

2. Link-directionality-based Dual Channel MAC Protocol for Ad-hoc Networks

The IEEE 802.11 standard is used as the benchmark and to implement the proposed concept in this research since it is the most widely deployed carrier sense multiple access (CSMA) protocol. It uses short request-to-send (RTS) and clear-to-send (CTS) messages to notify other nodes within the virtual carrier-sensing range (*VCSRange*) to update their Network Allocation Vector (NAV). The NAV includes the duration time of the ongoing transmission. Thus, no other nodes within the *VCSRange* can begin transmissions before the NAV expires. This is the carrier sensing mechanism. It prevents simultaneous transmissions that may lead to collisions. However, at the same time, it limits the network capacity. Figure 2.1a shows an example. Under the 802.11 protocol with RTS/CTS access mode, none of the links B, C or D can transmit at the same time with link A. This is because R_A has to receive the DATA frame from T_A while T_A has to wait for the ACK from R_A. Any other simultaneous transmissions within the *VCSRange* region of R_A and T_A in the same channel will lead to collision of the transmission between R_A and T_A. To avoid such collision, the RTS of T_A and the CTS of R_A forewarns links B, C, and D not to transmit before link A transmits its DATA frame.

Note that there are two carrier-sensing ranges: 1) the virtual carrier-sensing range (*VCSRange*) and 2) the physical carrier-sensing range (*PCSRange*). For 1), RTS/CTS can be detected and demodulated if the distance of transmission is less than the virtual carrier sensing range (*VCSRange*). The network allocation vector (NAV) included in the RTS/CTS frames would prevent nodes from transmitting. For 2), physical carrier sensing may also prevent simultaneous transmissions. When the preamble of the physical header can be decoded, the length field in the physical header informs the receiver of the duration of the payload that follows. In the simulations, physical headers are set to be transmitted at the same rate as RTS/CTS frames. Thus, *VCSRange* is the same as *PCSRange*.

To allow simultaneous transmissions, the transmission channels of two nodes of a link can be assigned with two independent channels based on their link directionalities. Consider the case where there are two channels, *s* and *t*. Channels *s* and *t* use non-overlapping frequency bands which are independent of each other. Nodes transmit RTS and DATA in one channel (e.g., channel *s*) as they are in the same direction (from T_A to R_A) while CTS and ACK are transmitted in another channel (e.g., channel *t*). The channels are assigned dynamically based on the directionality, network topology, and who else is transmitting in the neighborhood. RTS and DATA can be transmitted in either channel *s* or *t*, and thus CTS and ACK will be sent in the other channel (*t* or *s*). The main idea is to allow the simultaneous transmission of another link *i* within the *VCSRange* region of R_A and T_A provided that the transmissions of link *i* do not interfere with the reception of the ACK at T_A or the DATA at R_A. There are two possible cases:

Case 1: the transmissions of link *i* within the *VCSRange* use a different channel, and thus these do not affect the reception of R_A (T_A) in another channel.

Case 2: the transmissions of link *i* use the same channel as the reception of R_A (T_A) but those transmissions are far enough from R_A (T_A).

Notice that here the conditions within the brackets in this chapter represent the scenario when the symbols swap their roles.

For Case 2, let d_{TA-RA} be the distance between T_A and R_A, d_{TB-RA} be the distance between T_B and R_A, *CPThreshold* be the SIR (signal-to-interference ratio) capture threshold with α being the path loss exponent. From [96], assuming noise is negligible, if the signal-to-interference ratio at R_A is larger than the *CPThreshold*, R_A can capture the signal from T_A when T_B is transmitting. That is,

$$SIR = (d_{TB-RA} / d_{TA-RA})^{\alpha} > CPThreshold$$

$$d_{TB-RA} > CPThreshold^{1/\alpha} * d_{TA-RA}. \qquad (2.1)$$

In the simulations, the transmission range (*TxRange*) is set to be 250m while *VCSRange* is 550m by assigning the data rate for sending DATA/ACK at 12Mbps (OFDM,QPSK) and the basic rate for transmitting RTS/CTS at 2Mbps (DSSS,DQPSK). The SIR (signal-to-interference ratio) capture threshold (*CPThreshold*) is set to be 10dB [97][98] since reference [99] reported that *CPThreshold* tends to hold at 10 dB until 24 Mbps in real-life experiments. The value of path loss exponent α is usually in the range of 2 to 4 which in turn determines the interference range. Here the two-ray propagation model [96] is assumed with $\alpha = 4$. In the worst case that T_A and R_A are separated by the maximum transmission range (250m), R_A can capture the signal from T_A if T_B is located at more than $CPThreshold^{1/\alpha} * d_{TA-RA} = \sqrt[4]{10} * d_{TA-RA} =$ 1.78*250m=445m (which is also known as the interference range) away from R_A. If T_B can not receive the CTS from R_A, T_B must be far enough so that its signal can not interfere with the reception of signal from T_A at R_A. In most of the 802.11 commercial products (e.g. Buffalo WLI2-CF-S11 card as shown in Appendix A), *VCSRange* is usually set to be larger than the interference range to ensure the carrier-sensing mechanism can signal nearby links of ongoing transmissions in order to avoid collisions. Therefore, the proposed protocol can utilize this property to assign transmission channels for links as long as *VCSRange* is set to be larger than the interference range.

Figure 2.1b shows the same scenario as Fig. 2.1a with the channel assignments based on the Cases 1 and 2. Assuming link A is using channel 1 to transmit RTS and DATA from T_A to R_A and another independent channel 2 to send CTS and ACK from R_A to T_A. For link B to transmit simultaneously with link A, channel 1 can be assigned for the transmission of RTS and DATA from T_B to R_B. This will not lead to collisions on link A because the signal from T_B is much weaker than the signal from T_A when they reach R_A (Case 2). R_B can then use channel 2 to transmit CTS and ACK. This, again,

will not incur collisions on R_A because R_B is using another independent channel for transmissions (Case 1). Similarly, for link C, T_C can use channel 2 to transmit RTS and DATA while R_C can use channel 1 to reply CTS and ACK. For link D, since both T_D and R_D are within the *VCSRange* of link A, link A and D can not transmit at the same time and thus they have to take turns to transmit.

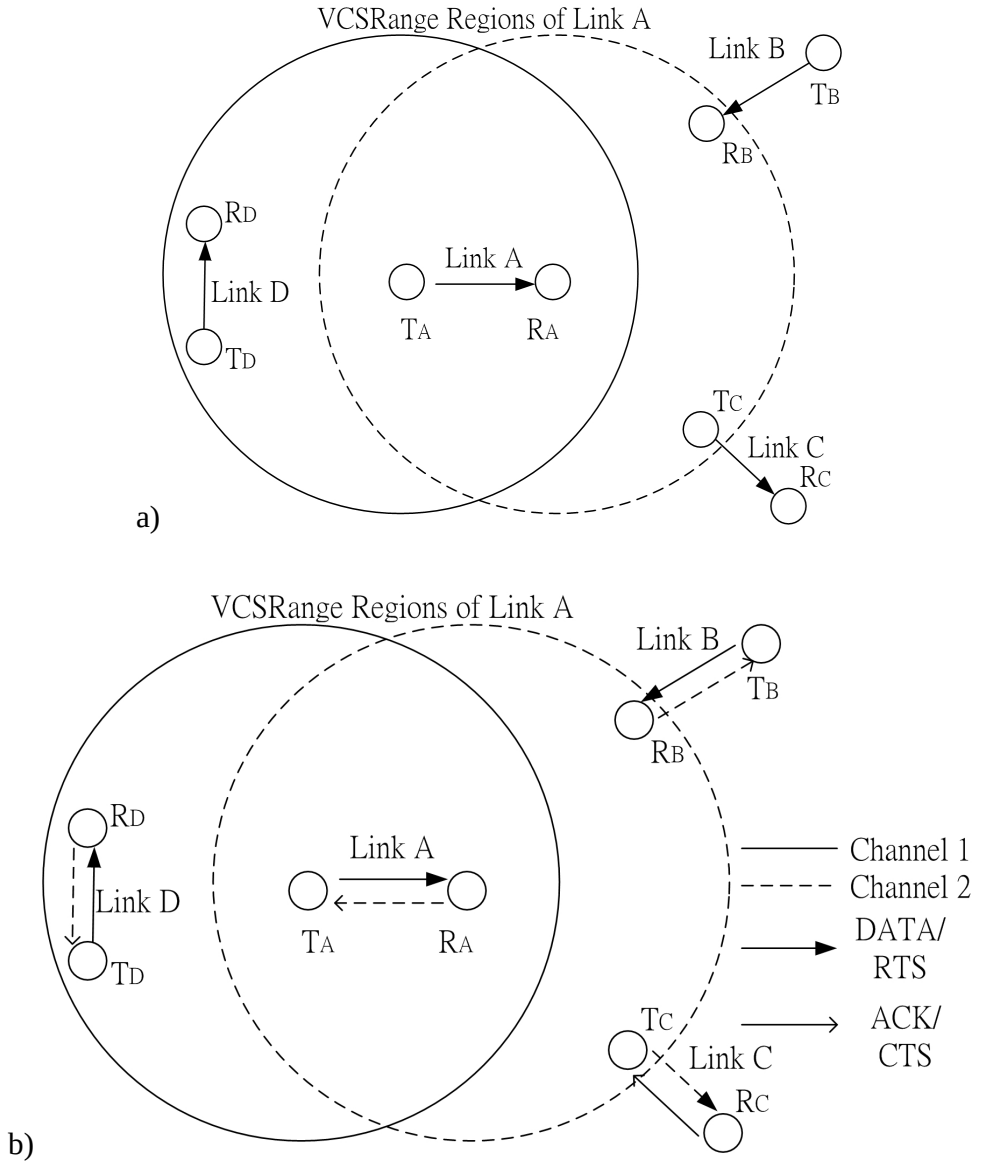


Figure 2.1. A network topology using a) the original 802.11 and b) the proposed scheme

2.1. The Proposed New MAC Protocol

In this sub-section, a MAC protocol is described to achieve the channel assignments as explained in the previous sub-section. The protocol assigns the transmission channels of each link based on the availabilities of the receptions of RTS and CTS from other links. The protocol is modified from the original 802.11 MAC protocol and it attempts to seek opportunities for simultaneous transmissions. Assume all nodes use the same power for transmissions and each node has a transmitter and a wideband receiver to monitor wireless channels. The receiver and transmitter do not need the ability to transmit and receive concurrently. This sub-section first outlines the basic concept of the proposed protocol. Then, it describes the algorithms required for the protocol.

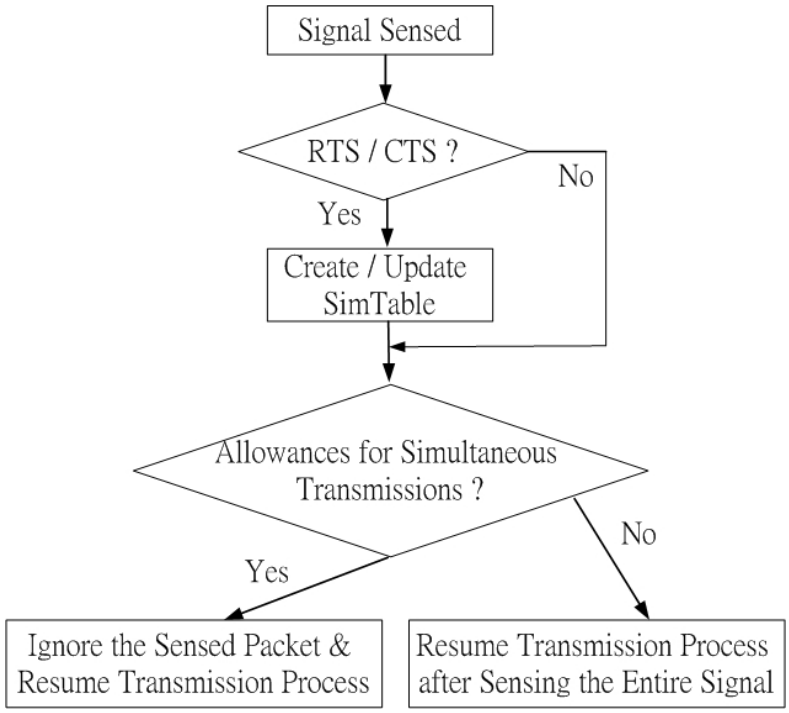


Figure 2.2. Flow chart for handling sensed signals of the proposed protocol.

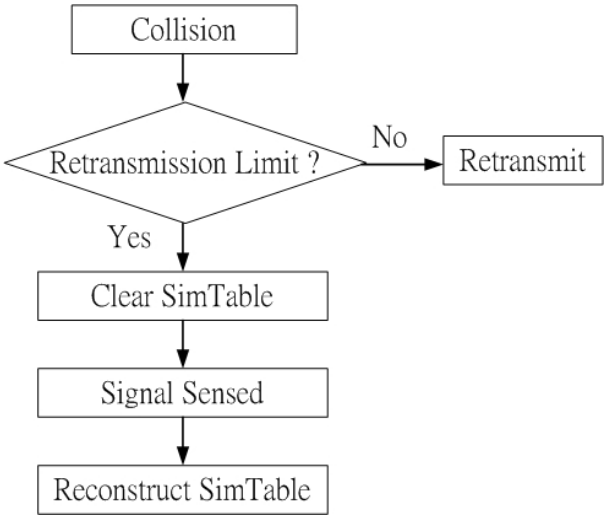


Figure 2.3. Flow chart for handling collisions of the proposed protocol.

2.1.1. Basic Concept

The main purpose of the protocol is to identify the transmission channel which does not interfere with the transmissions of nearby links based on the RTS/CTS frames received from neighborhoods. Consider two links, link *i* and link *j*. When a node (e.g., T_i) of link *i* receives the RTS_j but not the CTS_j of another link *j*, it will assign its RTS_i to the same channel as that of RTS_j. Thus, link $i_{T->R}$ can transmit simultaneously with $j_{T->R}$ because receiver R_j is located far enough away from the transmitter T_i (as explained in Case 2 in the previous sub-section) and T_j is receiving CTS or ACK in another channel (Case 1 in the previous sub-section). In other words, T_i knows that its RTS_i or $DATA_i$ transmitted on the assigned channel will not corrupt the reception at T_j and R_j, and so it is safe for T_i to transmit its RTS_i and $DATA_i$. Similarly, when a node (e.g., T_i) of link *i* receives the CTS_j but not the RTS_j of another link *j*, it will assign its RTS_i to the same channel as that of CTS_j. If a node can receive both the CTS_j and RTS_j of another link *j*, it will fall back to the original 802.11 protocol and will resume transmissions only after the NAV expires. In this case, links *i* and *j* have to

take turns to transmit. Various cases of link packing and node arrangements will be discussed in details in later parts of this sub-section.

2.1.2. Algorithms of the Protocol

To assign channels for simultaneous transmission links, the protocol requires three algorithms: i) construction of simultaneous transmission tables; ii) randomly assigned transmission channels; and iii) adding a priority field. The first algorithm identifies possible channels for simultaneous transmissions based on the received RTS/CTS frames from nearby links; the second algorithm chooses channels when RTS/CTS information is unavailable. The third algorithm gives priorities to nodes with channels assigned by the first algorithm over those assigned by the second one. Figures 2.2 and 2.3 outline the flows of the protocol.

i. Construction of Simultaneous Transmission Tables

The proposed MAC protocol constructs a simultaneous transmission table (*SimTable*) in each node based on the receptions of RTS and CTS from other links. Each entry in the table corresponds to the channel number used. Each node attempts to seek opportunities for simultaneous transmissions according to the sensed signals and the records of its *SimTable*. Table II.A. shows an example of the *SimTable* of node T_A of link A in Fig. 2.4. In the topology of Fig. 2.4, consider link B begins the transmission first. T_A receives the CTS from R_B and then updates its $SimTable_{TA}$ (as shown in Table II.A.) with a new record (the first row). The *CTSChannel* field is set to Channel 2. Since T_A cannot receive the RTS from T_B, the *RTSChannel* field remains *null*. According to $SimTable_{TA}$, T_A realizes that it can transmit simultaneously with R_B in Channel 2 without interfering with reception at T_B as T_B is far enough from T_A. Similarly, T_A receives the RTS from T_C and then updates its $SimTable_{TA}$

with another record (the second row). The *RTSChannel* field is set to Channel 2. Since T_A cannot receive the CTS from T_C, the *CTSChannel* field remains *null*. T_A thus recognizes that it can transmit concurrently with T_C in Channel 2 without interfering with R_C. When T_A has a packet to transmit, it examines its $SimTable_{TA}$. If simultaneous transmissions are allowed, T_A will transmit an RTS to R_A. Otherwise, it will wait for the expiration of NAV and then resume the transmission process.

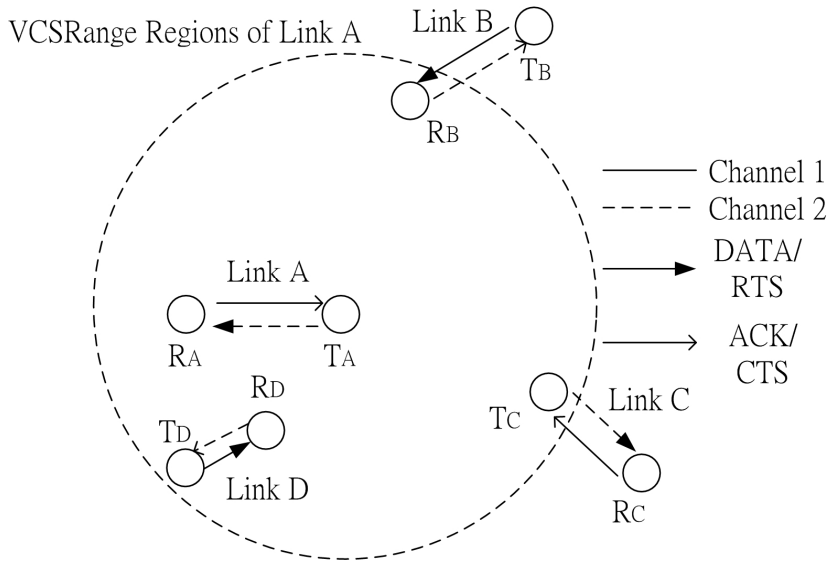


Figure 2.4. A network topology using the proposed channel assignment scheme

Table II.A. Simultaneous Transmission Table of Node T_A in Figure 2.4.

Index	From	To	RTSChannel	CTSChannel
1	T_B	R_B	*null*	2
2	T_C	R_C	2	*null*
3	T_D	R_D	1	2

Table II.B. The Priority Field of Nodes in Figure 2.4.

Link	Node	Priority Field	Node	Priority Field
B	T_B	0	R_B	1
C	T_C	1	R_C	0

Consider link D in Fig. 2.4. T_D sends RTS to R_D and R_D replies CTS back to T_D. T_A receives both the RTS_D and CTS_D of link D. Thus, the *RTSChannel* and *CTSChannel* fields of the record (the third row in Table II.A) are set to 1 and 2 respectively. So, in this case, link A cannot transmit at the same time with link D and they must take turns to transmit.

ii. Randomly Assigned Transmission Channels

When a transmitter of a link does not receive RTS/CTS signals from its nearby links for channel allocations, it will just randomly pick up one of the two channels for sending its RTS to the receiver of the link. If it can receive the CTS replied from the receiver, it will retain the channel for transmissions. Otherwise, it will swap to the other channel for a retransmission. This algorithm allows a node to identify the suitable transmission channel to avoid collisions when RTS/CTS information is unavailable. Figure 2.5 shows an example when a receiver R_2 is in silence for later transmissions. Assume T_1 is transmitting DATA to R_1 on Channel 1 when T_2 begins its transmissions to R_2. T_2 cannot identify the available channel for simultaneous transmissions since T_2 cannot receive the RTS and CTS from link 1. T_2 will then randomly pick one of the two channels for sending RTS to R_2.For example, Channel 1 is chosen, RTS_2 will collide with $DATA_1$ at R_2. Thus R_2 will not reply a CTS back to T_2. When the timer of T_2 expires, it will switch to another channel (Channel 2) for a retransmission. In this case, R_2 can now receive RTS_2 successfully and will reply a CTS_2 to R_2 in Channel 1. Link 2 will then retain these channel assignments for ongoing transmissions. Note that here the exponential backoff will not be triggered unless and until the second attempt also fails to get a response from R_2.

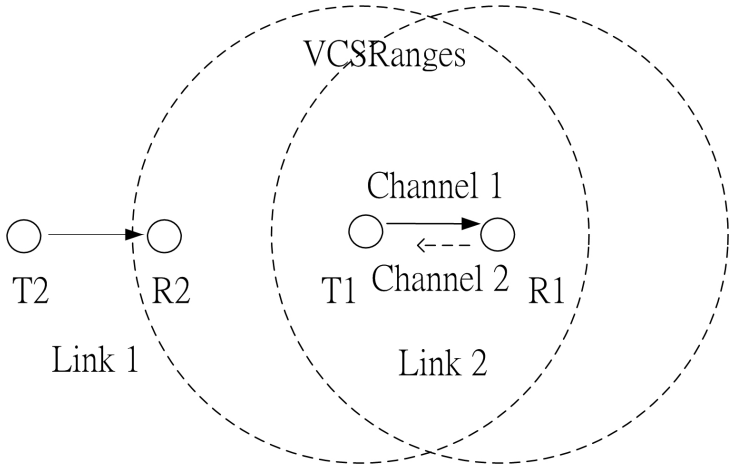


Figure 2.5. Choosing transmission channels with algorithm *ii) randomly assigned transmission channels*

iii. Adding a Priority Field

A priority field is recorded in each node and transmitted in the RTS initiated by it, for the purpose of choosing channels in case there is a conflict between the channel choice of the transmitter and receiver of a link. To do this, an extra bit indicating this priority field is added to the RTS frame after the MAC header. It only induces very little overheads since the priority field (1bit) is much smaller than the size of physical header (24bytes), MAC header (28bytes) and DATA (up to 2312bytes). Note that the channel choice based on algorithm *i* is a deliberate attempt to avoid collision, while the channel choice based on algorithm *ii* is a random choice. So, in case of a conflict, the channel choice of algorithm *i* should take precedence. In terms of implementation, if a node can assign its transmission channel based on the received RTS/CTS signal (by algorithm *i*), it will set its priority field to 1. Otherwise, the field remains 0 when channel is randomly chosen by algorithm *ii*. For example, R_B in Fig. 2.4 can receive the RTS_A from link A to assign its transmission channel while T_B cannot receive RTS/CTS from nearby links. As shown in Table II.B., the priority field of R_B

will then be set to 1 while that of T_B will be assigned as 0. This priority field will be attached in the MAC header of the RTS frames. Table II.B. also shows the priority fields of links B and C in Fig. 2.4. Consider link B in Fig. 2.4. The RTS sent from T_B to R_B contains the priority field (0) which is less than the priority field (1) of R_B. If the RTS_B from T_B uses the same channel as the assigned channel for CTS by algorithm *i*, R_B will not reply CTS_B back to T_B. R_B retains its transmission channel as assigned by algorithm *i*. When T_B cannot receive CTS_B from R_B, it will then swap to the other channel for retransmission. This algorithm ensures the channel assigned by algorithm *i* always override the channel randomly picked by algorithm *ii*.

2.1.3. Assigning Channels in Various Topologies

Consider the pair-wise scenario with two links, link *i* and link *j*. As shown in Fig. 2.6, there are five possible configuration cases between links *i* and *j*:

A) The two nodes of link *i* are outside the VCSRanges of the two nodes of link *j* (as shown in Fig. 2.6a).

B) One of the two nodes of link *i* is within the VCSRange of one of the two nodes of link *j* (as shown in Fig. 2.6b).

C) The two nodes of link *i* are within the VCSRange of one of the two nodes of link *j* (as shown in Fig. 2.6c).

D) One of the two nodes of link *i* is within the VCSRanges the two nodes of link *j* (as shown in Fig. 2.6d).

E) The two nodes of link *i* are within the VCSRanges of the two nodes of link *j* (as shown in Fig. 2.6e).

In each configuration, there are four possible transmitter-receiver arrangements. Thus, there are twenty cases of network arrangements. Let {*a,b,c,d*} be the node arrangements, from one side to another, they are:

Arrangement 1): { R_i T_i T_j R_j }

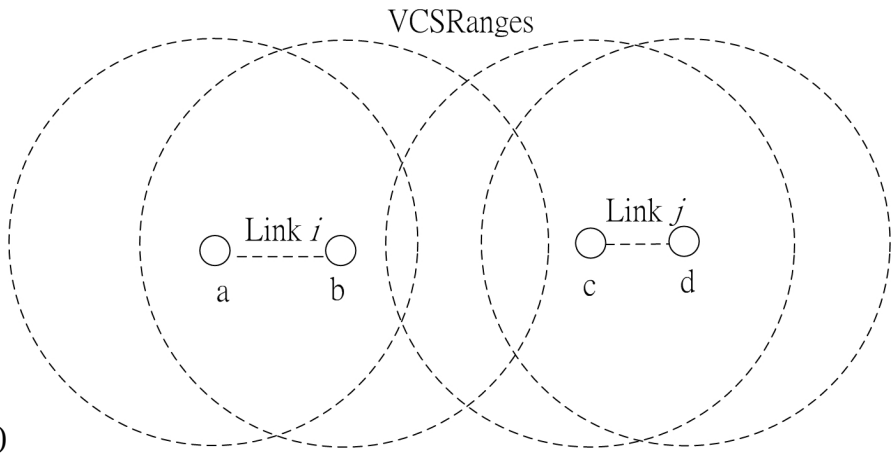
Arrangement 2): { R_i T_i R_j T_j }

Arrangement 3): { T_i R_i T_j R_j }

Arrangement 4): { T_i R_i R_j T_j }

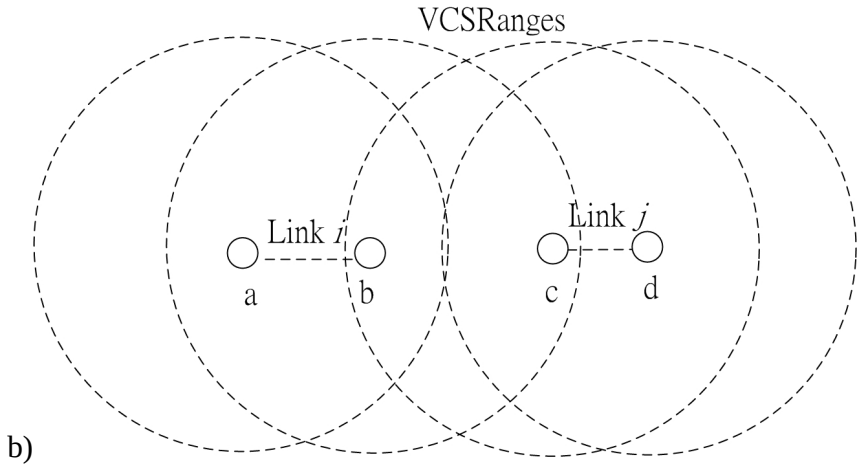
For example, Arrangement 1) { R_i T_i T_j R_j } with Configuration B represents the topology as shown in Fig. 2.7. There are a number of configurations:

Configuration A: For all arrangements 1 to 4, links *i* and *j* can transmit simultaneously since the nodes of link *i* are outside the *VCSRanges* of the nodes of link *j*. In the proposed protocol, T_i and T_j can randomly choose a transmission channel (e.g. channel *s*) for sending RTS and DATA. R_i and R_j then reply CTS and ACK by using the other channel (e.g. channel *t*).

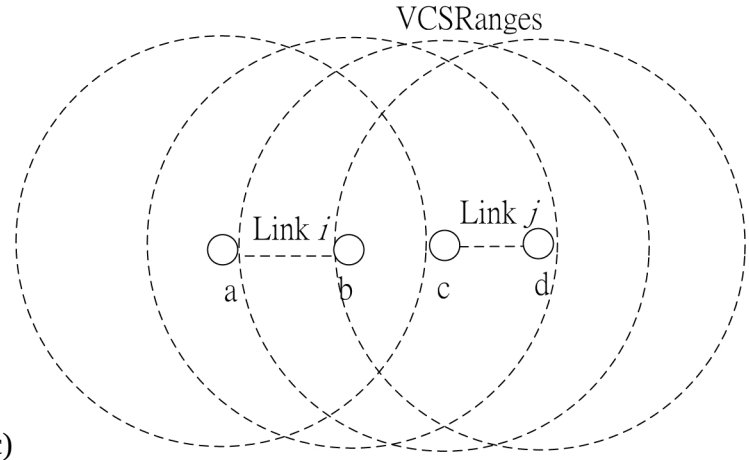


a)

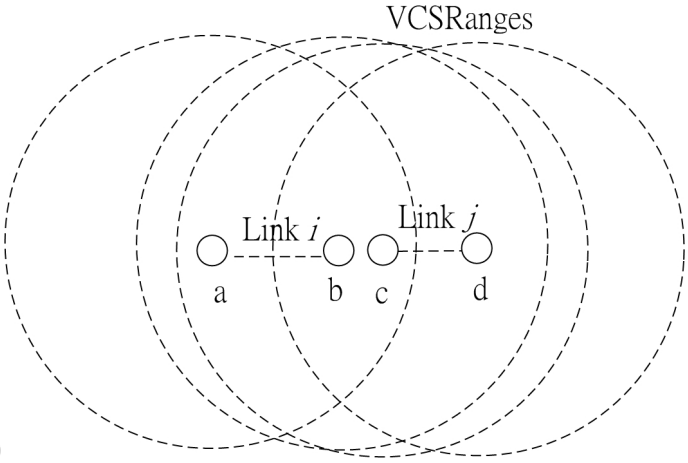
Figure 2.6.a Five configurations between links *i* and *j*



b)

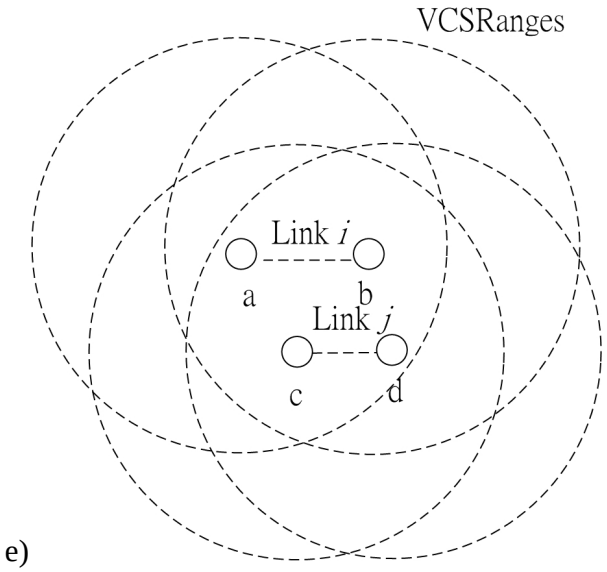


c)



d)

Figure 2.6.b, c and d. Five configurations between links *i* and *j*



e)

Figure 2.6.e Five configurations between links *i* and *j*

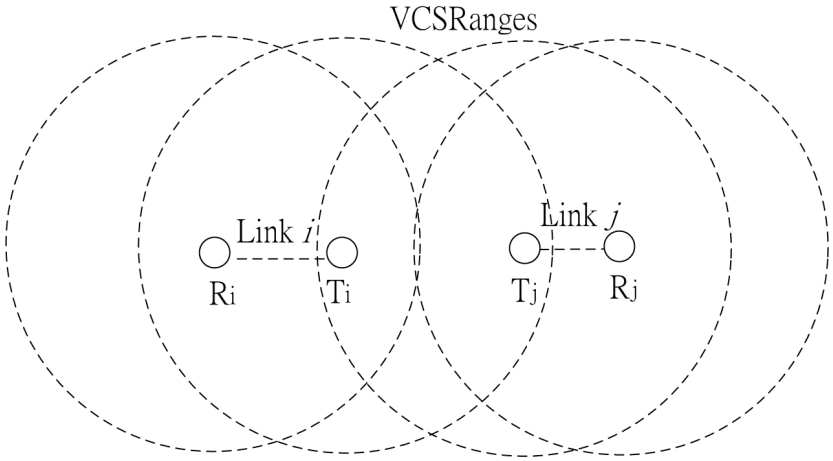


Figure 2.7. Case B's configuration with case 1's node arrangement

Configuration B: Simultaneous transmissions are permitted by the proposed protocol, but disallowed by the original 802.11 protocol. These are the scenarios in which the proposed protocol

increases the network capacities by assigning transmission channels to links arranged closely together for simultaneous transmissions.

Arrangement B.1: When T_i of link *i* receives the RTS_j but not the CTS_j of another link *j*, it will assign its RTS_i to the same channel as that of RTS_j. Thus, link $i_{T->R}$ can transmit simultaneously with $j_{T->R}$ because receiver R_j is located far enough away from the transmitter T_i and T_j is receiving CTS or ACK in another channel. Thus, there is no collision between link *i* and link *j*.

Arrangement B.2: If link *j* begins the transmissions before link *i*, T_i of link *i* receives the CTS_j but not the RTS_j of another link *j*, it will assign its RTS_i to the same channel as that of CTS_j. Link $i_{T->R}$ can then transmit simultaneously with $j_{R->T}$ because receiver T_j is located far enough away from the transmitter T_i and R_j is receiving RTS or DATA in another channel. Thus, link *i* and link *j* can transmit concurrently.

If link *i* begins the transmissions first, R_j of link *j* receives the RTS_i but not the CTS_i of link *i*, it will assign its CTS_j to the same channel as that of RTS_i and set the 'priority' field to 1 (by algorithm *iii*). However, T_j can not determine its transmission channel as it can not receive the RTS/CTS packets from link *i*. To solve this problem, T_j will randomly choose one of the two channels to transmit RTS_j to R_j (algorithm *ii*) with the priority field set to 0 (algorithm *iii*). If the randomly chosen channel for RTS_j is the same as the assigned channel for CTS_j, R_j will not reply CTS_j to T_j since the priority field of CTS_j is larger than that of RTS_j. T_j cannot receive CTS_j replied from R_j and will then choose another channel for sending RTS_j. This time, the channel for sending

RTS_j and the assigned CTS_j channel are different and R_j can reply a CTS_j back to T_j. Once T_j receive a CTS_j replied from R_j, it will keep using this channel assignment for transmissions.

Arrangement B.3: Similar to Arrangement 2 above. If link *i* begins the transmissions first, T_j of link *j* will assign its RTS_j to the same channel as that of CTS_i.On the other hand, if link *j* begins the transmissions before that of link *i*, T_i will randomly choose one of the two channels to transmit RTS to R_i with priority field set to 0.

Arrangement B.4: If link *i* begins the transmissions first, R_j of link *j* receives the CTS_i but not the RTS_i of link *i*, it will assign its CTS_j to the same channel as that of CTS_i and set the priority field to 1. However, T_j fails to determine its transmission channel as it can not receive the RTS/CTS packets from link *i*. T_j will randomly choose one of the two channels to transmit RTS to R_j with the priority field set to 0. R_j will not reply a CTS_j if the received RTS_j uses the same channel as the assigned channel for sending CTS_j. If there is no reply, T_j will choose another channel for retransmission. Once T_j receive a CTS replied from R_j, it will keep using this channel assignment for transmissions. Similar strategy applies to the arrangement that link *j* starts the transmissions before link *i*.

Configuration C: Simultaneous transmissions are not permitted by the proposed protocol. This configuration with node arrangement 3 or 4 can induce a hidden-node problem specific to the proposed protocol.

Arrangement C.1 and C.2: Both T_j and R_j are within the VCSRange of T_i. Suppose link *i* transmits first, link *j* (both T_j and R_j) will assign the RTS_j and CTS_j to the same channel (e.g. channel *s*) as that of RTS_i and both of them set their priority fields to 1. When T_j sends a RTS

packet to R_j in channel s, R_j will attempt to reply a CTS packet to T_j in another channel (e.g. channel t) as CTS_j has no priority over RTS_j due to the same value (1) of priority fields. If link *i* is not transmitting, R_j will then reply a CTS_j back to T_j. When T_i of link *i* captures both the RTS_j and CTS_j packets from link *j*, it will recognize that links *i* and *j* cannot transmit at the same time and they must take turns to transmit. After that, once T_i senses the signals from link *j*, it will pause its transmission process until the NAV of link *j* expires. Similar strategy applies to the arrangement that link *j* begins the transmissions first.

Arrangements C.3 and C.4: These scenarios induce hidden-node problems specific to the proposed protocol. Consider link *j* transmits first. R_i of link *i* receives both the RTS_j and CTS_j from link *j*, thus it realizes that links *i* and *j* must take turns to transmit. However, T_i which is outside the VCSRanges of link *j* does not recognize this and it may send RTS_i to R_i while link *j* is still transmitting. In this way, the RTS_i from T_i is corrupted because of collision from link *j* on link *i*. Thus, R_i cannot reply a CTS_i to T_i. T_i then times out and doubles its count-down window size for retransmissions. At the same time, link *j* transmits successfully and does not realize link *i* suffering from a collision. Link *j* keeps sending data and dominates the channel bandwidth from link *i* since link *j* is hidden from T_i. This hidden-node problem induces an unfairness problem. However, this does not degrade the achievable capacity as the protocol only permits one of the links *i* and *j* to transmit at one time. To achieve fair throughput allocation, a possible solution will be outlined in sub-section 2.2.2.

Configuration D: Simultaneous transmissions are prohibited by the proposed protocol.

Arrangements D.1 and D.3: T_j can hear both RTS_i and CTS_i. It realizes that links *i* and *j* have to take turns to transmit. Thus, when link *i* is transmitting, T_j will halt its transmission process and resume only after the NAV of link *i* expires.

Arrangement D.2 and D.4: R_j can hear both RTS_i and CTS_i. It recognizes that links *i* and *j* have to share the channel. However, T_j which can only sense the signals from T_i (Arrangement D.2) or R_i (Arrangement D.4) may send RTS_j to R_j. R_j will only reply a CTS_j to T_j when link *i* is not sending packets.

Arrangement E: Simultaneous transmissions are disallowed by the proposed protocol. Links *i* and *j* will fall back to the original 802.11 protocol and will resume transmissions only after the NAV from the other link ceases. In this arrangement, links *i* and *j* take turns to transmit.

2.2. Handling Collisions

In the original 802.11 protocol, if a transmitter can not receive the corresponding CTS/ACK replied from a receiver, it will declare a collision and double its contention window for re-transmissions. There are two possible cases for this to happen: A) contention window collisions between links which can not transmit simultaneously, and B) the hidden-node problem.

2.2.1. Contention Window Collisions

When two links which can not transmit simultaneously begin transmissions at the same time after counting down their contention windows, these two signals will collide at the receivers. However, as shown in [19], the binary exponential back-off algorithm of the 802.11 protocol is efficient in preventing such collisions between links. As long as the number of stations within a *VCSRange* is

less than or equal to 5, the average number of transmissions per packet is less than 1.2 [19]. In addition, both the original 802.11 protocol and the proposed protocol experience contention window collisions. This does not worsen the achievable network capacity when comparing the proposed protocol with the original 802.11 protocol.

2.2.2. Hidden-node Problem

The hidden-node problem in wireless networks has been studied extensively (e.g. [89][76][90]). Figure 2.8a shows a hidden-node scenario with the original 802.11 protocol. When node 3 sends a frame to node 4, node 2 senses the channel to be busy while node 1 senses the channel to be idle, since node 3 is inside the carrier-sensing range of node 2 but outside that of node 1. Once node 1 senses the channel as idle, it may count down its back-off contention window until zero and transmit a frame to node 2. If the transmission from node 4 is still in progress, node 2 will continue to sense the channel as busy, and it will not receive the frame from node 1. As a result, node 2 will not return an ACK to node 1. Node 1 may then time out and double the contention window size for retransmission later.

Meanwhile, node 3 transmits the frame successfully and is not aware of the collision at node 2. When transmitting the next frame, node 3 will use the minimum contention window size. The hidden-node scenario favours node 3, and the chance of collision at node 2 can not be reduced even though node 1 backs off before the next retry.

The RTS/CTS mechanism in 802.11 was designed with an attempt to solve the hidden node problem. However, using RTS/CTS in ad-hoc networks does not fully eliminate the hidden node problem [18]. The effectiveness of RTS/CTS mechanism is based on the assumption that transmissions by mutually hidden nodes are to a common receiver. Before the transmission of a hidden node begins, the receiver will forewarn other hidden nodes to prevent them from transmitting. This assumption may not hold in an ad-hoc network.

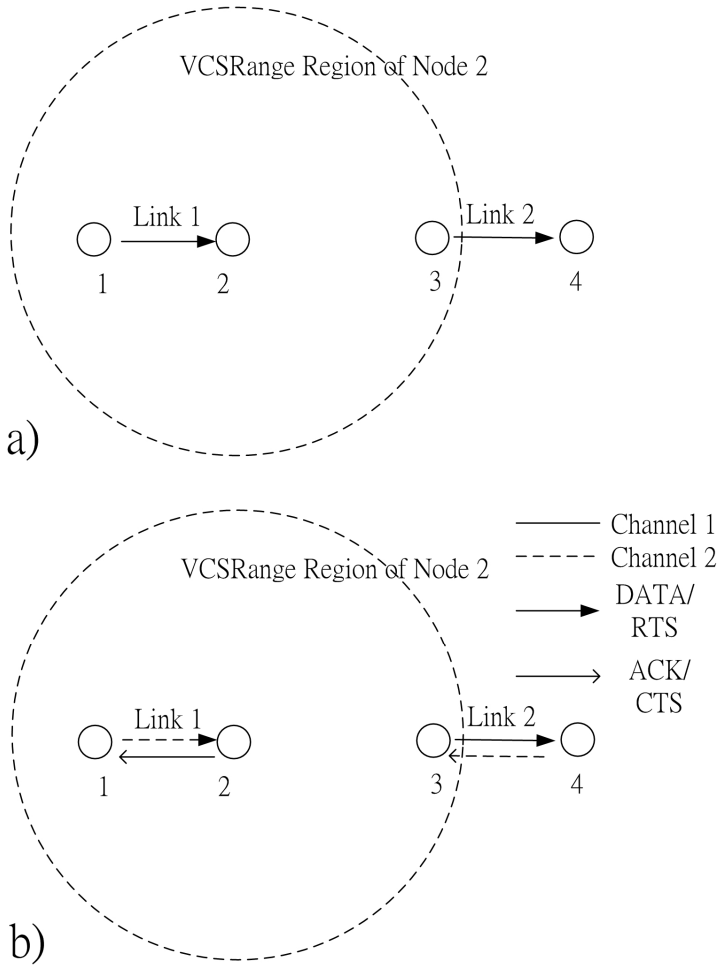


Figure 2.8. a) Hidden-node problem in orginial 802.11 protocol does not exist in b) the proposed MAC protocol

In the proposed MAC protocol, the above hidden-node scenario does not exist thanks to the channel assignment property of the protocol. If node 3 uses channel 2 to send RTS/DATA to node 4, node 1 will use channel 1 to transmit RTS/DATA to node 2 (as shown in Fig. 2.8b). Since the transmissions are in independent channels, both node 2 and node 4 can receive the signals successfully.

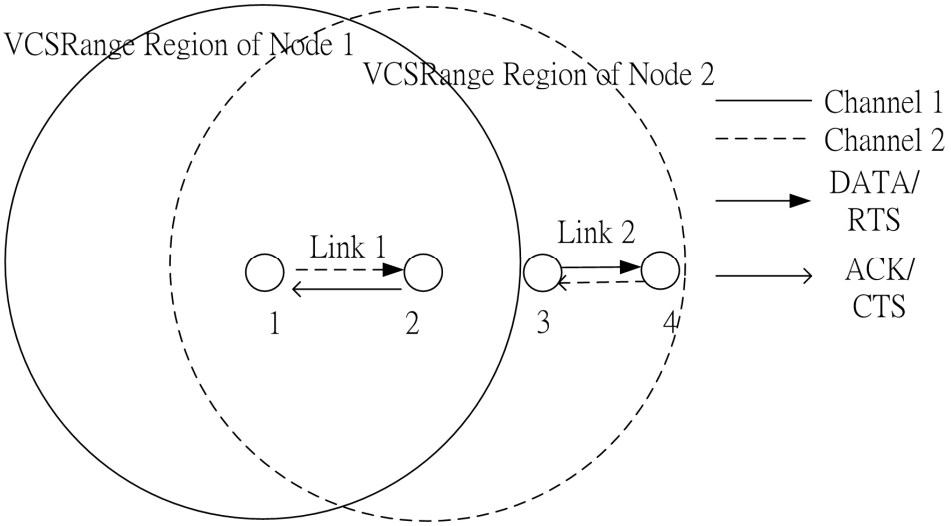


Figure 2.9. Hidden-node problem in the proposed protocol

Table III. System Parameters Assumed in Simulations of the proposed MAC Protocol [17]

Packet payload (*DATA*)	1460 bytes
UDP/IP header	20 bytes
MAC header	28 bytes
PHY header	24 bytes
ACK size	14 bytes
RTS size	20 bytes
CTS size	14 bytes
Data rate (DATA/ACK)	12 Mbps
Basic rate (RTS/CTS)	2 Mbps
PHY header bit rate	2 Mbps
Slot time σ	20 μs
SIFS	10 μs
DIFS	50 μs
$CW_{\min}$	31
$CW_{\max}$	1024
$CW_{average}$	310 μs
Retransmission Limit	7
Virtual Carrier-sensing Range (*VCSRange*)	550 m
Transmission Range (*TxRange*)	250 m
SIR Capture Threshold (*CPThreshold*)	10 dB

Beside the above scenario, there is a "hidden-node" scenario specific to the proposed protocol. Consider Fig. 2.9. Since nodes 3 and 4 are within the *VCSRange* of node 2, node 2 can receive both the RTS and CTS of link 2. Thus, links 1 and 2 must take turns to transmit. However, node 1 cannot receive the RTS and CTS from link 2 as nodes 3 and 4 are outside the *VCSRange* of node 1. In this

way, node 1 may send RTS to node 2. If the transmission of link 2 is still in progress, node 2 will not reply CTS to node 1. Thus, node 1 may time out and double its contention window for retransmission. This will induce an unfairness problem between links 1 and 2. From the protocol's point of view, only one of links 1 and 2 is allowed to transmit at each time. Although link 2 dominates most of the channel bandwidth, the overall capacity achieved by links 1 and 2 remains the same as allowed by the protocol.

Many solutions (e.g. [24] [100] [101]) have been proposed in the literature to solve the hidden-node problem. A possible solution for this unfairness problem is to use a so-called "re-start mode" chip set and extend the *VCSRange* to sufficiently large in order to cover all potential interfering nodes by the RTS/CTS mechanism. Reference [100] shows that the hidden-node problem of original 802.11 networks can be avoided when restart mode is enabled and the carrier-sensing range is sufficiently large. In particular, [100] proves two conditions that can guarantee a hidden-node-free operation in a general network: 1) restart mode and 2) a lower-bound requirement on the carrier-sensing range. With the "re-start mode", if the receiver is in the midst of receiving a signal, another signal with sufficiently large power margin arrives (say, 10dB stronger), the receiver will switch to receive the new signal. In Fig. 2.9, if the *VCSRange* is set to 700m and the transmission range (*TxRange*) is retained as 250m, node 4 will be at least 450m away from node 2. The signal from node 1 at node 2 will then be at least 10dB stronger than the signal from node 4. Thus, node 2 can always capture the frames from node 1 successfully [100].

In summary, both the original 802.11 protocol and the proposed protocol experience contention window collisions. Thus, this does not deteriorate the attainable network capacity when comparing the proposed protocol with the original 802.11 protocol. The hidden-node problem also does not worsen the overall network capacity but induces unfairness problems. References [100][24][101] have proposed some possible solutions for the hidden-node problem.

2.3. Simulation Results

The proposed MAC protocol has been implemented in the NS-2 [102] simulator which has been widely adopted in wireless ad-hoc network research (e.g. [24][13][46]). In Appendix A, the measurements of real-life experiments were compared with NS-2 simulation results. It indicated that NS-2 simulations do not contain major deficiencies. In Appendix B, an example will be provided to explain how the source codes of NS-2 are modified to implement the proposed protocol. For fair comparisons, settings of the original 802.11 protocol in NS-2 are used so that *VCSRange*=550m and *TxRange*=250m by assigning the data rate (for sending DATA/ACK) at 12Mbps (OFDM, QPSK) and the basic rate (for transmitting RTS/CTS) at 2Mbps (DSSS, DQPSK). Table III shows the system parameters assumed in the simulations. RTS frame size is 20 bytes [103] with 2 bytes for Frame Control, 2 bytes for Duration Field, 6 bytes for Receiver Address, 6 bytes for Transmitter Address, and 4 bytes for Frame Check Sequence. CTS frame size is 14 bytes [103] with 2 bytes for Frame Control, 2 bytes for Duration Field, 6 bytes for Receiver Address, and 4 bytes for Frame Check Sequence. All data sources are saturated UDP traffic stream with fixed packet size of 1460bytes. The throughput result is the average of three simulations with 300 seconds run time.

2.3.1. A Lattice Topology

Figure 2.10 shows twelve links in an 8x3 lattice topology. As shown in Fig. 2.12a), using the original single-channel 802.11 protocol results in 19.9Mbps total network throughput, thus the targeted capacity for using dual channels is by definition 19.9Mbps*2=39.8Mbps. With the proposed scheme, a total network throughput of 56.5Mbps is achieved, which is 142% of the targeted capacity. In other words, the proposed protocol improves the capacity to 2.83 times with respect to the single-channel 802.11 protocol. This shows the proposed protocol can double the network capacity by using only two channels.

Figure 2.10 also shows the channel assignments of links using the proposed protocol. Assume

node 11 uses channel 2 to transmit RTS/DATA to node 12. Since nodes 3, 10 and 19 are within the *VCSRange* of node 11, they can receive the RTS but not the CTS of link 6. Node 3, 10 and 19 then assign their transmission channels to channel 2. As they are far enough from node 12, nodes 3, 10, 11 and 19 can transmit simultaneously without interfering the reception of signals at node 12. However, when using the original 802.11 protocol, once link 6 is transmitting, links 2, 5 and 10 can not transmit because they can receive the CTS from node 11 of link 6. Any simultaneous transmissions from links 2, 5 and 10 will lead to collisions on link 6. The proposed protocol significantly increases the network capacity by allowing simultaneous transmissions.

2.3.2. An Irregular Topology

Figure 2.11 shows an irregular topology with channel assignments. The proposed scheme obtains total network throughput at 31.4Mbps, which is 106% of the targeted capacity (14.8Mbps*2=29.6Mbps). In other words, the protocol increases the capacity to 2.13 times when compared to the single-channel 802.11 protocol. Again, the proposed protocol doubles the network throughput. In addition to the capacity enhancement, the proposed protocol achieves a fairer bandwidth allocation in both the lattice and irregular topologies (as shown in Fig. 2.12).

2.3.3. Random Topologies

Figure 2.13 shows the total throughputs of random topologies with n links. In each random network, n single-hop links are randomly placed inside a 3000m x 3000m square. In all cases, as shown in Fig. 2.14, the capacity increases to more than 1.7 times that of the single-channel 802.11 protocol. The throughput improvements, however, are highly dependent on the network topologies. In the best case when $n=70$, the protocol increases the total network throughput to 2.04 times.

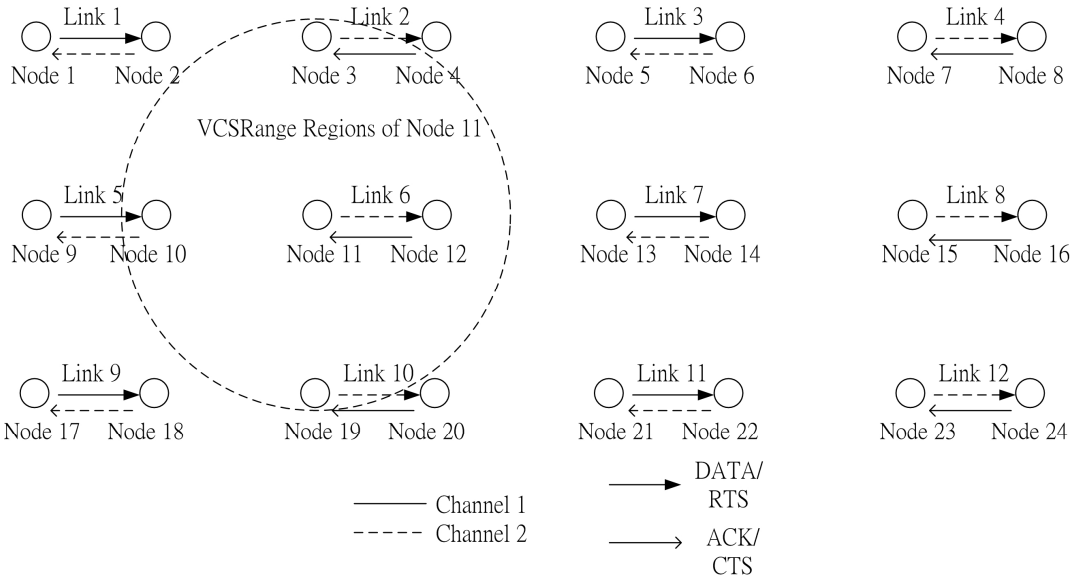


Figure 2.10. The proposed scheme increases the capacity to 2.83 times with respect to the single-channel 802.11 protocol in a lattice topology with twelve links

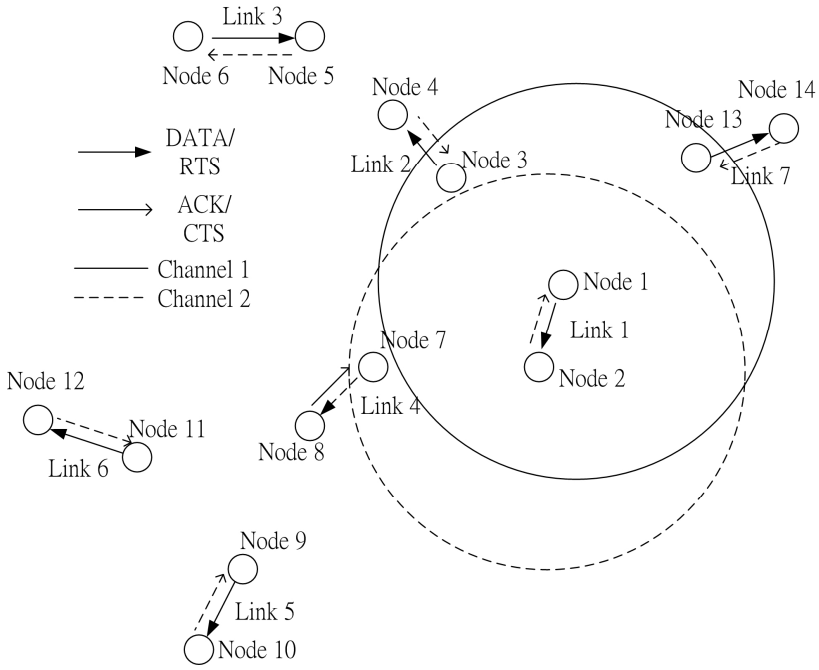
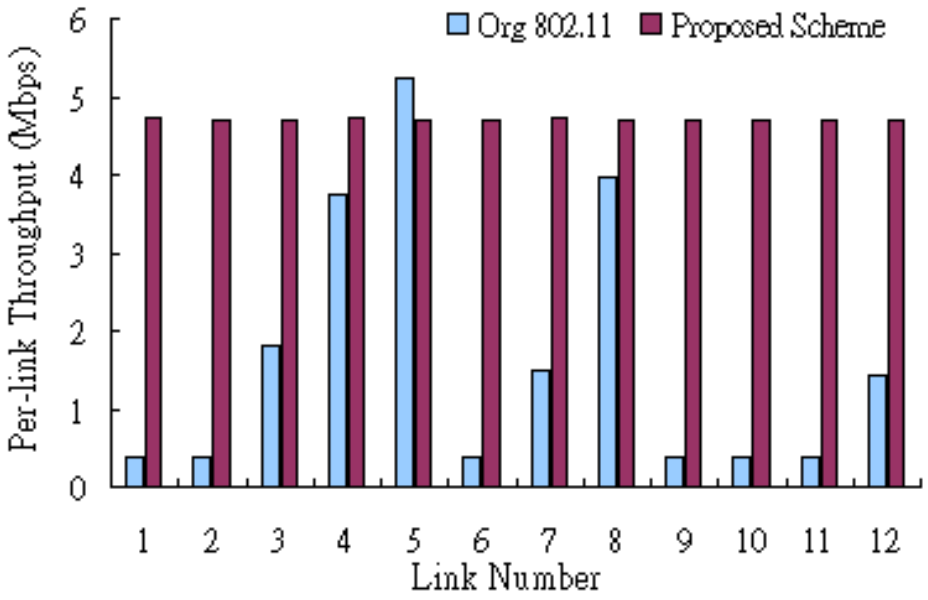
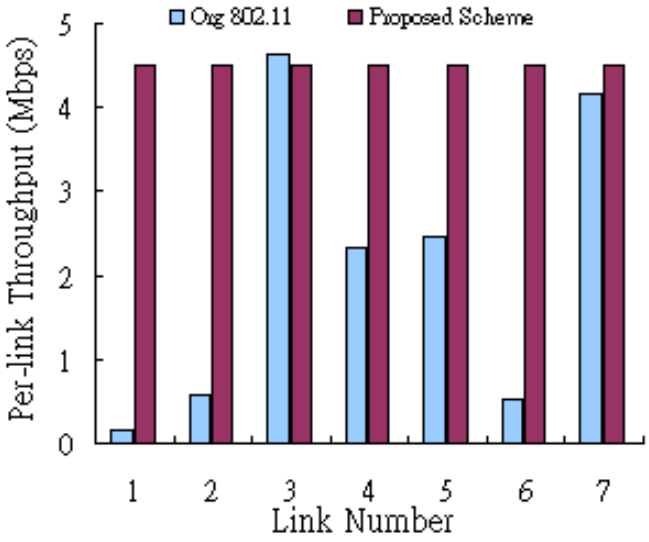


Figure 2.11. The proposed scheme increases the capacity to 2.13 times with respect to the single-channel 802.11 protocol in an irregular network topology



a)



b)

Figure 2.12. Simulated Per-link throughput of the networks of a) Fig. 2.10 and b) Fig. 2.11 with the original 802.11 protocol and the proposed MAC protocol

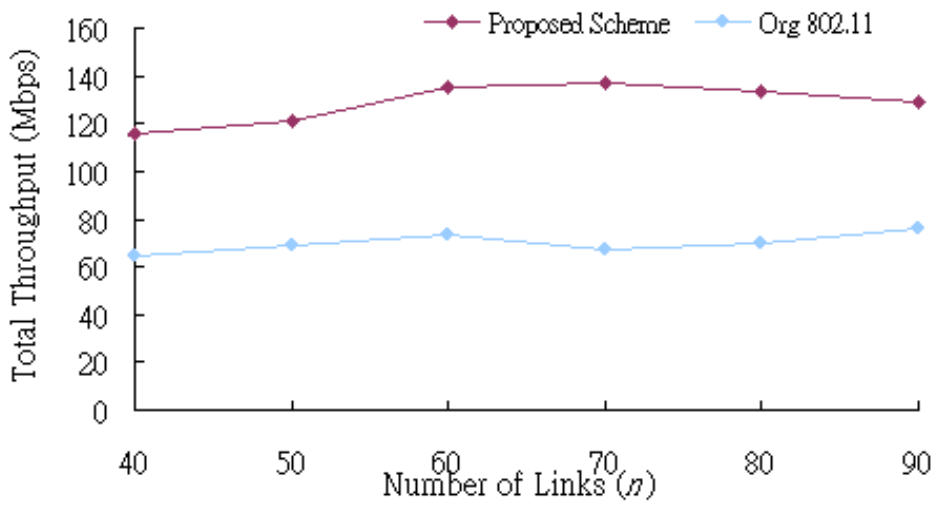


Figure 2.13. Simulated total throughputs of random networks with *n* single-hop links

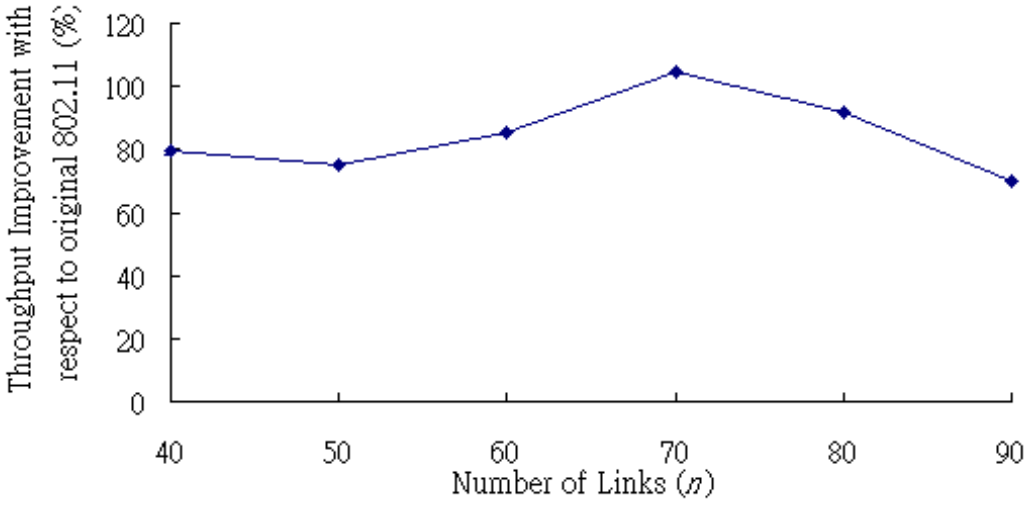


Figure 2.14. Percentage of net throughput enhancements by using the proposed dual-channel protocol with two wireless receivers with respect to the single-channel 802.11 protocol in random networks with *n* single-hop links

2.4. Conclusion

This chapter has presented an approach with the aim of doubling the network capacities of 802.11

ad-hoc networks by using a link-directionality-based dual channel MAC protocol (DCP). Simulations have showed that the proposed scheme can increase the network capacities of single channel 802.11 ad-hoc networks to 2.83 times in a lattice topology, 2.13 times in an irregular topology and more than 1.7 times in large-scale random network topologies with respect to the single-channel 802.11 protocol. The capacity improvements are achieved by splitting the transmission and reception channels of links. Nodes using the same reception channel can then be packed closer to each other since their transmissions are in another independent channel.

It is believed that this research is the first in the literature to explore the potentials of splitting channels based on link-directionalities and the proposed scheme can outperform other multi-channel protocols in terms of capacity per channel resource. However, there is room for further improvement by eliminating the limitations imposed by the carrier-sensing mechanism. Chapter 3 will give the details.

3. Further Improving Capacity by SIR Comparison Algorithm (SCA)

Chapter 2 has described the channel pairing process in the link-directionality-based dual channel protocol (DCP) which assigns transmission channels based on availabilities of receptions of request-to-send (RTS) and clear-to-send (CTS) packets. In other words, pair-wise simultaneous transmission links must have one of their two nodes outside the virtual carrier-sensing range (*VCSRanges*) of the nodes of the other link (see link A with link B or C in Fig. 3.1). In certain cases, however, this unnecessarily limits the chances for simultaneous transmissions, due to the so-called exposed node phenomenon. Consider two links again, link *i* and link *j*. Deriving from the equation (2.1), the interference range of link *j* can be defined as

$$InRange_j = (CPThreshold)^{1/\alpha} * d_{Tj-Rj}$$

$$= 1.78 * d_{Tj-Rj} \quad (3.1)$$

where the path loss exponent $\alpha = 4$ and SIR (signal-to-interference ratio) capture threshold $CPThreshold = 10dB$ since reference [68] reported that *CPthreshold* tends to hold at 10 dB until 24 Mbps in real-life experiments.

Simultaneous transmissions are actually permitted if a node of link *i* using the channel 1 (or 2) for transmissions is at a distance larger than $InRange_j$ from a node of link *j* using the same channel 1 (or 2) for receptions. For example, in Fig. 3.2, links A and B can transmit concurrently as T_B is more than $InRange_A$ away from R_A. From equation (3.1), *InRange* varies with the distance between two nodes of a link. The closer the distance between T_j and R_j (d_{Tj-Rj}), the smaller is the $InRange_j$. Simultaneous transmission links can then be packed closer to each other. This can drastically improve the network capacities, particularly when d_{Tj-Rj} is small.

Consider Fig. 3.2 again. Assuming T_A uses channel 1 to transmit RTS and DATA to R_A while R_A uses another independent channel 2 to send CTS and ACK back to T_A. Since T_B is outside the

interference range of link A ($InRange_A$), it can also transmit RTS and DATA via channel 1. This does not affect the receptions of signals of R_A from T_A because the signal from T_A at R_A is more than 10dB stronger than the signal from T_B. In addition, R_B uses another independent channel (channel 2) for transmissions which do not interfere with the signal receptions of R_A. Therefore, links A and B can transmit at the same time.

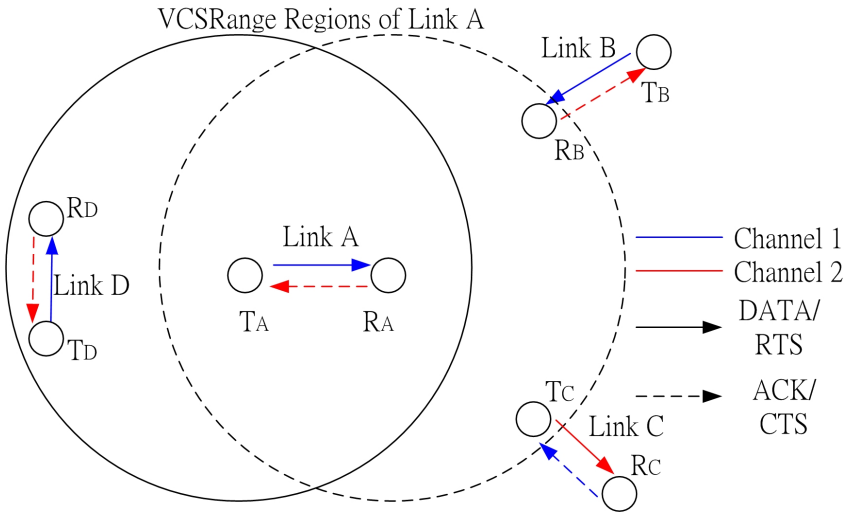


Figure 3.1. A network topology with transmission channels assigned by DCP

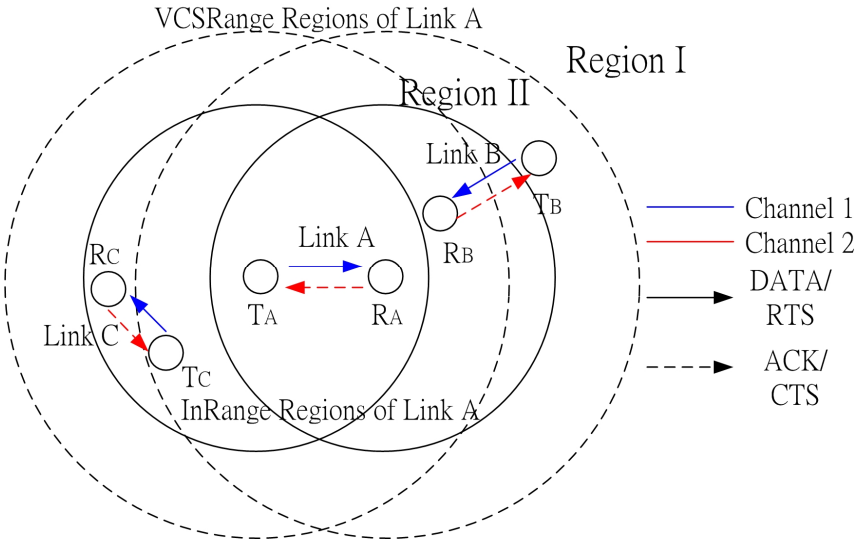


Figure 3.2. Closer configuration of simultaneous transmissions of links A, B and C are allowed after adopting SCA in DCP.

Comparing link B in Fig. 3.1 and Fig. 3.2, simultaneous transmission links (links A and B) can now be packed closer to each other. This can significantly improve the network capacity. The protocol, however, can no longer assign transmission channels based on availabilities of receptions of RTS and CTS packets as both nodes T_B and R_B can now receive the CTS packets from node R_A. To solve this problem, an SIR comparison algorithm is implemented on top of DCP to identify possible simultaneous transmission opportunities within *VCSRanges*.

3.1.1. DCP with signal-to-interference ratio SIR comparison algorithm (DCPwSCA)

This sub-section describes the signal-to-interference ratio SIR comparison algorithm (SCA) for releasing the protocol constraints of the link-directionality-based dual channel protocol (DCP). To realize the concept mentioned in the previous sub-section, nodes seek simultaneous transmission opportunities based on the information included in the packets received from other links. As shown in Fig. 3.2, the regions for simultaneous transmissions are divided into two parts:

Region I: A node of link *j* using channel 1 (or 2) for transmission is more than *VCSRange* away from a node of link *i* using channel 1 (or 2) for reception. (see Chapter 2)

Region II: A node of link *j* using channel 1 (or 2) for transmission is more than *InRange* but less than *VCSRange* away from a node of link *i* using channel 1 (or 2) for reception.

For region I, DCPwSCA follows the DCP and keeps using the availabilities of receptions of RTS and CTS packets to decide channel assignments. The reader is referred to Chapter 2 for details.

For region II, the SIR comparison algorithm (SCA) is introduced to assign channels based on the information included in the packets received from other links. The DCPwSCA first utilizes the information from the SIR comparison algorithm to look for simultaneous transmission opportunities (for region II). In the case that one of the two nodes of a link is located at region I (outside the

VCSRange of another link) such that RTS/CTS packets can not be received, the DCPwSCA will then fall back to use the availabilities of receptions of RTS and CTS packets to select channels. To assign channels for simultaneous transmissions in regions I and II, DCPwSCA requires three algorithms: i) the SIR comparison algorithm; ii) randomly chosen transmission channels; and iii) adding a priority field. Algorithms ii) and iii) are inherited and modified from DCP in Chapter 2.

i. SIR comparison algorithm (SCA)

The main purpose of the signal-to-interference ratio comparison algorithm (SCA) is to assign channels for nodes located within *VCSRanges* but outside *InRanges* of nodes of other links. The proposed algorithm inserts the signal strength and interference level information of the received packet (RTS/CTS) obtained from the measurements of wireless transceivers in the MAC header of the replied packets (CTS/DATA). Nearby nodes can then extract the signal strength and interference level information attached with the MAC header (as shown in Fig. 3.3) to decide their corresponding transmission channels.

In a network topology with a pair of links (link *i* and link *j*), one of their nodes is within the region II of the other link. When R_i (T_i) of link *i* receives an RTS (CTS) packet from T_i (R_i), it records the signal strength $S_{Ti->Ri}$ ($S_{Ri->Ti}$) and interference level $I_{Ti->Ri}$ ($I_{Ri->Ti}$) of the packet received and add an additional header in its MAC header of the replied CTS (DATA) packet. Notice that here the conditions within the brackets in this sub-session represent the scenario when the transmitter T_i and the receiver R_i of link *i* swap their roles during in the reception of ACK/CTS, where T_i becomes the receiver and R_i becomes the transmitter. When other nodes (e.g. T_j) receive the CTS (DATA) packet, they will extract the signal strength $S_{Ti->Ri}$ ($S_{Ri->Ti}$) and interference level $I_{Ti->Ri}$ ($I_{Ri->Ti}$) information from the MAC header. In addition, they will record the receive power $Power_{Ri->Tj}$ ($Power_{Ti->Tj}$) of the CTS (DATA) packet received. Owing to the reciprocal nature of the

wireless radio link, $Power_{Tj->Ri} \approx Power_{Ri->Tj}$ ($Power_{Tj->Ti} \approx Power_{Ti->Tj}$). The algorithm then compares $Power_{Tj->Ri}$ ($Power_{Tj->Ti}$) with $S_{Ti->Ri}$ ($S_{Ri->Ti}$) and $I_{Ti->Ri}$ ($I_{Ri->Ti}$). If $S_{Ti->Ri}/(I_{Ti->Ri} + Power_{Tj->Ri}) > CPThreshold$ ($S_{Ri-Ti}/(I_{Ri-Ti} + Power_{Tj->Ti}) > CPThreshold$), simultaneous transmissions are allowed and the protocol will then assign the same transmission channel to T_j.

The SCA also inherits two algorithms from DCP as the following:

ii. Randomly Assigned Transmission Channels

When a transmitter of a link is allowed by the protocol to choose either one of the two channels for simultaneous transmissions, it will randomly pick one of the two channels for sending RTS to the receiver of the link. If it can receive the CTS replied from the receiver, it will keep using that channel for forthcoming transmissions. Otherwise, it will swap to another channel for retransmissions. This algorithm allows the transmitter to identify the suitable transmission channel for the receiver.

iii. Adding a Priority Field

A priority field is recorded in each node and is added to the MAC header of RTS packet. If the protocol allows a node to use either one of the two channels for simultaneous transmissions (by algorithm i), it will set the priority field to 0. Otherwise, if only one channel is permitted, the field will be assigned as 1. This gives nodes with priority fields set to be 1 to have a higher priority to choose channels than nodes with the field assigned as 0.

3.1.2. Overheads of DCPwSCA

Comparing the DCPwSCA with the DCP, additional header overheads are incurred since DCPwSCA includes the signal strength and interference level of received packets (by algorithm i) and the priority field in the headers of replied packets (by algorithm iii). Figure 3.3 shows the modified structures of DATA, CTS and RTS packets. The size of the signal strength and interference

level header (1byte) and the priority field (1bit) in packets, however, are much smaller than the size of physical header (24bytes), MAC header (28bytes) and DATA(0-2312bytes) /CTS (14bytes)/RTS (20bytes). The header overheads add 9 bits to the original 224 bits MAC header. If DATA is set to be 1460 bytes with an11Mbps data rate and a 2Mbps basic rate for transmitting MAC and PHY headers, the additional 9 bits overheads will only cause 0.4% throughput degradation in a single link scenario. In contrast, a closer packing of simultaneous transmissions allowed by the DCPwSCA protocol significantly overrides this penalty.

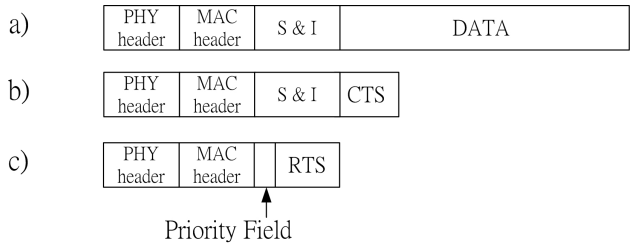


Figure 3.3. Signal strength and interference level is added to the headers of a)DATA and b)CTS packets while a priority field is added to c)RTS packets

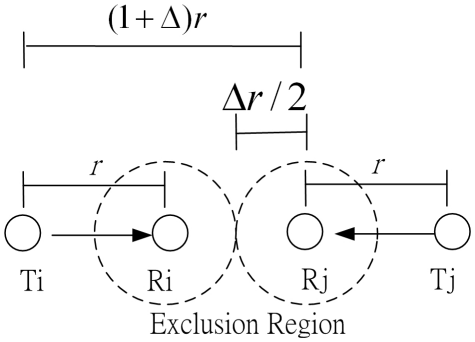


Figure 3.4. Exclusion regions of a pair of simultaneous-transmission links.

3.2. Analysis of Capacity Improvement

This sub-section analyzes the capacity enhancements of DCP, SCA and DCPwSCA. It first considers the upper bound on throughput capacity of random wireless networks defined by the

seminal work of Kumar [94][104]. Second, the maximum achievable capacity of ad-hoc network using the original 802.11 protocol is considered. It then calculates the upper capacity bounds of DCP, SCA and DCPwSCA in the same given network area. Finally, the capacity improvements are compared. Given a network with an area *S*. The upper capacity bound is the maximum number of simultaneous transmission links that can be packed in area *S.*

3.2.1. Optimal Upper Bound on Throughput Capacity of Random Networks

To calculate the upper bound on throughput capacity, the key is to identify the exclusion region consumed by each transmission link. In reference [104], an exclusion region is an area associated with an active receiver that must remain disjoint from the exclusion region of every other active receiver in the network. This concept of exclusion region can also be used to bound the capacities of networks using the original 802.11, DCP, SCA and DCPwSCA protocols. For general wireless networks, reference [94] showed that the exclusion region of a transmission link is a circular area of radius $\frac{\Delta r_i}{2}$ centered at the receiver, where r_i is the transmitter-receiver distance of a link *i* and $\Delta > 0$ is related to a power margin. Figure 3.4 shows an example with a pair of links and their exclusion regions. If the exclusion region of link *i* is disjoint with the exclusion region of link j, simultaneous transmissions of links *i* and *j* are allowed. For simplicity, consider the case where all links have the same transmitter-receiver length r in a network with area S with the link data rate *W*. The average area of exclusion region of a link, *E*,

$$E = \frac{\pi \Delta^2 r^2}{4}. \tag{3.2}$$

The optimal upper bound of throughput capacity of a random network in area *S* then becomes,

$$C = W \frac{S}{E}$$

$$= W \frac{4S}{\pi \Delta^2 r^2}. \quad (3.3)$$

Note that here this theoretical capacity bound is for general wireless networks with mono-directional traffic. In 802.11, each DATA transmission is followed by an ACK in the reverse direction, and this has not been taken into account in the original exclusion as defined in [104]. In addition, the existence of the carrier sensing mechanism as a protocol constraint has also not been taken into account. In the following sub-sections, the exclusion region concept will be extended for 802.11 networks.

3.2.2. Upper Capacity Bound of Original 802.11 Protocol

To calculate the upper capacity bound of network using the original 802.11 protocol, the key, again, is to identify the exclusion region consumed by each link. Figure 3.5 shows a pair of links that can transmit simultaneously. Node R_i and R_j of links *i* and *j* are located just outside the *VCSRanges* of the other link. R_i and R_j cannot sense the signals from each other and thus they can transmit at the same time. In the original 802.11 protocol, R_i and R_j have to reply ACKs back to the transmitters, T_i and T_j. When ACK is transmitting, R_i (R_j) becomes a transmitter while T_i (T_j) becomes a receiver. This bi-directional traffic of the original 802.11 protocol further enlarges the exclusion region consumed by each link. As shown in Fig. 3.5, the exclusion region can be defined as two disks of radius $\frac{v}{2}$ centered at two nodes of a link, where v is the virtual carrier-sensing range (*VCSRange*). Once the exclusion regions of links are disjoint, simultaneous transmissions are permitted by the protocol. To calculate the area of the exclusion region of a link, first the angle θ_{org} as shown in Fig. 3.5 is derived in term of r and v. Following the similar analysis as shown in [18],

$$\cos(\frac{\theta_{org}}{2}) = \frac{r}{2(v/2)}$$

$$\cos(\frac{\theta_{org}}{2}) = \frac{r}{v}$$

$$\theta_{org} = 2\cos^{-1}(\frac{r}{v}). \tag{3.4}$$

Thus, the area of exclusion region of a link using the original 802.11 protocol, E_{org}, is

$$E_{org} = \frac{\pi v^2}{2} - (\frac{v^2}{4}\theta_{org} - r \cdot \frac{v}{2} \cdot \sin\frac{\theta_{org}}{2}). \tag{3.5}$$

The upper bound of throughput capacity then becomes,

$$C_{org} = W\frac{S}{E_{org}}. \tag{3.6}$$

Thus, C_{org} depends on both the *VCSRange* (v) and the transmitter-receiver distance (r). In later parts of this sub-section, C_{org} is used to compare the capacity improvements obtained by DCP, SCA and DCPwSCA protocols.

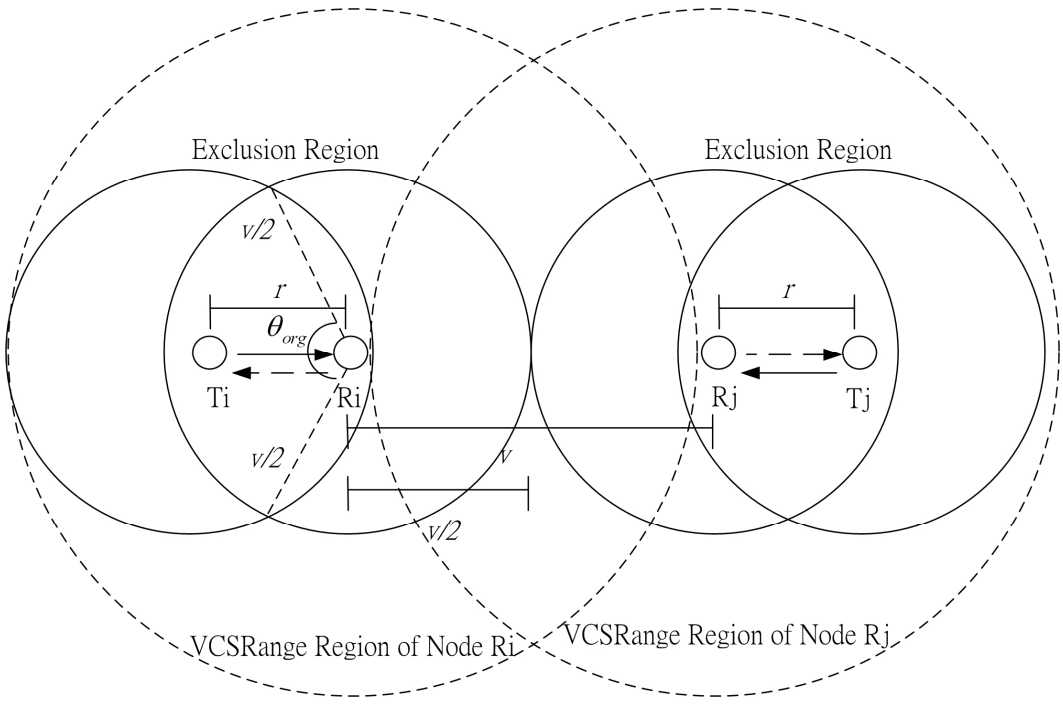


Figure 3.5. Exclusion regions of a pair of simultaneous-transmission links using the original 802.11 protocol.

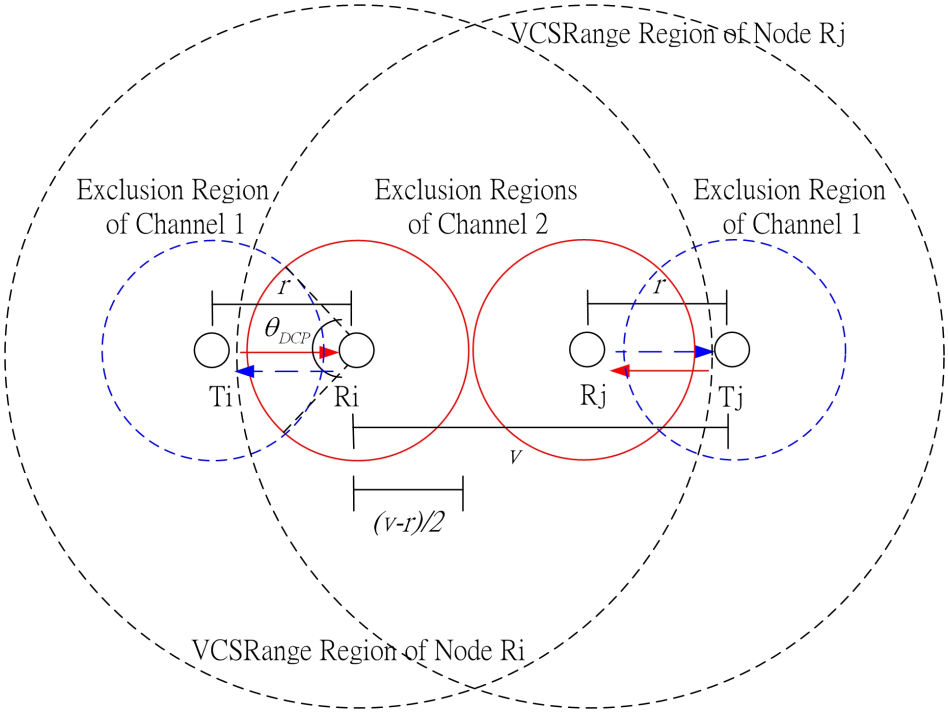


Figure 3.6. Exclusion regions of a pair of simultaneous transmission links using the DCP.

3.2.3. Upper Capacity Bound of Link-directionality-based Dual Channel MAC Protocol (DCP)

In DCP, simultaneous transmissions are allowed if one of the two nodes of link *j* is outside the *VCSRange* of either the transmitter or the receiver of link *i*. Figure 3.6 shows an example. Since node T_i (T_j) of link *i* (*j*) is outside the *VCSRange* of R_j (R_i), links *i* and *j* can transmit at the same time. When links *i* and *j* are packed with the closest distance, the distance between R_i and R_j becomes $v-r$. Since the transmitter and the receiver of a link use different channels for receptions, the exclusion region of each channel of a link is a circular disk of radius $\frac{v-r}{2}$ centered at the receiver of each channel of the link. The area of exclusion region of each channel of a link using DCP, E_{DCP}, is

$$E_{DCP} = \frac{\pi(v-r)^2}{4}. \tag{3.7}$$

DCP uses two channels for bi-directional traffic, RTS/DATA in one channel and CTS/ACK in

another. For fair comparisons, the upper bound of throughput capacity per channel then becomes,

$$C_{DCP} = \frac{W}{2} \cdot \frac{S}{E_{DCP}} = W \frac{2S}{\pi (v - r)^2}. \tag{3.8}$$

As a result, C_{DCP} can then be expressed in term of *v* and *r*.

3.2.4. Upper Capacity Bound of DCP with SIR Comparison Algorithm (DCPwSCA)

In the proposed protocol (DCPwSCA), link *i* can transmit successfully if one of the two nodes of link *j* is outside the interference range (*InRange*) of link *i*. As defined in [94], the interference range of link *i*,

$$InRange_i = (1 + \Delta) r_i. \tag{3.9}$$

Figure 3.7 shows an example when links *i* and *j* are packed with the closest distance. Since node $T_i (T_j)$ of link *i* (*j*) is outside the *InRange* of $R_j (R_i)$, links *i* and *j* can transmit concurrently. The distance between R_i and R_j equals to Δr. Thus, the exclusion region of each channel of a link is a circular disk of radius $\frac{\Delta r}{2}$ centered at the receiver of each channel of the link. The area of exclusion region of each channel of a link using DCPwSCA, $E_{DCPwSCA}$, is

$$E_{DCPwSCA} = \frac{\pi \Delta^2 r^2}{4}. \tag{3.10}$$

Due to the bi-directional traffic of each link, the upper bound of throughput capacity per channel then becomes,

$$C_{DCPwSCA} = \frac{W}{2} \cdot \frac{S}{E_{DCPwSCA}} = W \frac{2S}{\pi \Delta^2 r^2}. \tag{3.11}$$

Thus, $C_{DCPwSCA}$ only depends on the transmitter-receiver distance of a link (*r*) and is independent of the *VCSRange* (*v*). Note that the total number of nodes in the network is $n = 2 \cdot \frac{S}{E_{DCPwSCA}}$. Thus, the

upper capacity bound can be expressed from equation (3.11) as $O(Wn)$ which matches with the upper capacity bound $O(Wn\frac{m}{c})$ derived in reference [69] since the number of wireless interfaces per node $m=2$ and the number of channels $c=2$ in the DCPwSCA protocol.

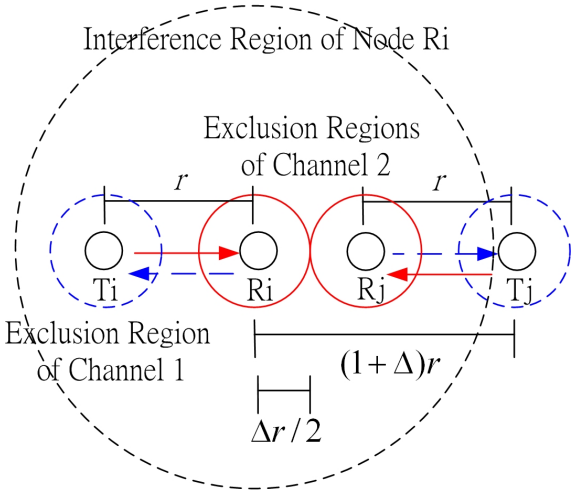


Figure 3.7. Exclusion regions of a pair of simultaneous transmission links using the DCPwSCA.

3.2.5. Upper Capacity Bound of SIR Comparison Algorithm (SCA) only (without DCP)

For comparing the capacity enhancements obtained by splitting channels based on link-directionalities (DCP) and adopting the SIR comparison algorithm (SCA) in the protocol, here the exclusion region of a single-channel protocol with SCA (without DCP) is also derived. Since only one channel is used by the protocol, simultaneous transmissions of links i and j are permitted only if R_i and T_i are outside the interference range (*InRange*) of R_j and T_j. Thus, the exclusion region of each link becomes two disks of radius $\frac{(1+\Delta)r}{2}$ centered at two nodes of the link. Using the similar approach as equation (3.4),

$$\theta_{SCA} = 2\cos^{-1}(\frac{1}{1+\Delta}). \tag{3.12}$$

The area of exclusion region of a link using SCA, E_{SCA}, is

$$E_{SCA} = \frac{\pi(1+\Delta)^2 r^2}{2} - (\frac{(1+\Delta)^2 r^2}{4}\theta_{SCA} - r \cdot \frac{(1+\Delta)r}{2} \cdot \sin\frac{\theta_{SCA}}{2}) \tag{3.13}$$

and the upper bound of capacity then becomes,

$$C_{SCA} = W\frac{S}{E_{SCA}}. \tag{3.14}$$

As a result, C_{SCA} can then be expressed in term of r and is independent of v.

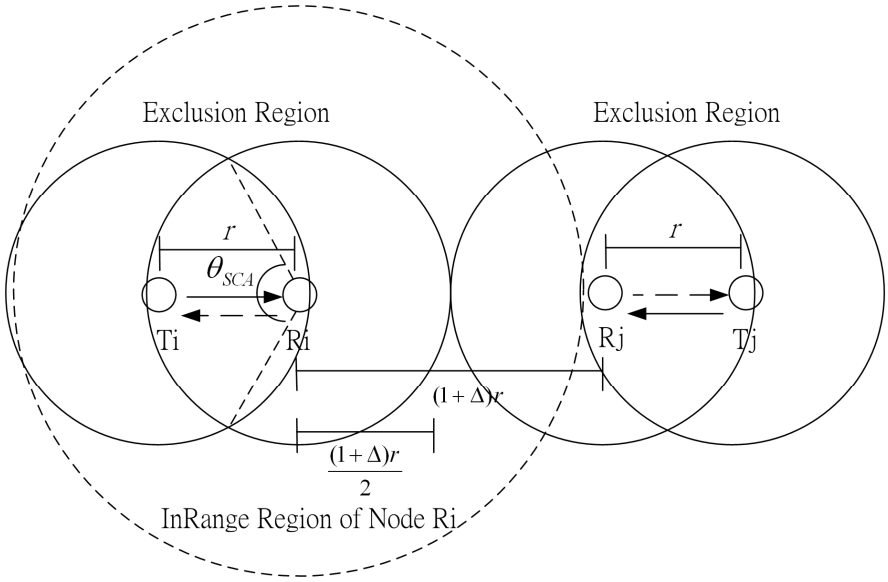


Figure 3.8. Exclusion regions of a pair of simultaneous transmission links using the SCA only (without DCP).

3.2.6. Comparisons

In summary, the areas of exclusion region of link using the original 802.11 protocol and DCP depend on the *VCSRange* (v) and the transmitter-receiver distance (r) while those links using DCPwSCA and SCA are determined only by r and are independent of v. The capacity improvement of DCPwSCA by comparing with the original 802.11 protocol is

$$I_{DCPwSCA}(r) = \frac{C_{DCPwSCA}(r)}{C_{org}(r)} = \frac{2 \cdot E_{org}}{\pi\Delta^2 r^2}. \tag{3.15}$$

Using the mean value theorem for integrals, the average capacity improvement is

$$I_{DCPwPEA} = \frac{1}{r_{\max} - r_{\min}} \int_{r_\min}^{r_\max} \frac{2 \cdot E_{org}(r)}{\pi \Delta^2 r^2} dr . \tag{3.16}$$

Consider the maximum transmitter-receiver distance (*r_max*) be 250m and the minimum (*r_min*) be 150m, the average capacity increases to 4.4 times with respect to the single-channel 802.11 protocol. This significantly multiplies the network capacities by using two channels. The capacity improvements are obtained by two factors:

1) permitting closer packing of simultaneous transmissions by splitting reception channels of nodes of each link. (by DCP)

2) releasing the protocol constraints induced by the virtual carrier-sensing mechanism. (by SCA)

For 1), DCPwSCA separates the transmission and reception channels of a node. This allows nodes using the same reception channel to be packed closer to each other since their transmissions use another independent channel which does not interfere with the receptions of the other link.

For 2), both the 802.11 and DCP relay on their carrier-sensing conditions to justify their transmission processes. DCPwSCA, on the other hand, bases on its SIR comparison algorithm (SCA) instead of the virtual carrier-sensing mechanism to seek simultaneous transmission opportunities. This, again, allows simultaneous transmissions to be packed closer to each other with inter-link distances less than *VCSRange.*

Figure 3.9 plots the capacity improvements obtained by DCPwSCA ($I_{DCPwPEA}(r)$), DCP ($I_{DCP}(r)$) and SCA ($I_{PEA}(r)$) when comparing with the original 802.11 protocol versus transmitter-receiver distances (*r*). The curves of DCP and SCA intercept when $r = 210$. When $r \geq 210$, the benefit of DCP (factor 1) plays a more important role than that of SCA (factor 2) in term of capacity improvement. When r increases, the advantage of SCA diminishes since the size of the *InRange* of a link expenses and gets closer to the size of *VCSRange*. This reduces the benefit obtained by releasing the protocol constraints induced by the virtual carrier-sensing mechanism. On the other

hand, when r increases, the area of exclusion region of DCP (E_{DCP}) decreases as shown in equation (3.7) and thus links can be packed closer to each other. This reduces inter-link distances and makes factor 1 the dominating factor for capacity improvements.

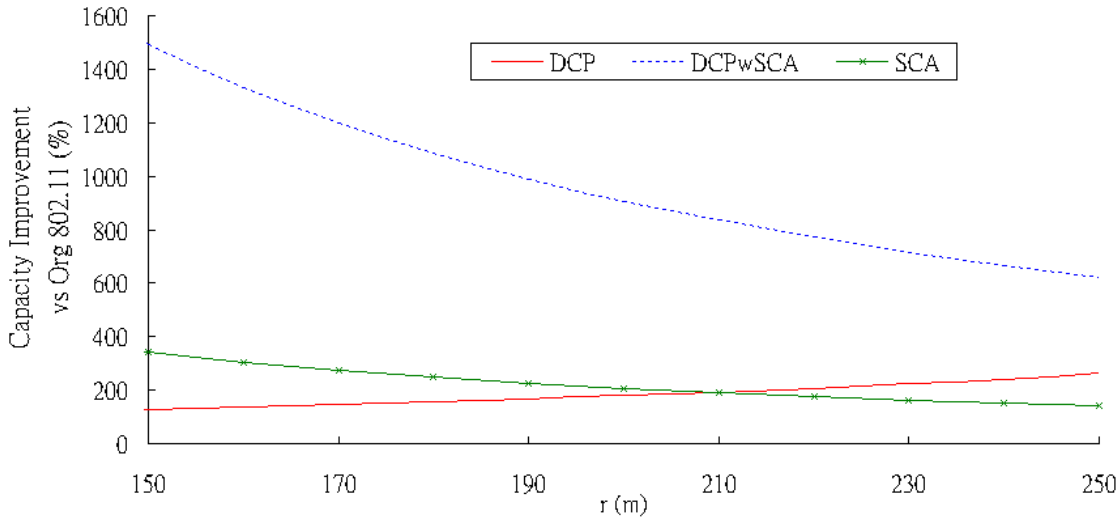


Figure 3.9. Theortical capacity improvements $I_{DCPwSCA}(r) = C_{DCPwSCA}(r)/C_{org}(r)$, $I_{DCP}(r) = C_{DCP}(r)/C_{org}(r)$, and $I_{SCA}(r) = C_{SCA}(r)/C_{org}(r)$ of protocols against the original 802.11 protocol verus the transmitter-receiver distance (r)

When $r \le 210$, the area of exclusion region, on the other hand, increases when the transmitter-receiver distance (r) decreases and thus the advantage of factor 1 diminishes. However, since the *InRange* decreases with r (see equation (3.9)), factor 2 overrides factor 1 by permitting closer link packing and becomes the prominent factor for capacity improvements.

DCPwSCA integrates the benefits of DCP (factor 1) and SCA (factor 2) in long-range ($r \ge 210$) and short-range ($r \le 210$) transmitter-receiver distance r. This significantly reduces the exclusion region $E_{DCPwPEA}$ and increases capacities. Theoretically, Fig. 3.9 shows the capacity can be increased from 6.2 to 14.9 times of that of the original 802.11 protocol when r is between 150 to 250m. In next sub-section, the capacity improvements obtained by simulations in lattice and random network

topologies will be shown.

3.3. Simulation Results

The proposed MAC protocol (DCPwSCA) has been implemented in the NS-2 [102] simulator. The *VCSRange* and *TxRange* are set to be 550m and 250m respectively. The system parameters assumed in the simulations are the same as listed in Table III. All data sources are saturated UDP traffic stream with fixed packet size of 1460bytes. The simulation results are the average of three simulations with 300 seconds run time. Real-life experimental work in Appendix A has shown that the NS-2 simulator does not contain major deficiencies.

3.3.1. Lattice Topologies

Figure 3.10 shows the capacity improvements obtained by DCPwSCA in lattice topologies. Single-hop links with transmitter-receiver distance *r* are packed as many as possible in a 2000m x 2000m square. The inter-link distance is set to be $2.6 * r$. When $r = 50$, DCPwSCA improves the network capacity of the original 802.11 protocol drastically to 10.6 times. In the worst case, when $r = 200$, the improvement is 2.2 times. On average, the capacities are multiplied to 4.3 times.

3.3.2. Random Topologies

In each random network, ninety single-hop links with transmitter-receiver distance *r* are randomly placed inside a 3000m x 3000m square. The entire topology of each link-length simulation is randomly re-generated. On average, the capacities increase to 2.1 times that of the single-channel 802.11 protocol. The lowest improvement is 1.6 times when $r = 250$ and the highest is 3.1 times when $r = 50$.

3.3.3. Multi-hop Topologies

In this case, a lattice topology of three 7-hop chains is generated. The nodes in a chain are separated by 250m while inter-chain distance is 500m. Simulations show that the total throughput of DCPwSCA is 3.9Mbps while that of the original 802.11 protocol is 1.9Mbps. The capacity is improved to 2.1 times when compared to the single-channel 802.11 protocol..

Simulations show that DCPwSCA can significantly multiply the network capacities in lattice, random, and multi-hop topologies. The protocol can out-perform other dual-channel schemes (e.g. [105]) previously proposed in the literature.

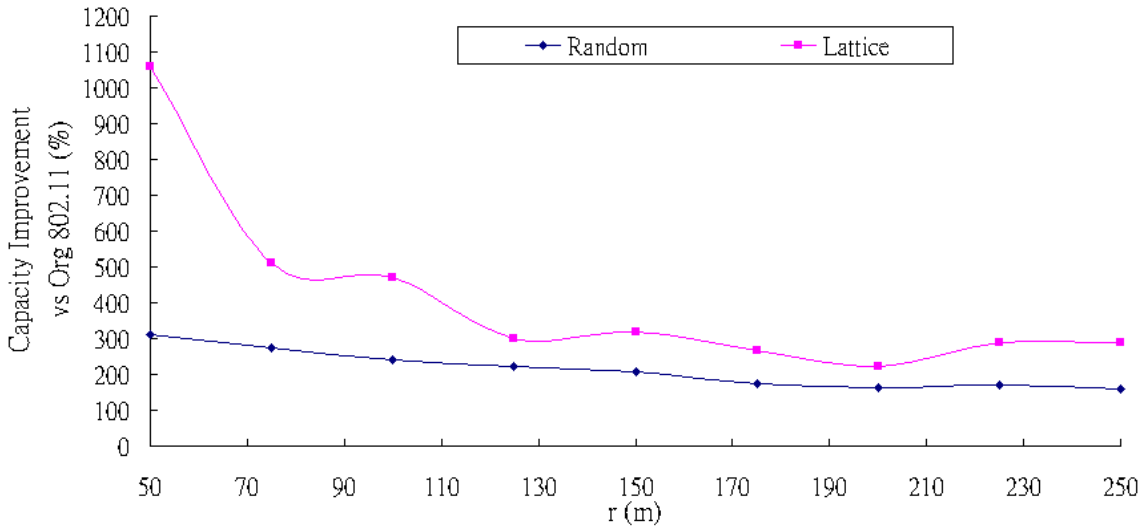


Figure 3.10. Simulation results of capacity improvements $I_{DCPwSCA}(r) = C_{DCPwSCA}(r) / C_{org}(r)$ of DCPwSCA with respect to the single-channel 802.11 protocol against the transmitter-receiver distance (r) in lattice and random topologies

3.4. Conclusion

This chapter has described an attempt to increase network capacities of IEEE 802.11 ad-hoc networks by two channels. The scheme presented (DCPwSCA) integrates two algorithms to increase network throughputs: 1) the dual channel link-directionality-based MAC protocol (DCP) in Chapter

2, and 2) the signal-to-interference ratio SIR comparison algorithm (SCA).

For 1), the transmission and reception channels of a node are split so that transmissions in one channel do not interfere with receptions in another non-overlapping channel. This allows more compact packing of nodes using the same reception channel.

For 2), the protocol constraints imposed by the virtual carrier-sensing mechanism are released. Links can then decide their transmission processes based on the physical interference constraints instead of the receptions of RTS/CTS packets as in the original 802.11 protocol.

The performance improvements achieved by algorithms 1) and 2) have been studied. Algorithm 1) outperforms algorithm 2) in long intra-link distances while 2) outweighs 1) in short intra-link distances. Interesting, integrating these two algorithms allows the protocol to compensate the downside of each other. Simulations have shown that the integrated approach of these two algorithm can increase the network capacities of single-channel IEEE 802.11 ad-hoc networks to 4.3 times in lattice and 2.13 times in random topologies with respect to the single-channel 802.11 protocol. The proposed algorithms can significantly increase the network capacities when compared to the original single-channel 802.11 protocol. It induces smaller protocol overheads than other dual-channel schemes (e.g. [12], [13], [105]) proposed in the literature. As demonstrated in Chapters 2 and 3, the proposed approach can be implemented with current technologies based on the well-defined IEEE 802.11 industrial standard.

However, the capacity improvements also depend on the network topologies and link packing densities. The capacity advantages could be diminished in networks which have nodes densely packed together. Therefore, in Chapter 4, a generic approach for capacity analysis will be introduced to allow one to determine if the approach of link-directionality should be applied to a given network. Chapter 4 will turn the attention to the fundamental analysis of wireless networks by using link interference graphs. It will also apply the concept of link-directionality for capacity improvements in wireless local area network (WLAN).

Chapters 2 and 3 have focused on the capacity improvement of ad-hoc networks. Chapter 4 will turn the attention to the infrastructure mode of carrier sense wireless networks. The concept of link-directionality will also be applied to wireless local area network (WLAN) for performance enhancements.

4. Eliminating Interference in WLANs by Colouring Link-directional Interference Graphs

In Chapters 2 and 3, a novel medium access control (MAC) protocol has been proposed which is based on two algorithms: 1) link-directionality-based dual channel protocol (DCP) and 2) signal-to-interference ratio comparison algorithm (SCA). The concept of link-directionality has been implemented on the protocol level in these two chapters. To have a better understanding of the principle of this concept and its advantages, this chapter turns the attention back to the fundamental analysis of wireless networks. It introduces the link interference graph to refine the interference relationships between links. A generic approach for capacity analysis is then used to demonstrate whether the concept of link-directionality should be applied to a given network. Moreover, the link interference graphs provide insights in eliminating the hidden-node and exposed-node problems in wireless local area networks (WLAN).

Physical interference in wireless networks

The physical interference between links can be represented by two inequalities [94]. Consider two links, links 1 and 2. Let T_i and R_i be the transmitter and receiver of link *i*, respectively. Link 2 can interfere with link 1 if

$$\left|X_{T2} - X_{R1}\right| < (1+\Delta)\left|X_{T1} - X_{R1}\right| \tag{4.1}$$

and link 1 can interfere with link 2 if

$$\left|X_{T1} - X_{R2}\right| < (1+\Delta)\left|X_{T2} - X_{R2}\right| \tag{4.2}$$

where X_i is the location of node i, and $\Delta > 0$ is related to a power margin. The physical interference range of a link *i* is then

$$PInRange_i = (1+\Delta)\left|X_{Ti} - X_{Ri}\right|.$$

For example, in a two-ray propagation model with the SIR (signal-to-interference ratio) capture threshold set to 10dB [97], $\Delta = 0.78$ according to equation (3.1). Simultaneous transmissions on links 1 and 2 are not possible if either (4.1) or (4.2) is true. In other words, when T_1 (T_2) is located within the $PInRange_2$ ($PInRange_1$) of R_2 (R_1), links 1 and 2 cannot transmit concurrently. Otherwise, collisions will occur.

4.1. Physical Interference Graph (P-graph)

These two physical constraints can also be graphically represented by constructing physical interference graphs (p-graph) of wireless networks [88]. In a p-graph, a vertex represents a wireless link. There is an interference edge between vertices 1 and 2 if (4.1) or (4.2) is satisfied.

Note that the physical interference range $PInRange_1$ is the distance of T_2 from R_1 where the transmission of link 1 is independent of the transmission of link 2. In fact, the interference relationship between two links is not a sharp cut between no and severe interference. When $d_{T2-R1} \geq PInRange_1$ where d_{T2-R1} is the distance between T_2 and R_1 , the p-graph assumes the interference impact factor $\beta(d_{T2-R1}) = 0$. When $d_{T2-R1} < PInRange_1$, the p-graph assumes the interference impact factor $\beta(d_{T2-R1}) = 1$. Indeed, the transmissions of link 1 can be interfered and the capacity of link 1 can be degraded by an interference impact factor $\beta(d_{T2-R1})$ where $0 \leq \beta(d_{T2-R1}) \leq 1$. In this section, an interference edge is drawn between vertices 1 and 2 when $\beta(d_{T2-R1}) > 0$ and even if links 1 and 2 can occasionally transmit together. This allows a colouring algorithm to eliminate interference between links for simultaneous transmissions. In sub-section 4.4, a generic approach for capacity analysis will be proposed to take into account the interference impact factor $\beta(d_{T2-R1})$ when it is not a 0-1 parameter.

Figure 4.1 shows an example of mapping a network topology to a p-graph. Links P and Q can

transmit simultaneously since T_P and T_Q are outside the *PInRanges* of R_Q and R_P. On the other hand, link R cannot transmit at the same time with links P or Q since T_P and T_Q are within the *PInRange* of R_R. Thus link R and links P and/or Q must take turns to transmit.

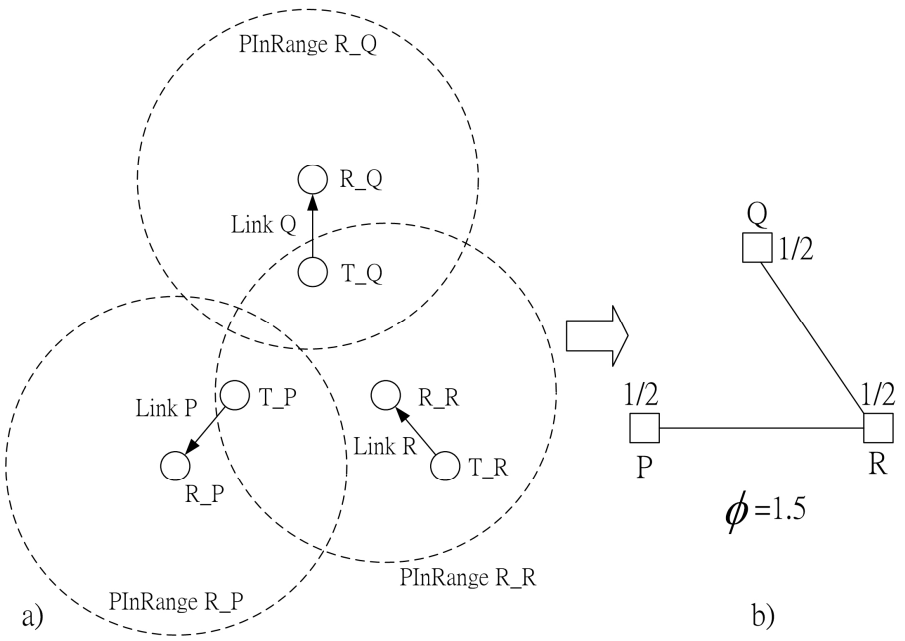
Based on the max-min fair share assignment proposed by [86], the expected capacity of the network can be obtained from the p-graph. The algorithm includes the following steps:

Step 1. Separate the graph into cliques with initial capacities set as 1.

Step 2. For the clique with the smallest value of capacity to number of vertices ratio, assign a fair share to all vertices in that clique.

Step 3. These vertices are then removed from the graph and the capacities of remaining cliques are updated.

The steps 2-3 are repeated until all vertices are assigned with a fair share [86].



** R_Q in the figure indicates node R_Q ;*

PInRange R_Q in the figure indicates the physical interference range of node R_Q

Figure 4.1. Mapping of a network topology a) to b) physical interference graph

Let ϕ be the sum of the "fair shares" of all vertices in the graph and C be the maximum throughput achieved by an isolated wireless link. The network capacity is then $C_{PHY} = \phi \cdot C$. All vertices in Fig. 4.1 are assigned by the algorithm with a fair share of 1/2. Thus, $C_{PHY} = 1.5C$ because links P and/or Q and link R each uses half of the total time for transmissions.

This capacity bound, C_{PHY}, however, is difficult to achieve in wireless ad-hoc networks due to two factors: 1) symmetric traffic generated by replying ACKs and 2) protocol constraints.

For 1), in many wireless medium access protocols (e.g. IEEE 802.11), the receiver (R_i) always replies an acknowledgement packet (ACK) back to the transmitter (T_i) after successfully receiving a DATA packet. This can ensure information integrity, particularly for data networks. Consider Fig. 4.1 again. When there are ACKs from the receivers (R_P and R_Q) to the transmitters (T_P and T_Q), links P and Q can no longer transmit simultaneously. This is because T_P (T_Q) are within the *PInRange* of T_Q (T_P). When R_P (R_Q) is replying an ACK to T_P (T_Q) and T_Q (T_P) is sending DATA, a collision will occur at T_P (T_Q). Since T_P (T_Q) fails to receive the corresponding ACK of the transmitted DATA, the medium access protocol (e.g. IEEE 802.11) may treat it as a collision and retransmit the DATA packet. Therefore, links P and Q have to take turns to transmit and fail to reach the maximum achievable capacity, $C_{PHY} = 1.5C$. Notice that here the conditions within the brackets in this chapter represent the scenario when the symbols swap their roles.

For 2), wireless medium access protocols may limit the spatial reuse by imposing unnecessary protocol constraints. For example, reference [88] showed that simultaneous transmissions permitted by physical constraints (4.1) and (4.2) can be restricted by the virtual carrier sensing mechanism of the IEEE 802.11 protocol in ad-hoc networks. This is also well-known as the exposed-node problem. In addition, protocols may allow transmissions that will actually cause collisions (i.e., the

hidden-node problem). These hinder protocols to achieve their expected capacities.

In this chapter, solutions for factor 1) are proposed so as to increase the capacities of networks. For factor 2), orthogonal data streams obtained by multi-carrier code division multiple access (MC-CDMA) are used to eliminate the hidden-node and exposed-node problems in WLANs. For solutions in ad-hoc networks for factor 2), the interested reader is referred to references [88] and [106] in which solutions were proposed to modify the 802.11 MAC protocol to eliminate these protocol constraints.

4.2. ARQ Physical Interference graph (ARQ P-graph)

To take into account the symmetric traffic induced by replying ACKs, six additional inequalities are needed for the physical constraints. When a link is transmitting ACK, its transmitter becomes a receiver and may collide with the DATA or ACK of other links. Thus, collisions due to the ARQ could occur if one of the following is true [88]:

$$|X_{R2} - X_{R1}| < (1+\Delta)|X_{T1} - X_{R1}| \tag{4.3}$$

$$|X_{T1} - X_{T2}| < (1+\Delta)|X_{R2} - X_{T2}| \tag{4.4}$$

$$|X_{T2} - X_{T1}| < (1+\Delta)|X_{R1} - X_{T1}| \tag{4.5}$$

$$|X_{R1} - X_{R2}| < (1+\Delta)|X_{T2} - X_{R2}| \tag{4.6}$$

$$|X_{R2} - X_{T1}| < (1+\Delta)|X_{R1} - X_{T1}| \tag{4.7}$$

$$|X_{R1} - X_{T2}| < (1+\Delta)|X_{R2} - X_{T2}| \tag{4.8}$$

As examples, figures 4.2a and 4.2b show the scenarios of inequalities (4.3) and (4.8) respectively. In Fig. 4.2a, if T_1 is sending DATA and R_2 is sending ACK at the same time, there will be a collision at R_1. Similarly, in Fig. 4.2b, if R_1 and R_2 are sending ACKs at the same time, a collision will occur at T_2. Thus, T_2 cannot receive the ACK successfully and will re-transmit DATA to R_2.

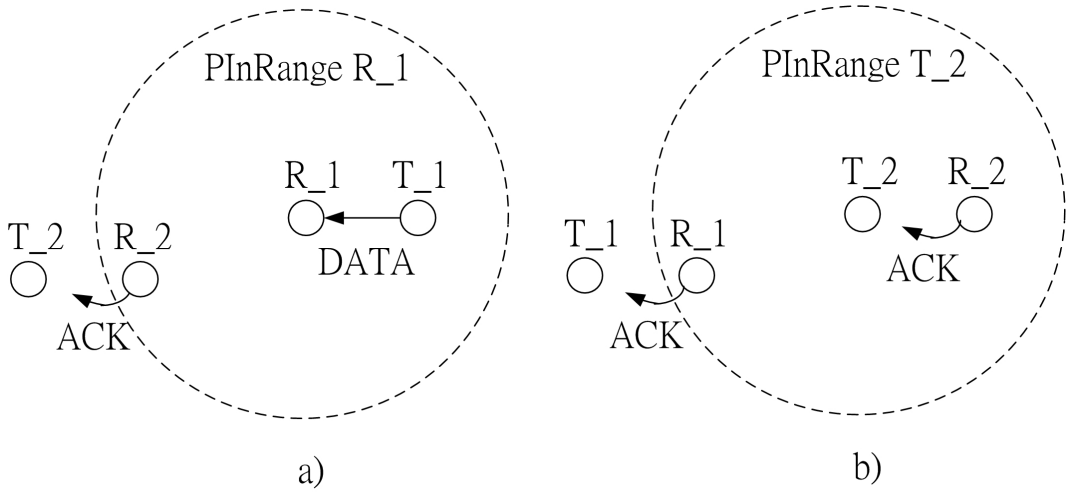


Figure 4.2. Network scenarios represented by inequalities a) (4.3) and b) (4.8)

Inequalities (4.3)-(4.8) are then added in constructing the ARQ p-graphs. Figure 4.3b shows the ARQ p-graph of the network topology in Fig. 4.1. Since T_P and T_Q are within the *PInRanges* of T_Q and T_P (inequalities (4.4) and (4.5) are true) respectively, there is now an edge between vertices P and Q which means links P and Q cannot transmit simultaneously. Therefore, links P, Q and R must take turns to transmit. In addition, the transmissions of ACKs take parts of the total transmission time. The capacity of a network with ARQ is then

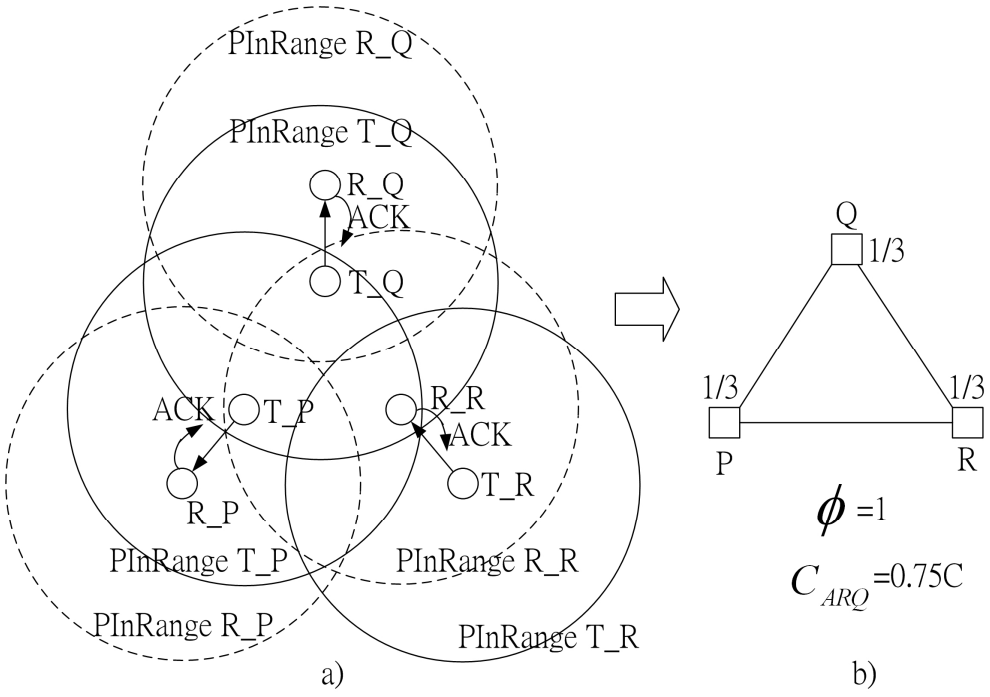
$$C_{ARQ} = \frac{T_{DATA}}{T_{DATA} + T_{ACK}} \cdot \phi \cdot C \tag{4.9}$$

where T_{DATA} is the time for transmitting a DATA packet while T_{ACK} is the time for sending an ACK packet. In this chapter, the data rate is set to 11Mbps and the basic rate for ACK is 2Mbps. DATA size is fixed at 500 bytes and ACK is 30 bytes. With these settings,

$$C_{ARQ} = 0.75 \cdot \phi \cdot C\ . \tag{4.10}$$

Here the protocol overheads are not taken into account since the proposed model is not specified to a particular protocol. As shown in Fig. 4.3, $C_{ARQ} = 0.75C$. Comparing C_{ARQ} with C_{PHY}, the capacity

is drastically degraded from 1.5C to 0.75C.



** R_Q in the figure indicates node R_Q ;*

PInRange R_Q in the figure indicates the physical interference range of node R_Q

Figure 4.3. Mapping of a network topology with ARQ a) to b) ARQ physical interference graph

4.3. Link-directional Interference graph (l-graph)

To clarify the interference relationships between links, the vertices in ARQ p-graph are further separated into directional vertices based on their link-directionalities. In a link-directional interference graph (l-graph), an arrow-shape vertex represents a wireless link with the arrowhead pointing toward the receiver. Therefore, there are two vertices for a link with ARQ in a l-graph. One vertex represents the DATA traffic while the other represents the ACK traffic. The name of the destination node of a directional link is used as the name of the directional vertex. For example, the DATA traffic from T_Q to R_Q is represented by the directional vertex R_Q in the l-graph with the

arrow head pointing to the receiver R_Q. Figure 4.4 shows the l-graph of the network topology in Fig. 4.1. There is an edge between two directional vertices if one of the inequalities (4.1)-(4.8) is true. For example, vertex R_Q is connected to vertex T_P, thus links R_Q and T_P cannot transmit simultaneously. In other words, collisions will occur if link Q is sending DATA while link P is replying ACK at the same time. On the other hand, links R_Q (T_Q) and R_P (T_P) can transmit DATA (ACK) concurrently since there is no edge between vertices R_Q (T_Q) and R_P (T_P) in the l-graph. The network capacity can then be improved by allowing non-interfering links to transmit simultaneously. The construction of l-graph can give us a clearer picture of the interference relationships which provides a new insight to increase the capacity by proper scheduling or channel allocations.

Based on the insights obtained from l-graphs, 1) time division multiple access (TDMA) and 2) frequency division multiple access (FDMA) can be used to increase network capacities. There are many TDMA and FDMA schemes proposed in the literature for ad-hoc networks. They can be modified with the proposed schemes. This chapter focuses on the conceptual ideas of the proposed schemes in scheduling transmissions and assigning channels instead of the protocol implementations. The interested reader is referred to [107][108][109][110] for the details of TDMA and FDMA protocols in ad-hoc networks.

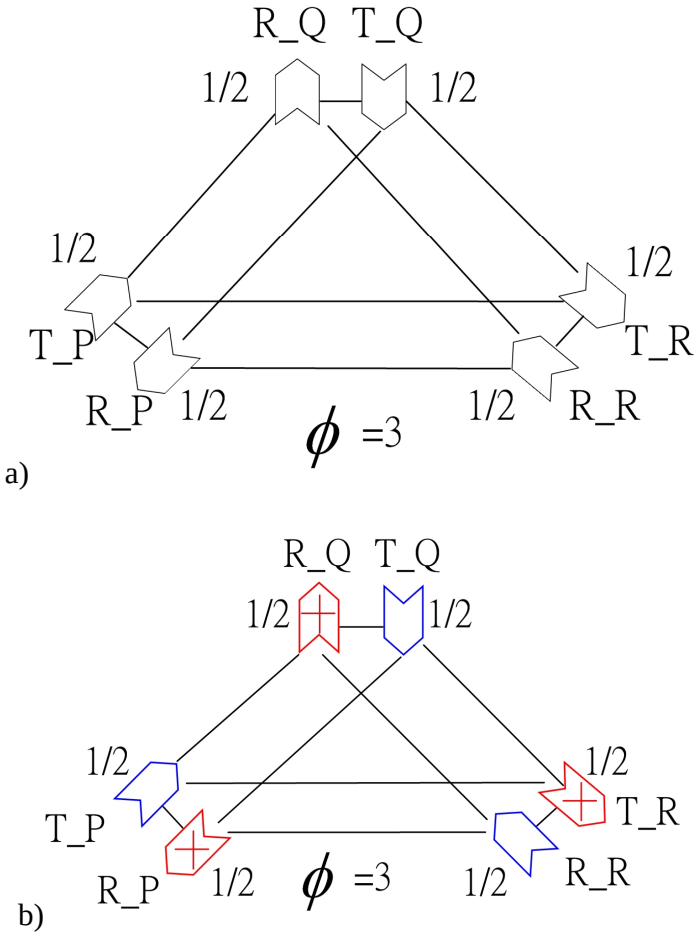


Figure 4.4. a) Link-directional interference graph of the network topology in Fig. 4.3b and b) its colouring result

For 1) TDMA, the groups of links that can transmit together have to be identified. For 2) FDMA with two sub-channels, one of the two sub-channels has to be assigned to vertices to eliminate interference between connected vertices. A colouring algorithm is applied in l-graphs with *two* colours and the colouring results are then used for transmission scheduling or channel assignments. The colouring algorithm here is modified from the "degree of saturation" (DSATUR) algorithm proposed in [111] [87]. First, the "degree of saturation" is defined as the number of differently coloured neighbours of a vertex. The algorithm consists of the following steps:

Step 1. Initialize the degrees of saturation of all vertices to 0.

Step 2. Select the uncoloured vertex of highest degree of saturation. If more than one vertex has the same degree of saturation, choose the one with the highest number of uncoloured neighbours.

Step 3. If the chosen vertex is connected to other vertices coloured with one of the two colours (say colour 1). Colour the chosen vertex with another colour (say colour 2). Otherwise, randomly pick one of the two colours for the chosen vertex.

Step 4. Update the degrees of saturation of the uncoloured vertices connected to the chosen vertex.

The steps 2-4 are repeated until all vertices are coloured.

Figure 4.4b shows the colouring of the l-graph. The result is used to schedule transmissions and assign channels for TDMA and FDMA. If a vertex with colour 1 (2) is connected to another vertex in the same colour, these two vertices must take turns to transmit. Figure 4.5 shows an example. Since T_Z and R_Z are both within the *PInRanges* of R_X and T_X, links X and Z must take turns to transmit even though T_X and R_Z are in blue colour while R_X and T_Z are in red. Otherwise, collisions will occur.

For 1) TDMA, after colouring the l-graph, links assigned with the same colour can transmit concurrently without causing collisions. As shown in Fig. 4.6, links T_Q, T_P and R_R in Fig. 4.3a can transmit in one time slot while links R_Q, R_P and T_R can send packets in another time slot. In this way, all three links P, Q and R can transmit concurrently to increase the network capacity. Since the TDMA protocol needs two time slots for transmitting DATA and ACK of a complete transmission, the capacity of using TDMA is then

$$C_{Colour} = \frac{C}{2} \cdot \phi \,. \tag{4.11}$$

Note that here a transmission of ACK still takes a whole time slot because ACK and DATA are now transmitting simultaneously. The link that sends ACK must wait for the completions of the

transmissions of DATA by other vertices before sending DATA again. Otherwise, collisions may occur.

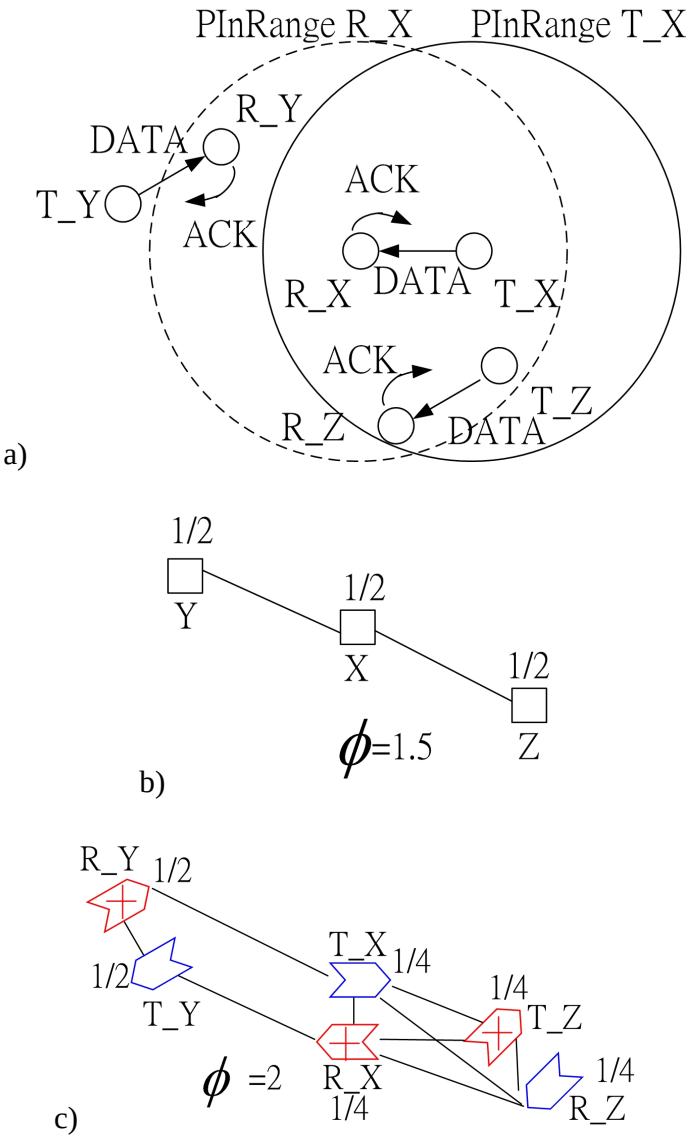


Figure 4.5. Mapping of a network topology a) to b) ARQ physical interference graph and c) coloured link-directional interference graph

In this example, the capacity is increased by up to $C_{Colour} = 1.5C$ which doubles the $C_{ARQ} = 0.75C$ of the network. However, TDMA requires synchronizations between links. This may not be easily achieved in distributed wireless ad-hoc networks unless a broadcast clock is available.

For 2) FDMA, the channel is divided into two sub-channels and assign each of them for sending either DATA or ACK packets of a link. Consider the case of two sub-channels, sub-channels 1 and 2. DATA packets can be sent via sub-channel 1 while ACK packets can be transmitted in sub-channel 2. Note that here sub-channel assignments depend on link directionalities. Other links may use sub-channel 1 (or 2) for sending ACK while sub-channel 2 (or 1) for DATA.

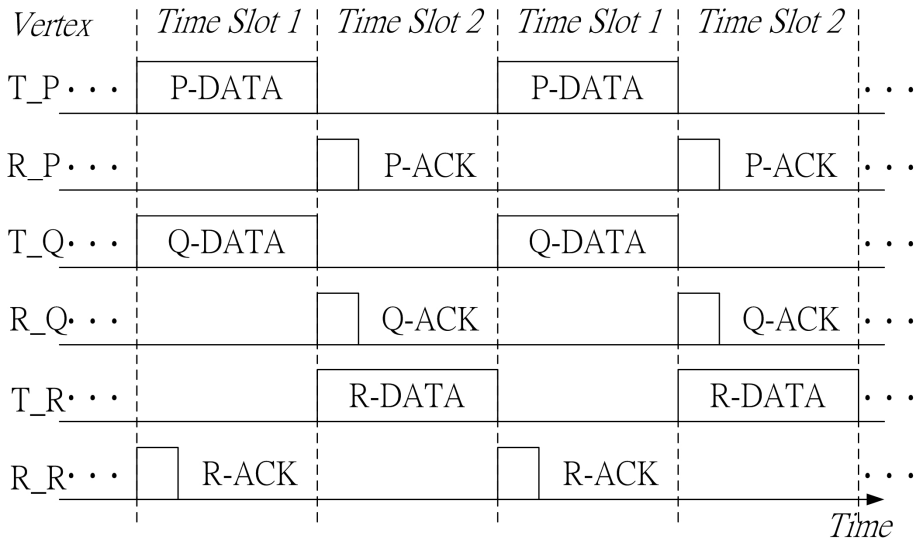


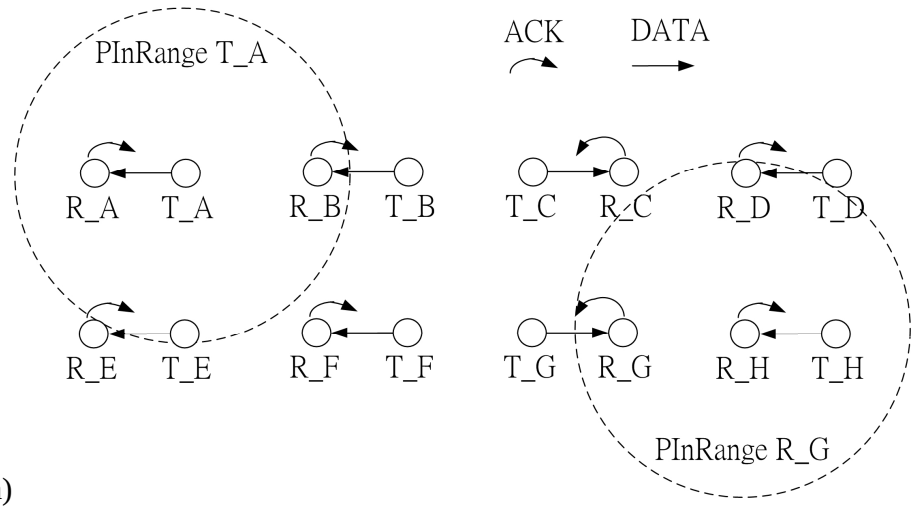
Figure 4.6. Scheduling the transmissions of links in the network topology of Fig. 4.3a according to the colouring result of l-graph in Fig. 4.4b

This time, the colouring result is used to assign sub-channels instead of grouping simultaneous transmission links. After colouring the l-graph, links assigned with the same colour will use the same sub-channel for transmissions. In Fig. 4.4b, vertices T_P , T_Q and R_R use sub-channel 1 for transmissions while vertices R_P , R_Q and T_R use sub-channel 2 instead. In this way, T_P, T_Q and R_R (R_P , R_Q and T_R) can transmit simultaneously without causing collisions. Synchronizations between wireless nodes are no longer needed since links use independent sub-channels for transmissions to

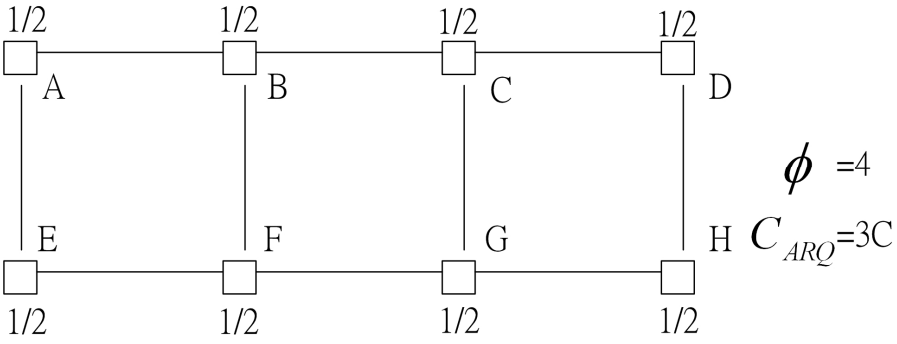
avoid interference. Since the channel is divided into two sub-channels which in turn halves the transmission bit rate, the achievable capacity C_{Colour} is then the same as that achieved by TDMA in equation (4.11). This solution, however, does not require time synchronizations between wireless nodes which makes it more suitable for the distributive character of ad-hoc networks.

4.3.1. An example in a Lattice Topology

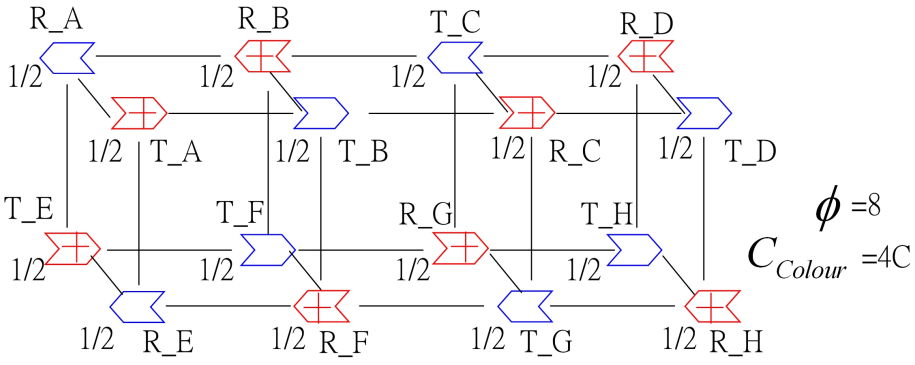
Figure 4.7a shows a 2x8 lattice topology. In ARQ p-graph as shown in Fig. 4.7b, neighbour links (e.g. links A and B or links D and H) have to take turns to transmit since they are within the *PInRange* of each other. This yields $\phi = 4$ and $C_{ARQ} = 3C$ according to equation (4.10). Figure 4.7c shows the coloured l-graph. With TDMA, blue coloured vertices can transmit at the same time in one time slot while vertices in red can use another time slot for concurrent transmissions. With FDMA, blue coloured vertices use sub-channel 1 while those in red use sub-channel 2 for transmissions. It does not require synchronizations between links which means red and blue vertices can transmit simultaneously as they use independent sub-channels. As a result, the proposed schemes yield $\phi = 8$ and $C_{Colour} = 4C$ which is 33% higher than C_{ARQ}.



a)



b)



c)

Figure 4.7. Mapping of a 2x8 lattice topology a) to b) ARQ physical interference graph and c) coloured link-directional interference graph

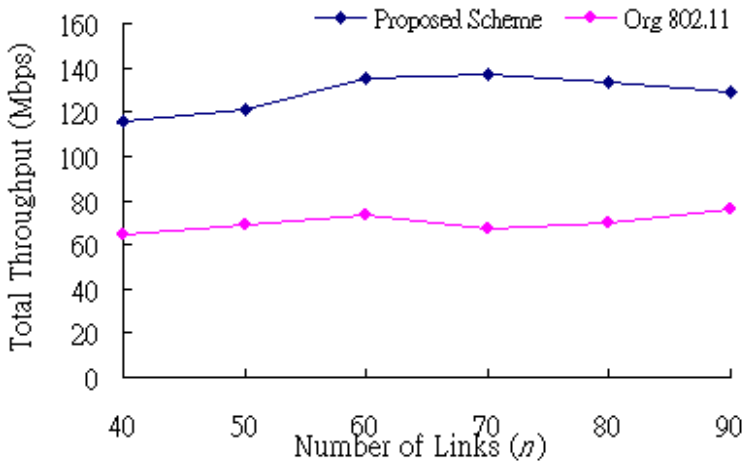


Figure 4.8. Total throughputs of random networks with *n* single-hop links

4.3.2. Simulation Results

It has been shown that the proposed schemes can improve the capacities of the networks in Fig. 4.3a and Fig. 4.7 to 2 times and 1.33 times respectively. The TDMA and FDMA schemes mentioned above, however, require the knowledge of network topology which may be difficult to obtain in distributed ad-hoc networks. In Chapter 2, a distributed link-directionality-based dual channel MAC protocol (DCP) for channel allocations has been proposed. The protocol is modified from the original 802.11 MAC protocol and it attempts to seek opportunities for simultaneous transmissions based on the concept of link-directionality. Transmission channels of each link are assigned according to the availabilities of receptions of RTS and CTS from other links. The reader is referred to Chapter 2 for details. The DCP protocol has been implemented in the NS-2 [102] simulator. The data and basic rates are set at 12Mbps and 2Mbps respectively. The transmission range is 250m and the carrier-sensing range is 550m. In the simulations, all data sources are saturated UDP traffic stream with fixed packet size of 1460bytes.

Figure 4.8 shows the total throughputs of random topologies with *n* links. In each random network, *n* single-hop links are randomly placed inside a 3000m x 3000m square. In all cases, the capacity

improvements achieve more than 1.7 times with respect to the single-channel 802.11 protocol. The throughput improvements, however, are highly dependent on the network topologies. In the best case when *n=70*, the DCP protocol increases the total network throughput to 2.04 times.

4.4 A Generic Approach for Capacity Analysis

In previous chapters, a specific propagation model (i.e., two-ray propagation model), MAC protocol (i.e., IEEE 802.11) and modulation scheme (i.e., QPSK) have been assumed in the simulations. In fact, the idea of link-directionality is not limited to these models. In this sub-section, a generic approach is introduced to investigate the capacity advantage of using link-directionality for channel allocations. This approach can be adopted with various propagation models, MAC protocols, modulation schemes and probability models. The value of achievable capacity obtained from this generic approach can then be compared with the single-channel scheme to decide if link-directionality should be applied to a given network for improving capacity. Indeed, there are scenarios in which link-directionality cannot provide better network capacities than the single-channel scheme, particularly in densely packed network topologies. In those cases, the single-channel scheme should be maintained. At the end of this sub-section, an example with chosen models is presented to demonstrate how to use this generic approach for capacity analysis.

Moreover, previous sub-sections have assumed a 0-1 interference relationship between two links. When the distance (d_{TB-RA}) between the transmitter of link B and the receiver of another link A is within *InRange* (physical interference range), there is an edge between these two link vertices in the l-graph. On the other hand, when $d_{TB-RA} \geq InRange$, these two links are assumed to be able to transmit at the same time. In fact, instead of a fixed sharp-cut *InRange*, there is a range of distances within which a link suffers from variable interference impacts. The generic approach in this sub-section can take this factor into account. It includes the following steps:

Step 1: To determine the range of interference distances

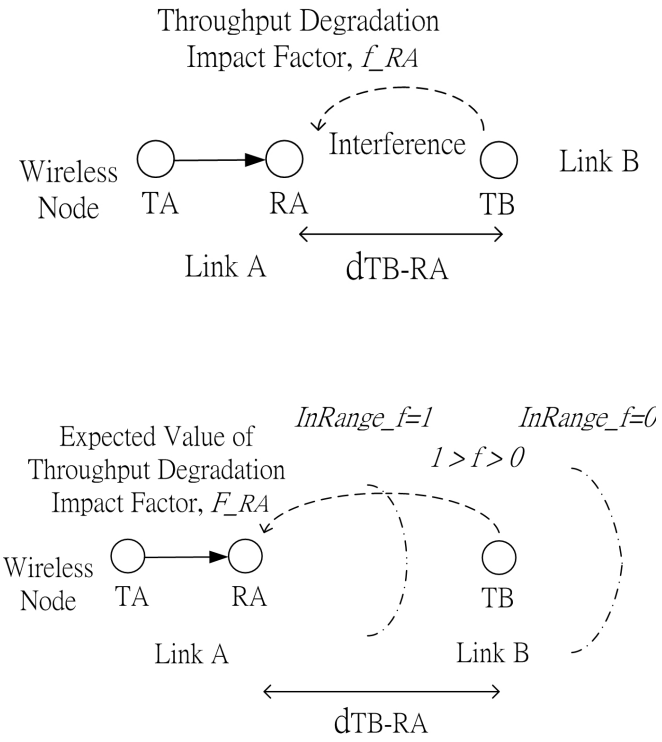


Figure 4.9. a) Throughput degradation of link A caused by interference from link B; b) Throughput degradation of link A when T_B is within the range of interference distances

Consider two links, link A and link B as illustrated in Fig. 4.9a. When the distance (d_{TB-RA}) between the transmitter of link B (T_B) and the receiver of link A (R_A) is within the range of interference distances, the throughput of link A is reduced by a throughput degradation impact factor f_{RA} if links A and B are transmitting simultaneously. f_{RA} is a probability function defined by the assumed channel probability model and $0 \leq f_{RA} \leq 1$. When the bit error rate (BER) is smaller than a specific value ($BER_{f=0}$) chosen by the pre-assumed protocol, the receiver R_A can perfectly receive every packet successfully from T_A even if T_B is transmitting at the same time. In this case, the throughput

degradation impact factor $f_{RA} = 0$. On the other hand, when the bit error rate (BER) is larger than a specific value ($BER_{f=1}$) indicated by the protocol used, the receiver R_A cannot decode a single packet successfully from T_A when T_B is transmitting at the same time. Thus, in this scenario, the throughput degradation impact factor $f_{RA} = 1$. Given the modulation scheme used in the network, the relative signal-to-noise ratios ($SNR_{f=0}$ and $SNR_{f=1}$) for $BER_{f=0}$ and $BER_{f=1}$ can be determined. The relative interference ranges ($InRange_{f=0}$ and $InRange_{f=1}$) can therefore be calculated according to the propagation model and the value of path loss exponent assumed in the network.

Step 2: To determine the throughput degradation impact factor on each suffering link

Let *d* be the interferer-receiver distance as defined above. When $InRange_{f=1} < d < InRange_{f=0}$, the receiver of a link suffers a throughput degradation. According to the assumed probability model, an expected throughput degradation impact factor, F, can be assigned to a link. Figure 4.9b shows an example of link A and link B. When $InRange_{f=1} < d_{TB-RA} < InRange_{f=0}$, receiver R_A of link A is assigned with an expected throughput degradation impact factor F_{RA}. This step is repeated until all links which suffer from interference have been assigned with their respective throughput degradation impact factors.

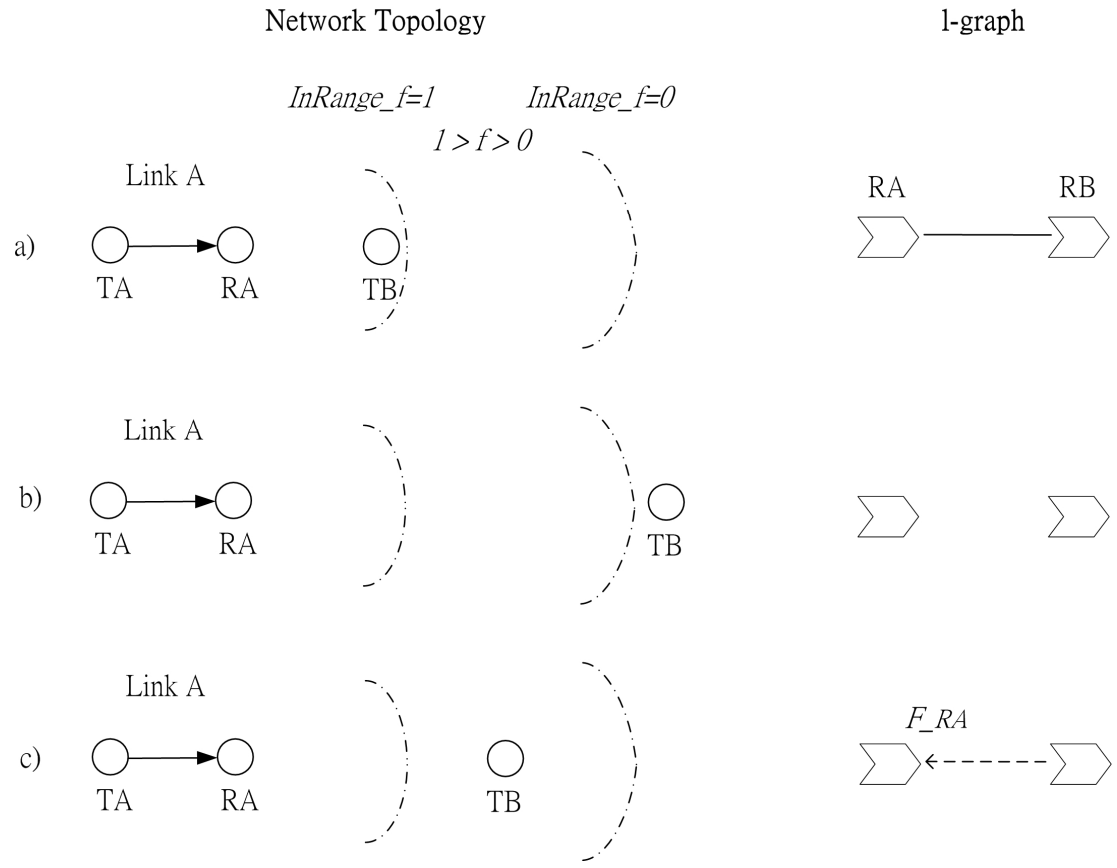


Figure 4.10. Using solid or dot edges to represent interference relationships between links in l-graph

Step 3: Converting the network topology into a link-directional interference graph (l-graph)

Consider link A and link B again. When $d_{TB-RA} \le InRange_{f=1}$, a solid interference edge is drawn between vertices R_A and R_B in l-graph as shown in Fig. 4.10a. This implies nodes T_A and T_B cannot transmit simultaneously.

When $d_{TB-RA} \ge InRange_{f=0}$, there is no interference edge between vertices R_A and R_B in the l-graph which means nodes T_A and T_B can transmit at the same time without causing interference at R_A.

As shown in Fig. 4.10c, if $InRange_{f=1} < d_{TB-RA} < InRange_{f=0}$, a dot edge is drawn between vertices R_A and R_B. This dot edge is assigned with the expected throughput degradation impact factors F_{RA}

on vertex R_A. According to the conditions as mentioned above, a network topology can then be converted into an l-graph with solid and dot interference edges.

Figure 4.11 shows an example. Node T_Q is within the $InRange_{f=1}$ of node T_P, therefore, a solid edge is drawn between vertices T_P and R_Q. Node T_P is within the $InRange_{f=0}$ but outside the $InRange_{f=1}$ of node R_Q, thus a dot edge is drawn between vertices R_Q and R_P with expected throughput degradation impact factors F_{RQ} and F_{RP} respectively.

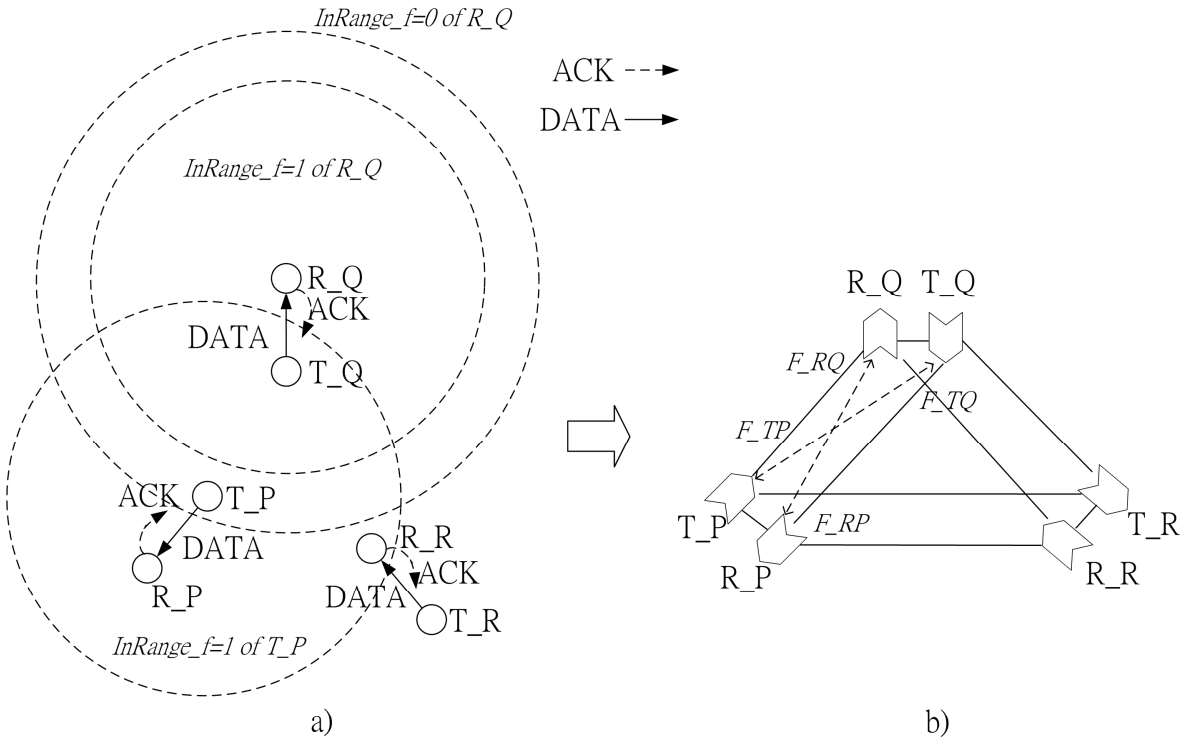


Figure 4.11. Converting a) a network topology into b) an l-graph with solid and dot interference edges

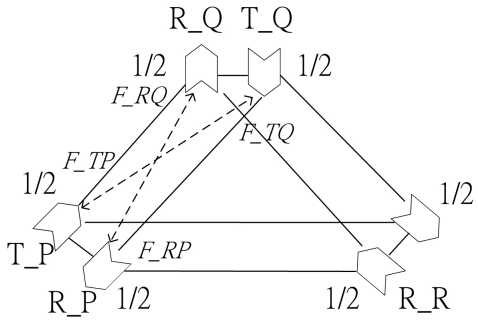


Figure 4.12. Assigning capacity share for each vertex in l-graph

Step 4: To compute the share of each vertex in l-graph according to the solid edges

Using the same algorithm as described in sub-section 4.1, the capacity share of each vertex can be calculated based on the solid edges in the l-graph. Figure 4.12 shows an example. The algorithm results in 1/2 capacity share for each vertex. Let S_i be the capacity share of vertex *i*. The summation of the capacity shares in the network

$$\phi = \sum_i S_i \,. \tag{4.12}$$

And thus, from equation (4.11), the total network capacity

$$C_{Colour} = \frac{C}{2} \cdot \phi = \frac{C}{2} \sum_i S_i \,. \tag{4.13}$$

Where C is the maximum throughput achieved by an isolated wireless link as defined in section 4.1. Since the channel is divided into two sub-channels for channel allocations which in turn halves the transmission bit rate, the total network capacity is therefore the summation of shares of all vertices divided by two.

Step 5: To adjust the achievable network capacity according to the impact factor F

As mentioned in step 3, each vertex with a dot edge is assigned with an expected throughput degradation impact factor F. In this step, the total achievable capacity is adjusted by taking this

factor into account. For vertex i with a dot edge, its throughput is degraded by F_i. Therefore, the total network capacity

$$C_{Colour} = \frac{C}{2}\sum_i S_i(1-F_i). \tag{4.14}$$

This is the achievable network capacity by using link-directionality scheme. It can be compared with the capacity achieved by a single-channel scheme as shown in Fig. 4.3. If there is a capacity improvement, the colouring algorithm as described in sub-section 4.3 can then be used to allocate channels according to link-directionalities for performance enhancements.

Table IV. Network models and parameters assumed in the example for capacity analysis

Modulation Scheme	QPSK
$BER_{f=0}$ (bit error rate)	10^{-5}
$BER_{f=1}$	10^{-4}
Propagation Model	Path loss model
Environment	Shadowed urban area
Path loss exponent β	2.7
Transmission Range (*TxRange*)	250m
Throughput degradation impact factor at interferer-receiver distance d f_d	Normal distribution
The expected value of f_d, F_d	Linear proportional with d
Multiple Access Protocol	FDMA
DATA size	1400 bytes
Data transmission rate	10Mbps
ACK size	40 bytes
ACK transmission rate	2Mbps

* BER (bit error rate) does not include any ARQ (automatic repeat-request)

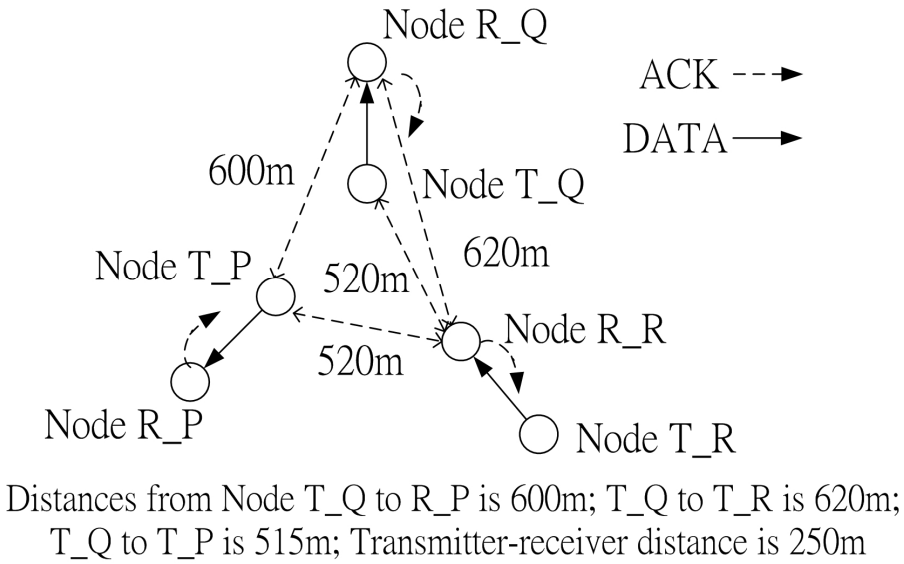


Figure 4.13. A network topology with three links

4.4.1 An Example of the Generic Approach for Capacity Analysis

This sub-section shows an example of the generic approach for capacity analysis to demonstrate how the achievable capacity according to link-directionalities can be calculated. It uses the network topology as shown in Fig. 4.13 as an example with the assumed network and channel models as listed in Table IV. Note that this generic approach is not restricted to the assumed topology and models. Other network topologies, models and system parameters can also be adopted in the approach for capacity analysis.

Step 1: To determine the range of interference distances

Given QPSK as the modulation scheme, the bit error rate for QPSK [112]

$$BER = \frac{1}{2} erfc(\sqrt{\frac{E_b}{N}}) \tag{4.15}$$

where $erfc(\cdot)$ is the complementary error function and E_b / N is the signal-to-noise ratio per bit.

Therefore, *BER* can be plotted against *SNR* as shown in Fig. 4.14 [112]. Since the assumed bit error

rates $BER_{f=0}=10^{-5}$ and $BER_{f=1}=10^{-4}$, $SNR_{f=0}=10.5$ and $SNR_{f=1}=9.25$ from Fig. 4.14.

In the path loss model, a close-in distance d_0 is used as a reference. The received power $P_r(d)$ at a distance d is computed relative to $P_r(d_0)$

$$\frac{P_r(d_0)}{P_r(d)}=(\frac{d}{d_0})^{\beta}. \tag{4.16}$$

Consider the transmitter of another link is at distance d_f from link Q and transmits simultaneously. The signal-to-noise ratio at R_Q

$$[SNR_{RQ}]_{dB}=10\log\frac{P_r(d_{TQ-RQ})}{P_r(d_f)} \tag{4.17}$$

$$=10\log\frac{P_r(d_0)/(d_{TQ-RQ}/d_0)^{\beta}}{P_r(d_0)/(d_f/d_0)^{\beta}}$$

$$=10\beta\log(\frac{d_f}{d_{TQ-RQ}}).$$

In an outdoor shadowed urban area environment, path-loss exponent β is 2.7 [113]. Therefore,

$$SNR_{f=0}=27\log(\frac{InRange_{f=0}}{d_{TQ-RQ}}) \quad \text{and}$$

$$SNR_{f=1}=27\log(\frac{InRange_{f=1}}{d_{TQ-RQ}}). \tag{4.18}$$

Thus, the physical interference ranges are $InRange_{f=0}$ =612m and $InRange_{f=1}$ =550m for $SNR_{f=0}$ and $SNR_{f=1}$ respectively when transmitter-receiver distance is 250m.

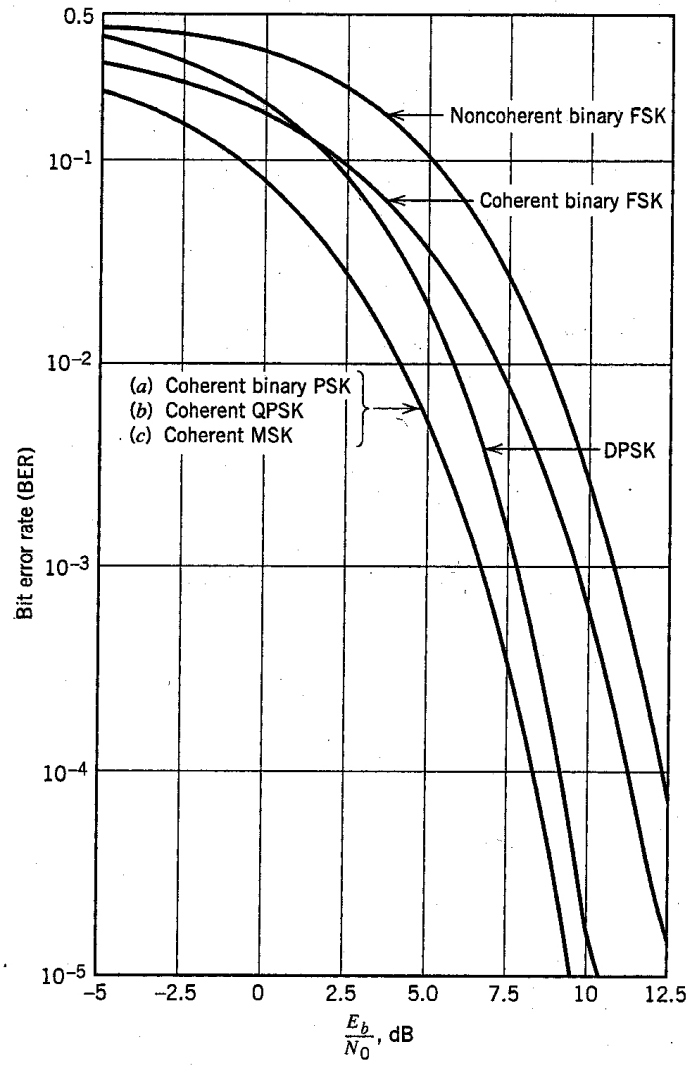


Figure 4.14. Bit error rate (BER) against vs E_b / N (signal-to-noise ratio per bit) of QPSK [112]

Step 2: To determine the throughput degradation impact factor on each suffering link

The expected throughput degradation impact factor F against interferer-receiver distance d can be plotted as in Fig. 4.15. In this example, the expected throughput degradation impact factor F is linear proportional to the interferer-receiver distance d . When the interference transmitter T_P of link P is located at 600m away from R_Q , the impact factor at R_Q , F_{RQ} =0.2 as shown in Fig. 4.15. Similarly, the same approach can be repeated to determine the expected throughput degradation impact factor of each suffering link in the network.

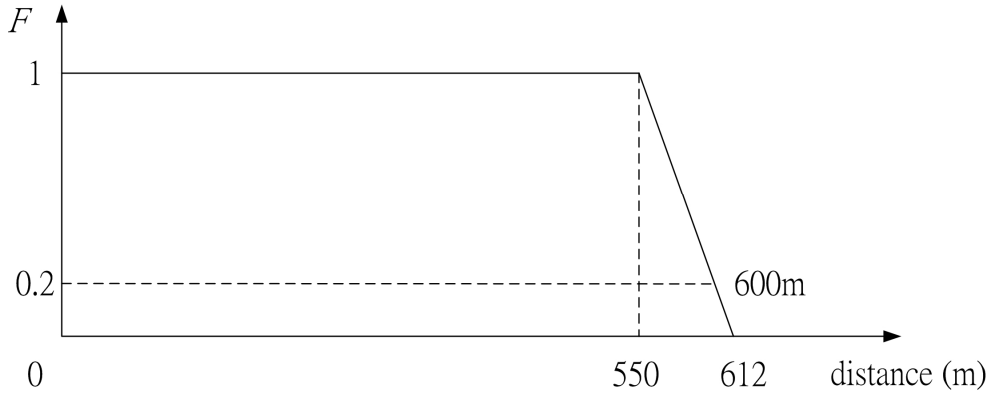


Figure 4.15. Expected throughput degradation impact factor *F* against interferer-receiver distance *d*

Step 3: Converting the network topology into a link-directional interference graph (l-graph)

Figure 4.16 shows the conversion of the network topology into the l-graph with both solid and dot interference edges. The throughput degradation impact factors *F* for vertices are also specified in the l-graph.

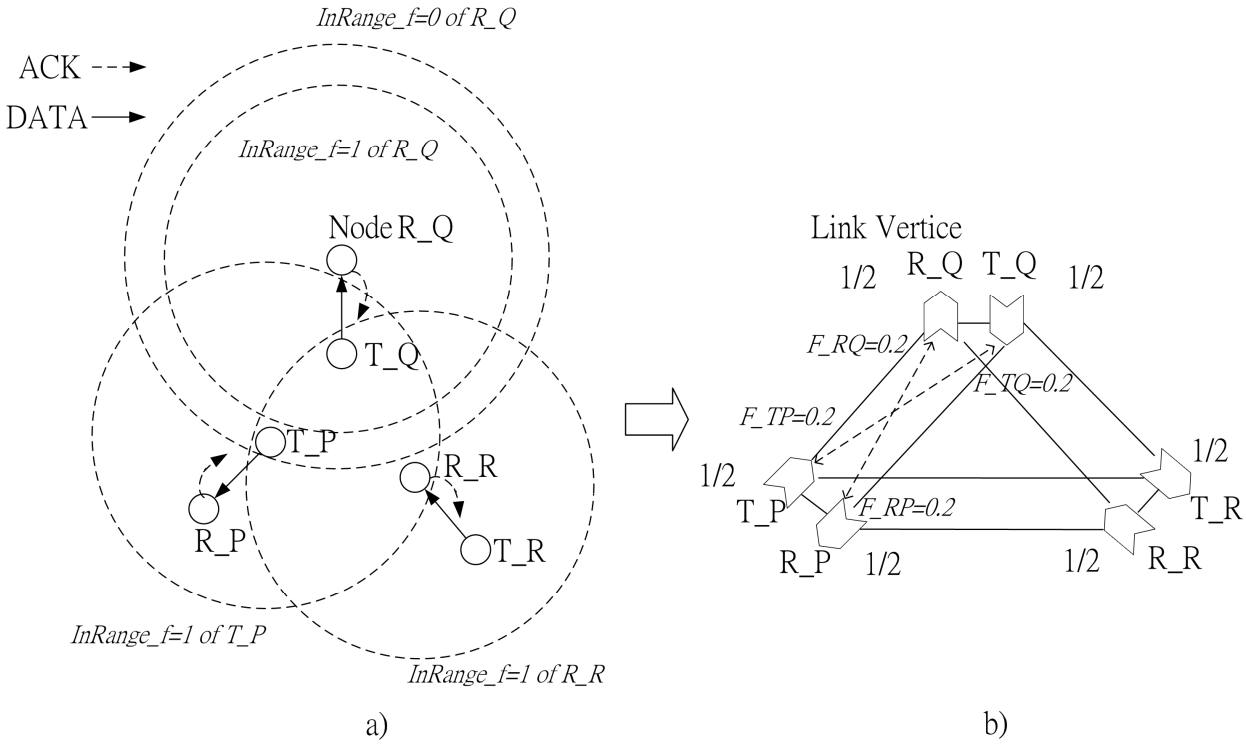


Figure 4.16. Converting a) the network topology of Fig. 4.13 into b) the l-graph

Step 4: To compute the share of each vertex in l-graph according to the solid edges

As shown in Fig. 4.16b, the capacity share of each vertex in the l-graph can be calculated based on the solid edges using the algorithm as described in sub-section 4.1.

Step 5: To adjust the achievable network capacity according to the impact factor F

According to equation (4.11), the total capacity of the network which uses link-directionality becomes

$$C_{Colour} = \frac{C}{2}\sum_i S_i(1-F_i) \tag{4.19}$$

$$= 1.3C\,.$$

Therefore, using link-directionality for channel allocations in this network results in $1.3C$ total network capacity. This value is then compared with the single-channel scheme to decide if link-directionality should be applied in the network for channel allocations.

Capacity comparison with the single-channel scheme

Figure 4.17 converts the network topology into an ARQ p-graph (ARQ physical interference graph). From the ARQ p-graph, the total network capacity of using a single-channel scheme can be determined as described in sub-section 4.2. In this case, according to equation (4.9), the DATA and ACK settings as shown in Table IV, the total network capacity for a single-channel scheme

$$C_{ARQ} = \frac{T_{DATA}}{T_{DATA}+T_{ACK}}\phi \cdot C = 0.875\mathrm{C} \tag{4.20}$$

where T_{DATA} is the time for transmitting a DATA packet while T_{ACK} is the time for sending an ACK. Since all three links are within the interference range of each other, they have to take turns to transmit and share the network capacity. Comparing C_{Colour} with C_{ARQ}, using link-directionality can improve the network capacity by 48.5%. For sub-channel allocations with FDMA, the colouring

algorithm as described in sub-section 4.3 can be applied in the l-graph. Note that there are dot interference edges between links Q and P in Fig. 4.16b. This means receivers of links Q and P cannot successfully receive every packet even if their transmissions are assigned with sub-channels according to the colouring algorithm. However, since $F_{RQ} = F_{TQ} = F_{RP} = F_{TP}$ =0.2, the throughput degradation impacts are relatively small and the capacity can still be increased by allowing simultaneous transmissions.

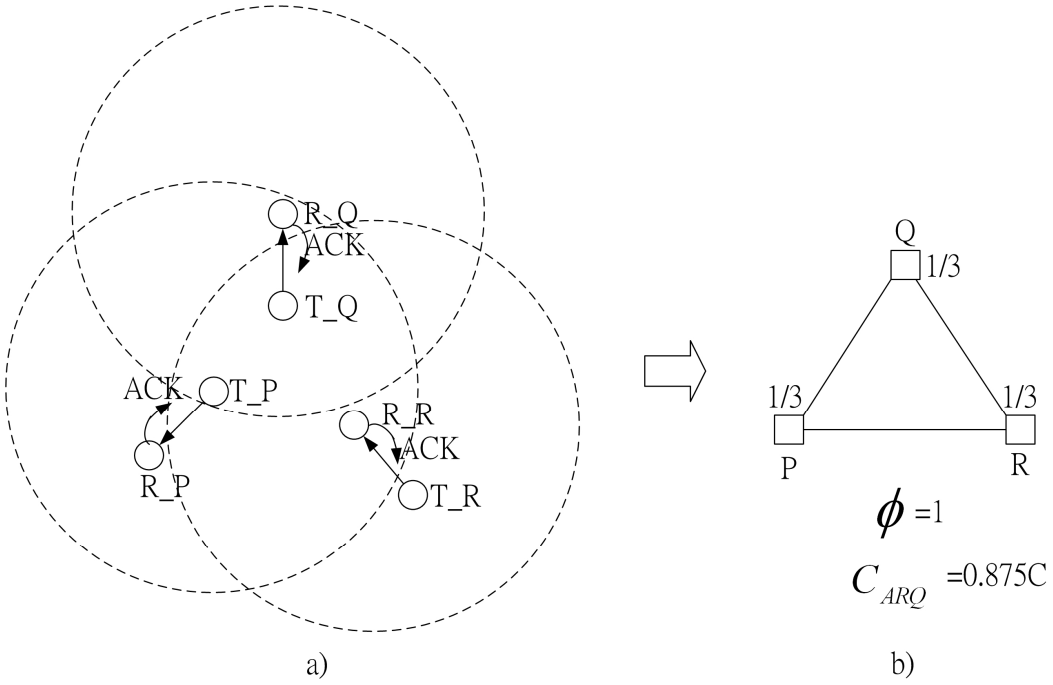


Figure 4.17. Converting a network topology into a ARQ p-graph

Finally, a graph of the total network capacity C_{Colour} against the expected throughput degradation impact factor F can be used to identify the range of F within which applying the link-directional scheme can yield better network throughput than a single-channel scheme. Figure 4.18 shows an example. Assume $F_{RQ} = F_{TQ} = F_{RP} = F_{TP}$ in the network of Fig. 4.16. The total network capacity C_{Colour} decreases when F increases. When $F < 0.625$, link-directionality is capable for performance

improvement when compared to the single-channel scheme ($C_{ARQ} = 0.875C$). On the other hand, when $F \geq 0.625$, using link-directionality for channel allocations does not yield performance enhancements in the network. This allows one to determine if link-directionality should be applied or not.

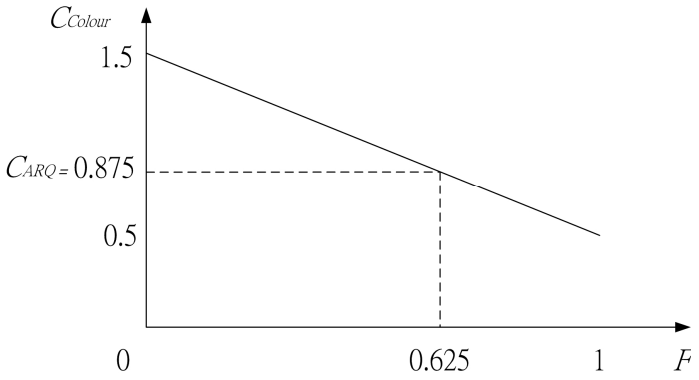


Figure 4.18. Achievable network capacity C_{Colour} by link-directional scheme against throughput degradation impact factor *F*

4.5 Insights in WLAN Channel Allocations

Besides modeling network topologies in ad-hoc networks, the proposed coloured l-graph can also provide insights into channel allocations of wireless local area network (WLAN) to eliminate the hidden-node and exposed-node problems. Figure 4.19a shows an IEEE802.11b WLAN scenario with three independent channels (channels 1, 6 and 11). The topology attempts to separate basic service sets (BSS) using the same channel with the largest physical distance to reduce interference. However, clients A, B and C still have to take turns to transmit as they are within the physical carrier sensing range (*PCSRange*) of each other. This limits the network capacity. Note that here the *PCSRange* is considered instead of the *PInRange* (physical interference range) as the 802.11 protocol sets the *PCSRange* larger than the *PInRange* to ensure wireless nodes within the *PInRange*

will not send packets at the same time to avoid collisions. The ARQ p-graph in Fig. 4.19b shows each of the basic service sets (BSS) A, B and C is assigned with 1/3 fair share. Reference [114] found that partially overlapped channels (channels 1, 4, 7, and 11) can be used without causing harmful interference. However, four channels are still insufficient to separate BSSs using the same channel so as to mitigate interference.

On the other hand, the l-graph as shown in Fig. 4.19c gives us an insight in improving the network throughput. Assume channel 1 can be separated into two sub-channels by Multi-carrier Code Division Multiple Access (MC-CDMA) [115][116] into sub-channel 1A & 1B such that transmissions in each sub-channel can still achieve the same data rate as transmissions in the original channel 1. Sub-channel 1A can then be assigned for downlink traffic from an access point (AP) to clients and sub-channel 1B for uplink traffic from clients to the access point. In this way, BSSs A, B and C can transmit concurrently. This drastically increases the sum of fair share of a BSS to 1.

The interested reader is referred to [115][116][117] for the details of the design of MC-CDMA. Reference [117] proposed a carrier interferometry (CI) approach to support $2N$ users on N carriers while maintaining the performance of N users. The CI spreading codes can double the MC-CDMA network capacity without loss in performance. The following sub-sections will describe the details of the channel assignment scheme in eliminating inter-BSS co-channel interference by MC-CDMA in WLANs.

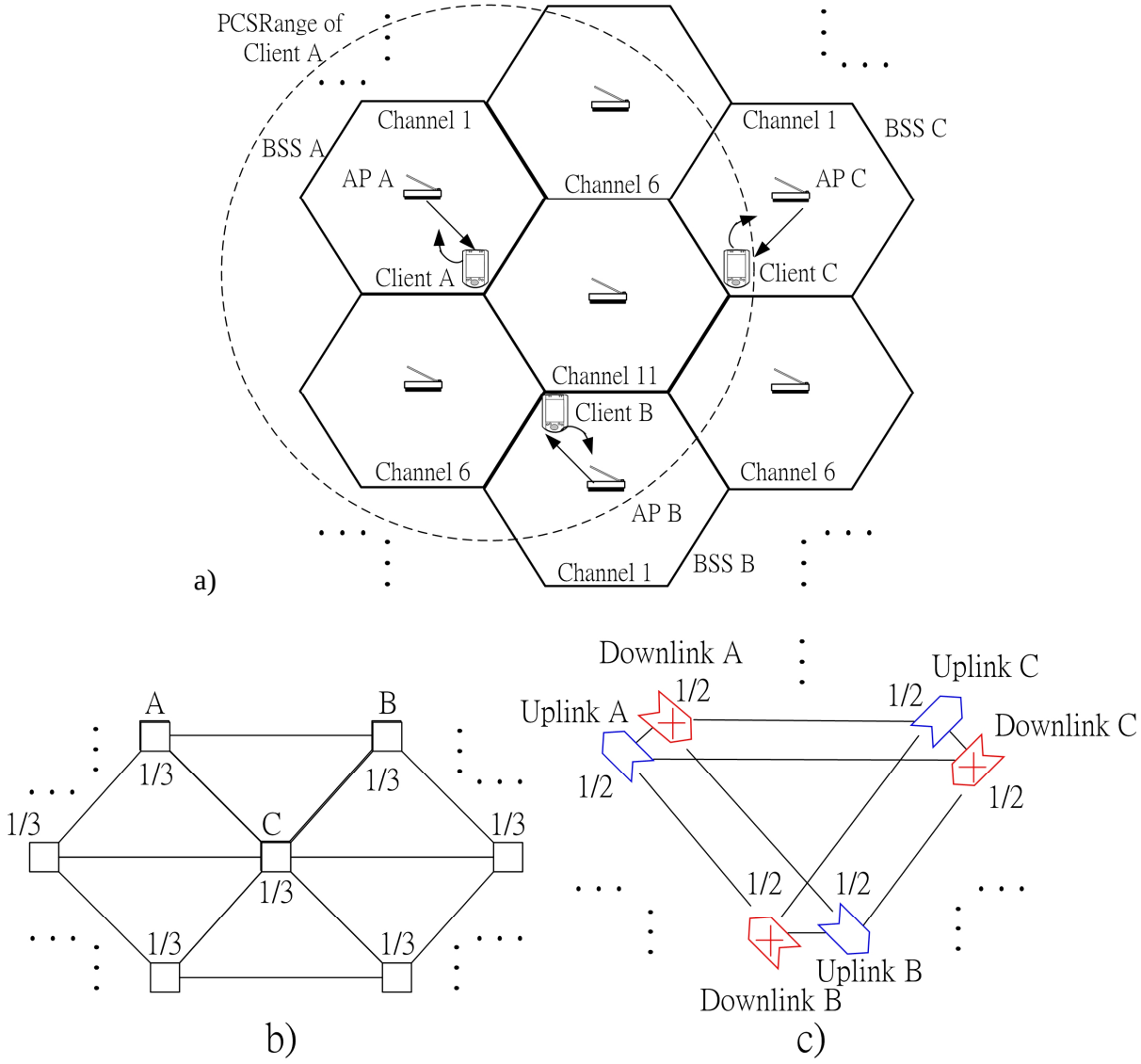


Figure 4.19. Mapping of a WLAN network a) to b) ARQ physical interference graph and c) coloured link-directional interference graph

4.5.1. Capacity Limitations in WLAN

There are three factors which limit the capacity of a BSS to reach its maximum achievable throughput: 1) channel sharing between two closely packed BSSs which use the same or over-lapping transmission channels, 2) the exposed-node problem, and 3) the hidden-node problem.

For 1), when two access points (AP) are within the physical carrier-sensing range (*PCSRange*) of

each other, they take turns to transmit and thus share the channel capacity. Figure 4.20a shows an example. APs A and B using the same transmission channel are within the *PCSRange* of each other. When access point (AP) A is sending DATA to client A, AP B senses the signal and halts its transmission process until the transmission of access point (AP) A completes. Therefore, the placement of APs can severely degrade the achievable throughput of a WLAN. However, it can be solved by careful channel planning. Figure 4.20b shows an example for the 802.11b/g. APs A and B are separated by a distance larger than the *PCSRange*. Since they cannot sense the signals from the other, simultaneous transmissions are now permitted. The throughput degradation caused by 1) can be improved by proper channel assignments. However, those induced by factors 2) and 3) remain even when APs using the same channel are separated by a distance larger than the *PCSRange.*

For 2), possible simultaneous transmissions are prohibited by the protocol due to the exposed-node problem. Figure 4.21 shows an example. When client B is sending data to AP B, client A senses the channel as busy since client B is within the *PCSRange* of client A. Thus, client A stops its transmission process until client B finishes its transmission. Therefore, clients A and B have to take turns to transmit and share the channel capacity. This, again, significantly limits the achievable throughput. In fact, clients A and B can transmit concurrently since the signal strength from client A (B) is much stronger than that from client B (A) at AP A (B).

For 3), collisions can be induced by the hidden-node problem. Figure 4.21 shows a scenario. When client D is sending DATA to AP D, client C senses the channel as busy while AP C senses the channel as idle since client D is inside the *PCSRange* of client C but outside that of AP C. Once AP C senses the channel as idle, it may count down its back-off contention window until zero and transmit DATA to client C. If the transmission from client D is still in progress, client C will continue to sense the channel as busy, and it will not receive the packet from AP C. As a result, client C will not return an ACK to AP C. This causes a collision. AP C then times out and doubles the contention window size for retransmission later. Meanwhile, client D transmits the packet

successfully and is not aware of the collision at client C. For the next transmission, client D keeps using the minimum contention window size. The hidden-node problem favours BSS D while BSS C suffers severe throughput degradation.

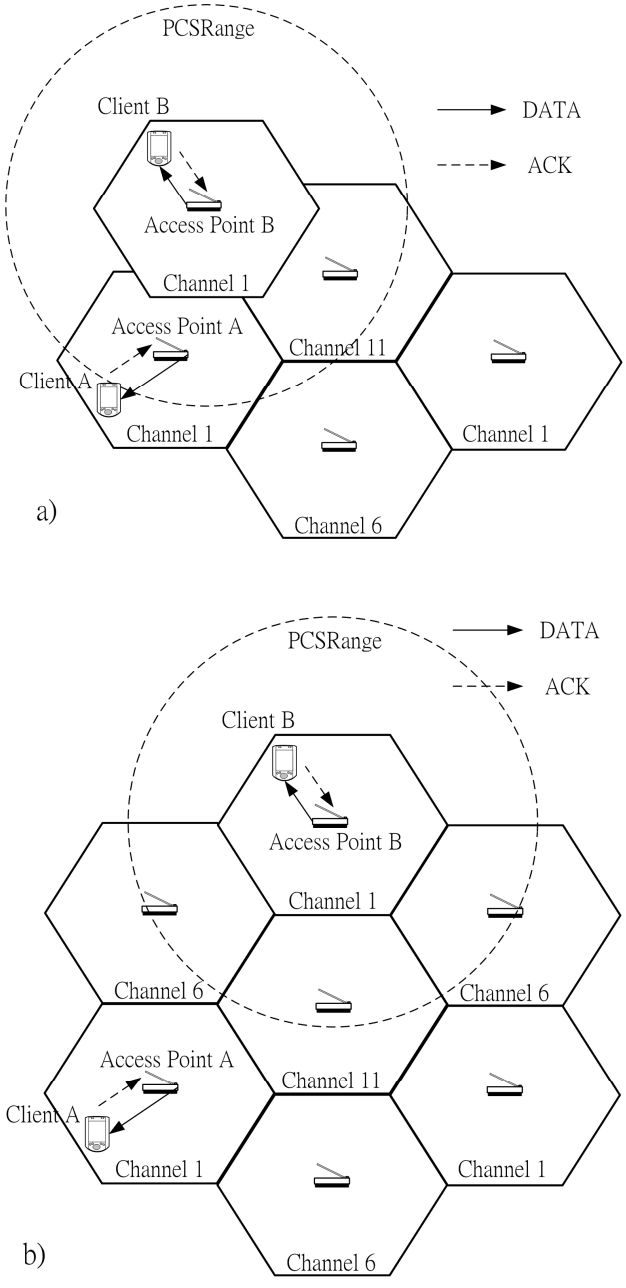


Figure 4.20. a) Interference between neighbour APs sharing the same channel; and b) assigning non-overlapping channels for neighbour APs to avoid interference

The above scenarios have been simulated in NS-2 [102] simulator with the parameter settings as listed in Table V. Real-life experimental work in Appendix A has shown that the NS-2 simulator does not contain major deficiencies. Data and basic rates set at 12Mbps (802.11g, OFDM, 1/2 coding rate, QPSK), without the RTS/CTS mechanism. A two-ray ground propagation model is used [96]. In the simulations, all data sources are TCP (transport control protocol) traffic streams with fixed packet size of 1460bytes. In an isolated BSS with an AP and a wireless client, the maximum achievable TCP throughput is 3.88Mbps. This is used as a benchmark for comparing the throughput degradations caused by factors 2) and 3). Appendix B shows an example of how to create a network scenario for simulations. The system parameters as listed in Table V, network topology, traffic flows are set in the simulation script.

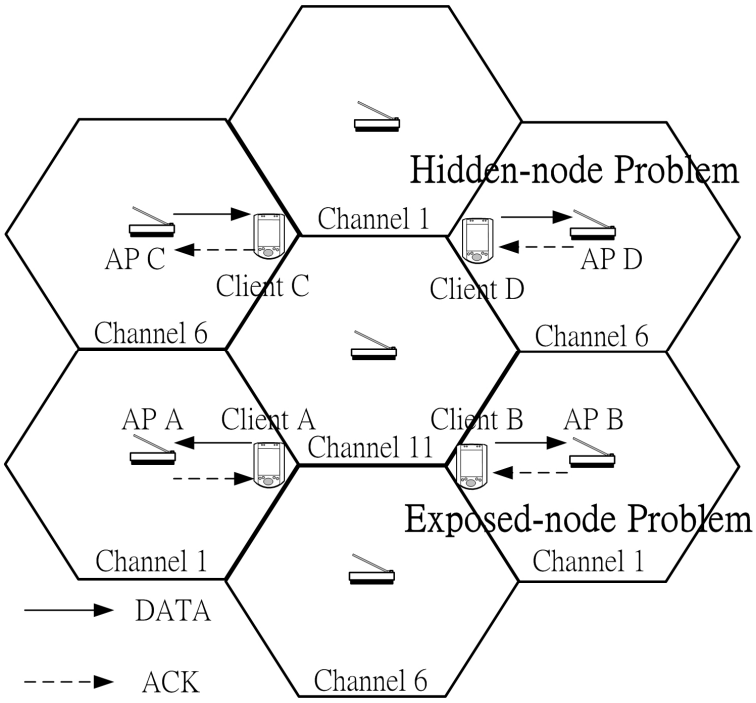


Figure 4.21. Exposed-node and hidden-node problems between co-channel BSSs

Table V. System Parameters Assumed in the Simulations

Data rate and basic rate	12 Mbps
Propagation model	Two-ray ground
Transmission range	250 m
SIR Capture threshold (CPThreshold)	10 dB
Interference range (InRange)	445 m
Physical carrier sensing range (PCSRange)	445 m
Data packet size	1460 bytes

Figure 4.22 shows the simulation results of the throughput degradations caused by factors 2) and 3). For 2) as shown in Fig. 4.21, AP A obtains a throughput of 1.8Mbps while AP B achieves a throughput of 1.9Mbps. Comparing to the benchmark throughput (3.88Mbps) of an isolated link, APs A and B suffer 54% and 51% throughput degradations respectively. They thus share the network capacity. For 3), client C has a throughput of 0.8Mbps while AP D attains a throughput of 2.9Mbps. They suffer 79% and 25% throughput degradations respectively. Both factors 2) and 3) significantly degrade network capacities of WLANs even though BSSs are separated by the maximum physical distance in appropriate AP placements with proper channel assignments.

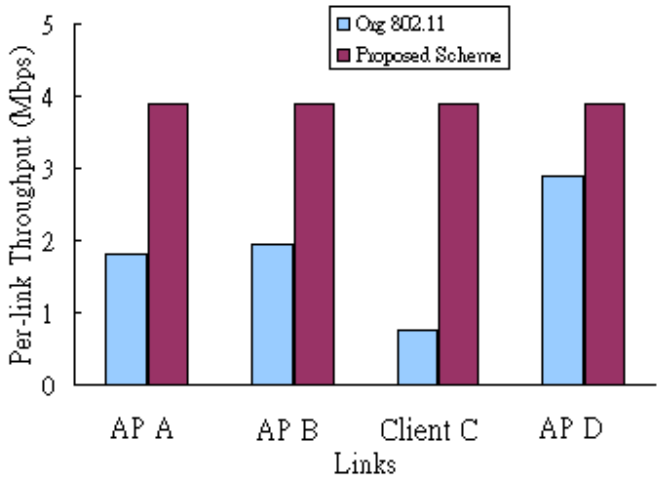


Figure 4.22. Simulation results of TCP per-link throughputs of the original 802.11 protocol and the proposed scheme in term of the per normalized channel in the exposed-node and hidden-node scenarios as shown in Fig. 4.21

4.5.2. Proposed Solution

The previous sub-section has shown that the capacity of a WLAN can be restricted by the hidden-node and exposed-node problems even under proper AP placements and careful channel assignments. In this sub-section, a solution is proposed for these issues. Multi-carrier code division multiple access (MC-CDMA) is used to create two orthogonal streams for each channel. Each wireless AP or client uses one stream for transmission and the other for reception.

Consider two orthogonal streams 1A and 1B are generated for channel 1 in the 802.11g. The main idea is to assign one stream (e.g. stream 1A) for down-link and the other (e.g. stream 1B) for up-link traffic in a BSS. This can effectively eliminate the hidden-node and exposed-node problems by increasing the distance from the interfering traffic to the receivers. Figure 4.23 shows the stream assignments in the same scenario as Fig. 4.21.

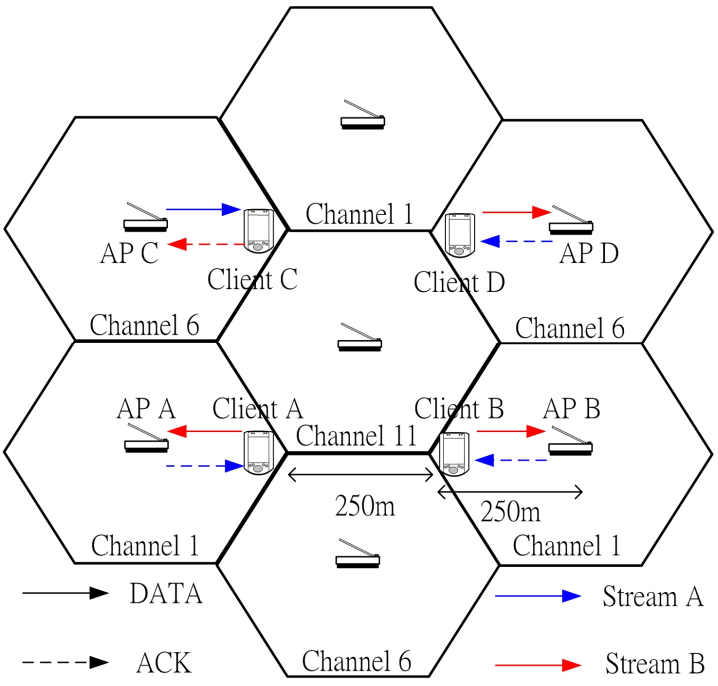


Figure 4.23. Eliminating the exposed-node and hidden-node problems by the proposed channel assignment scheme

4.5.2.1. Exposed-node Problem

To eliminate the throughput degradation caused by factor 2), the exposed-node problem as mentioned in sub-section 4.5.1., APs A and B use stream 1A for sending down-link packets to their clients while clients A and B use stream 1B for transmitting up-link packets, no matter the traffic are DATA or ACK. When client B is sending packets to AP B via stream 1B, client A can capture the signal but cannot decode it since client A uses another coding for stream 1A signal reception. Therefore, client A will ignore the signals from client B and transmit packets to AP A via stream 1B.

Consider the interference caused by client B on the signal reception of AP A. Let d_{A-iC} be the distance between A P A and client A in the same BSS, d_{A-eC} be the distance between AP A and client B in a neighbour BSS using the same transmission stream, and assume the SIR (signal-to-interference ratio) capture threshold (*CPThreshold*) is set to be 10dB. From [97], in a two-ray propagation model, assuming noise is negligible, if the signal-to-interference ratio at AP A is larger than the *CPThreshold*, it can decode the signal from client A when client B is transmitting. Similar to equation (2.1), that is,

$$SIR = (d_{A-eC} / d_{A-iC})^4 > CPThreshold$$

$$d_{A-eC} > 1.78 * d_{A-iC}. \quad (4.21)$$

In the worst case that AP A and client A are separated by the maximum transmission range ($d_{A-iC} = 250m$), AP A can capture the signal from client A if client B is located at more than 1.78*250m=445m away from AP A. With proper AP placements and channel allocations, client B is at least 500m away from AP A. Thus, AP A can receive the packets from client A successfully even though client B is transmitting at the same time. Simultaneous transmissions of clients A and B are now permitted. Figure 4.22 shows the simulation results of the proposed solution. Both BSSs A and B obtain their maximum achievable throughputs (3.88Mbps).

4.5.2.2. Hidden-node Problem

To get rid of the hidden-node problem (factor 3 in sub-section 4.5.1.), orthogonal streams are assigned for the transmissions of the hidden-node and the receptions of the suffering node. As shown in Fig. 4.23, client D (the hidden-node to AP C) is transmitting packets to AP D through stream 6B while client C (the suffering node) is receiving packets from AP C via stream 6A. Client C can receive both signals from AP C and client D. However, it can only decode the signal from AP C for packet receptions. This prevents collisions between two signals and thus eliminates the hidden-node problem.

In addition, client C can also receive the down-link transmissions from AP D via stream 6A. However, the signal from AP D is more than 10dB weaker than that from AP C because AP D is more than the maximum interference range (455m) away from client C. As a result, client C can receive packets from AP C successfully even if client D and AP D are transmitting packets at the same time. As shown in Fig. 4.22, both client C and AP D can now obtain their maximum achievable throughputs (3.88Mbps).

4.5.3. Hardware and MAC Requirements

Previous sub-sections have assumed the *PCSRange* (physical carrier-sensing range) is equal to the maximum interference range (*PCSRange*= *InRange*=1.78*TxRange*). *PCSRange* smaller than *InRange* is inefficient in preventing collisions. Thus, *PCSRange* is usually set to be equal or larger than *InRange.* This sub-section considers the hardware and MAC requirements when *PCSRange* is larger than *InRange.* The size of *PCSRange* can be separated into two cases:

A) $InRange \le PCSRange < 2 \cdot TxRange$; and

B) $PCSRange \ge 2 \cdot TxRange$

Since APs are placed at the centers of BSSs, they experience less interference than wireless clients

located at the edges of BSSs. Let say there are two neighbour BSSs, L and M, both using Channel 1. BSS L (M) has a AP L (M) using stream 1A for down-link transmissions and stream 1B for receptions while client L (M) using stream 1B for up-link transmissions and stream 1A for receptions. For each case, the worst case scenario is considered as shown in Fig. 4.24 with two clients located at the edges of BSSs L and M such that they are in the closest distance to each other.

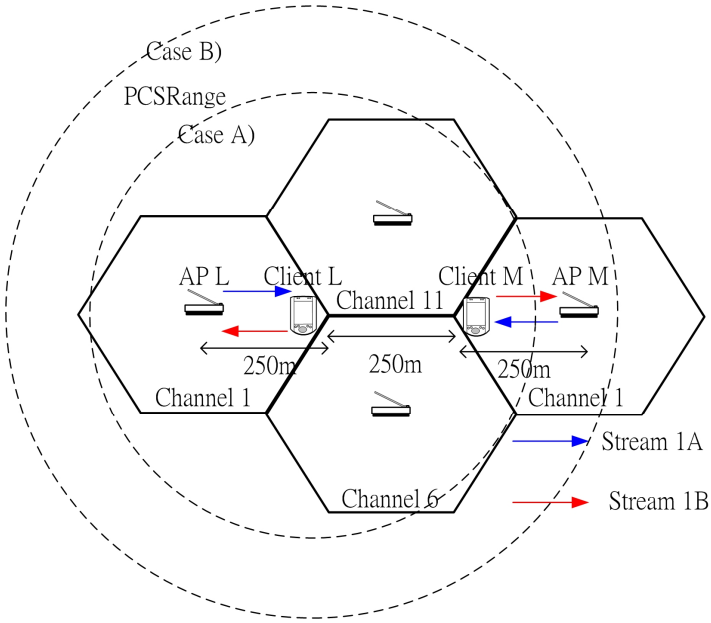


Figure 4.24. Various settings of physical carrier-sensing range in a WLAN

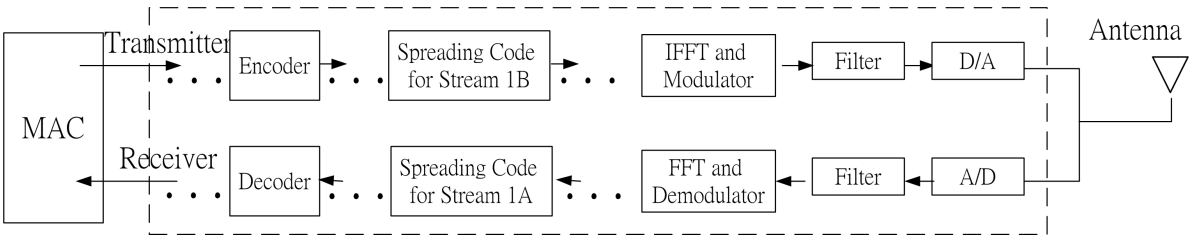


Figure 4.25. Parts of the hardware chip set used for the proposed scheme [115][116]

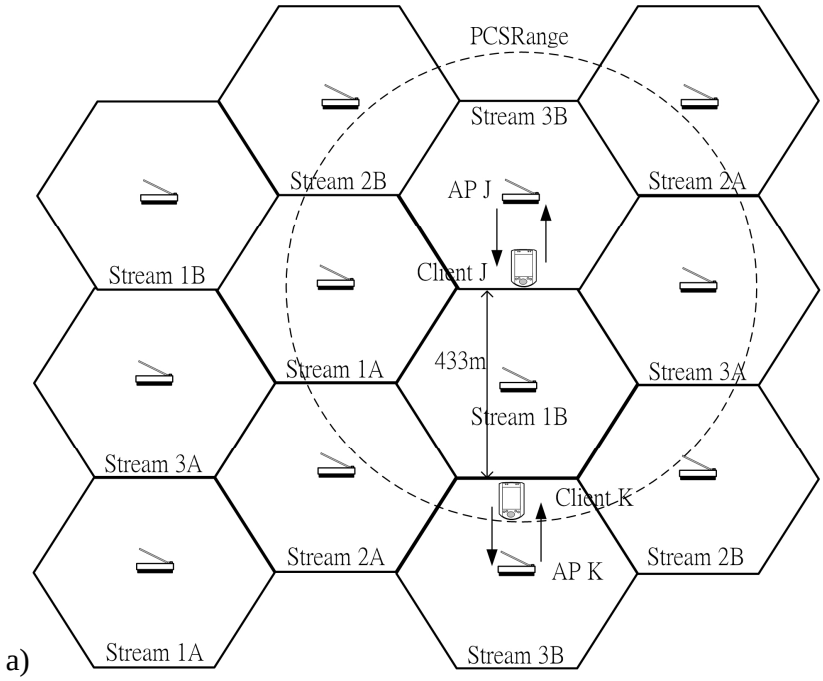
For case A), these settings are the same as the situation that have been discussed in previous sub-sections. Since client L in BSS L is at least $2 \cdot TxRange$ away from AP M, client L cannot sense

the signal from AP M via stream 1A. Thus client L can keep sending data to AP L even when AP M is transmitting. When client M is transmitting via stream 1B, client L cannot decode the signal because it uses stream 1A for reception. It will simply ignore the signals from client M and thus both BSSs L and M can transmit simultaneously. In this scenario, the original 802.11 MAC protocol is used without modifications. However, a decoder for one stream (e.g. stream 1A) and an encoder for another stream (e.g. stream 1B) are needed in each wireless node. An example of a wireless client is shown in Fig. 4.25 [115][116].

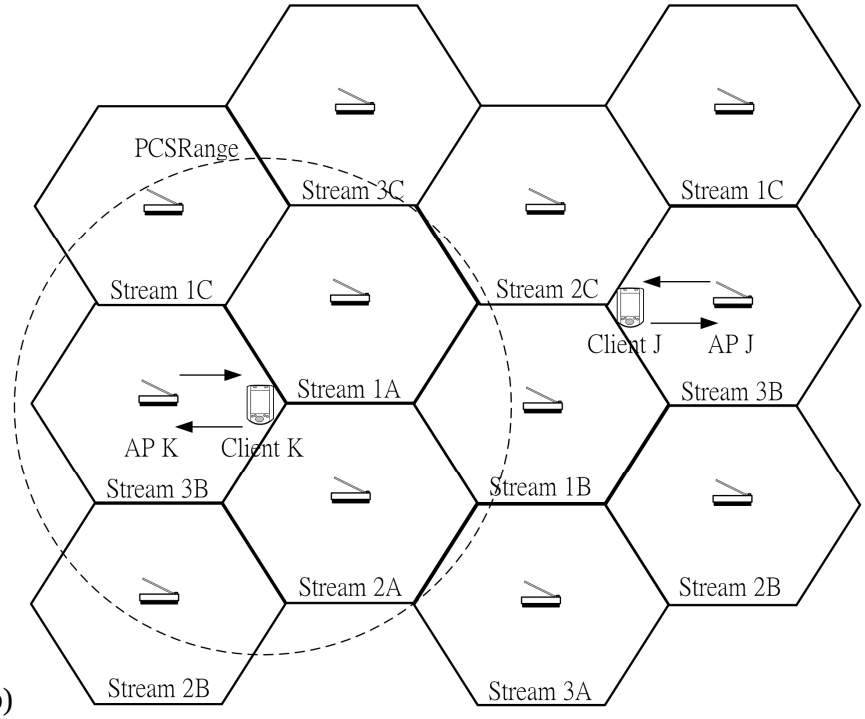
For B), this is the assumption widely adopted by previous work in the literature. In the NS-2 simulator [102], the default setting is $PCSRange \approx 2.2 \cdot TxRange$. The real-life experimental results of reference [97] showed that Buffalo WLI2-CF-S11 IEEE 802.11b Wireless LAN card has similar $PCSRange$ setting. When $PCSRange > 2 \cdot TxRange$, the hardware and the MAC protocol of wireless nodes have to be modified.

For the transmission process, client L can now sense the transmissions from AP M via stream 1A. With the original 802.11 MAC protocol, client L will then halt its transmission process and wait for the completion of the sensed signal. In this way, BSSs L and M cannot have concurrent transmissions. This is because client L cannot identify the source of the sensed signal. If the signal is from AP L, client L should halt its transmission process to prevent collisions within BSS L. On the other hand, if the signal is from AP M, client L can actually transmit at the same time without causing interference. A possible solution is to identify the source based on the received signal strength. Since the distance between an associated AP and its wireless clients are much shorter than the distance between those clients and other neighbour APs. A signal strength threshold (*SSThreshold*) can be set to identify the sensed signal. If $SIR < SSThreshold$, the signal will be discarded and clients will carry on their transmission procedures. On the other hand, if $SIR \geq SSThreshold$, most likely the signal is from the associated AP and thus client will halt its

transmission until the Network Allocation Vector (NAV) expires.



a)



b)

Figure 4.26. Assigning one of the orthogonal data streams to each BSS; a) interference between APs sharing the same channel stream when spreading factor SF=2; b) APs K and J can transmit simultaneously when spreading factor SF=3

For the signal reception at client L, the signal from AP M may overlap with those from AP L to induce collisions even though the signal from AP M is more than *CPThreshold* (10dB) stronger than the signal from AP L. This is because, under the original 802.11 protocol, the success of the signal reception depends on the signal arrival order. According to reference [97], in most of the commercial 802.11 products and in the NS-2 simulator, if client L senses the signal from AP M, it will then consider the channel as being busy. In that case, a newly arriving packet from AP L will be ignored even if it is more than *CPThreshold* stronger than that from AP M. This will cause a collision at client L. To remove this problem, a possible solution is to use a specific chip set with "re-start mode". In some commercial 802.11 chips (e.g., Atheros Chip [97]), if the receiver is in the midst of receiving a signal, another signal with sufficiently large power margin arrives (e.g. 10dB stronger), the receiver will switch to receive the new signal. The receiver can then receive the packet successfully. For more details about the "restart-mode", the interested reader is referred to sub-section 2.2.2 and reference [91]. In summary, when $PCSRange > 2 \cdot TxRange$, the proposed scheme requires 1) the SSThrehold setting in the MAC protocol for signal strength comparisons and 2) the adoptation of chip sets with "restart-mode".

4.5.4. Why Not Assign One Data Stream to One BSS?

In the proposed scheme as mentioned in sub-section 4.5.2., two orthogonal data streams are assigned to each BSS, one stream for up-link traffic, the other for down-link. Another way to allocate channels is to set each of the six independent streams (three channels, each with two orthogonal streams) to different BSSs for both up-link and down-link traffic. Figure 4.26a shows an example of this channel allocation. In this way, clients J and K are still within the *PCSRange*(=*InRange*) of each other. This will induce the previously mentioned exposed-node and hidden-node problems and cause throughput degradations. Therefore, with this scheme, two orthogonal data streams for each channel are not sufficient to separate BSSs. Three orthogonal streams (SF=3) are needed indeed for each

channel to yield nine independent streams in total. Then, channels can be assigned as shown in Fig. 4.26b. The distances between BSSs using same stream are now large enough to avoid interference. Note that here the more data streams are used the higher is the complexity for the decoder and encoder in the transceiver which in turn consumes more power. Power consumption has to be considered, particularly when handheld devices like PDAs or mobile phones are used as the mobile clients since they have limited battery capacities.

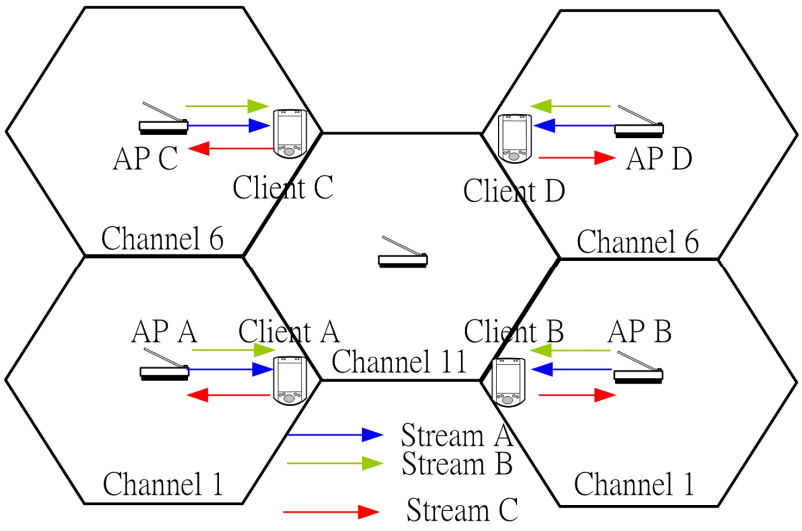


Figure 4.27. Assigning two streams for downlink traffic and one for uplink with the proposed scheme and SF=3

Assume three orthogonal data streams per channel can be obtained without the considerations of chip set complexity and power consumption. Let *T* be the maximum throughput that can be achieved by TCP traffic in a BSS with one stream. When one stream is allocated to each BSS (as shown in Fig. 4.26b), the maximum throughput of each BSS would be *T*. There is another method of channel allocation (as shown in Fig. 4.27) which is to assign three data streams for each BSS with the proposed scheme, two streams for down-link traffic and one for up-link. This can eliminate the exposed-node and hidden-node problems while achieving throughput more than *T* per BSS,

particularly when there are more down-link traffic than up-link in WLAN (wireless local area network). To achieve this, however, the 2x2 transmitter-receiver antenna arrays are required.

4.5.4.1. IEEE 802.11a

Another possible way to achieve the proposed scheme as well as increasing capacities is to group the twelve orthogonal channels of the 802.11a into three groups, each with four channels. By using a system with three transmit antennas and three receive antennas, three channels can be assigned for down-link traffic and one for up-link per BSS. Since pre-802.11n products (e.g. [118]) with multiple transmit and receive antennas has already been brought to the market, they can be modified to attain the proposed scheme. This can sufficiently increase the achievable throughput of a BSS without using MC-CDMA decoder/encoder in hardware chip sets.

4.6. Conclusion

This chapter has focused on channel allocations in the infrastructure networks (wireless local area networks). The link-directional interference graphs (l-graph) is presented to refine the interference relationships between directional links. A colouring algorithm has been applied to l-graphs to provide insights into transmission scheduling or channel allocation in time division multiple access (TDMA) or frequency division multiple access (FDMA) ad-hoc networks respectively. The proposed scheme can increase network capacity to 2 times with respect to a single-channel protocol in a triangular topology and 1.33 times in a lattice topology. Simulations also showed that more than 1.7 times capacity improvements can be achieved with a distributed link-directionality-based dual channel protocol when compared to the single-channel 802.11 protocol. It is believed that this is the first time in the literature to take into account the link-directionalities in interference graphs.

A generic approach for capacity analysis has also been proposed to justify the capacity advantage of using link-directionality in a network topology. This approach shows that the concept of

link-directionality is not limited to the propagation model, channel model, modulation scheme and medium access control (MAC) protocol assumed in the simulations in this thesis. In fact, link-directionality can be adopted with other network models, protocols and parameter settings. The achievable network capacity obtained by this approach for a given network can then be compared with the single-channel scheme. This allows one to determine whether channel allocations according to link-directionalities should be applied to the given network.

Based on the insight of colouring link-directional interference graph, the exposed-node and hidden-node problems between co-channel basic service sets (BSS) in wireless local area networks (WLAN) can be eliminated. In the proposed scheme, two orthogonal data streams are generated for each channel by using multi-carrier code division multiple access (MC-CDMA). They are then individually assigned for transmitting up-link and down-link traffic of a BSS. Simulations have showed that the proposed scheme can improve network throughputs to 2.06 times in an exposed-node scenario and to 2.13 times in a hidden-node scenario when compared to the single-channel 802.11 protocol.

5. Conclusion & Future Work

5.1. Conclusion

This thesis has proposed a novel approach to assign channels to links for simultaneous transmissions based on their link-directionalities. This concept has been applied to carrier sense ad-hoc networks and infrastructure network (wireless local area networks WLAN) in order to 1) increase network capacities of ad-hoc networks in the order of magnitude and 2) eliminate interference in WLANs. It has been shown that the proposed schemes can be implemented with the well-defined industrial standard (IEEE 802.11).

For 1), in Chapter 2, a dual-channel link-directionality-based MAC protocol (DCP) has been proposed. It has been shown that the scheme can increase the network capacities of single channel IEEE 802.11 ad-hoc networks to 2.83 times in a lattice topology, 2.13 times in an irregular topology and more than 1.7 times in large-scale random network topologies with respect to the single-channel 802.11 protocol. The capacity improvements are achieved by splitting the transmission and reception channels of each node of links. Nodes using the same reception channel can then be packed closer to each other since their transmissions are in another independent channel.

In Chapter 3, the SIR (signal-to-interference ratio) comparison algorithm (SCA) has been implemented with the proposed scheme (DCP) in chapter 2. This algorithm inserts the SIR information of the received request-to-send (RTS) and clear-to-send (CTS) packets in the MAC header of the replied packets (CTS/DATA). Nearby links can then decide their transmission processes based on the physical interference constraints instead of the receptions of RTS/CTS packets as in the original 802.11 protocol. It releases the protocol constraints imposed by the virtual carrier-sensing mechanism. The performance improvements achieved by DCP and SCA have been

analyzed. DCP can outperform SCA in long intra-link distances (the distance between the transmitter and the receiver of a wireless link) while SCA outweighs DCP in short intra-link distances. Integrating these two algorithms allows the protocol to compensate for the downside of each other. Simulations have shown that the integrated scheme (DCPwSCA) can increase the network capacities of single-channel IEEE 802.11 ad-hoc networks to 4.3 times in lattice and 2.13 times in random topologies when compared to the single-channel 802.11 protocol.

For 2), in Chapter 4, the link-directional interference graph (l-graph) has been presented to refine the interference relationships between directional links. A colouring algorithm can then be applied to l-graphs to provide insights into transmission scheduling or channel allocation. The proposed scheme can increase network capacity to 2 times in a triangular topology and 1.33 times in a lattice topology. According to the insight of colouring link-directional interference graph, a scheme has been proposed to eliminate the exposed-node and hidden-node interference between co-channel basic service sets (BSS) in WLANs. Two orthogonal data streams generated by multi-carrier code division multiple access (MC-CDMA) are individually assigned for transmitting up-link and down-link traffic of a BSS. Simulations have showed that the proposed scheme can improve network throughputs to 2.06 times in an exposed-node scenario and 2.13 times in a hidden-node scenario with respect to the single-channel 802.11 protocol.

It is believed that this research is the first to propose splitting channels based on link-directionalities in carrier sense wireless networks. Although this thesis has focused on carrier sense wireless networks, similar schemes with the concept of link-directionality can be applied to other wireless networks for capacity enhancements. This has been demonstrated by the generic approach for capacity analysis in sub-section 4.4. It shows that the concept of link-directionality can

also be adopted with other network models, protocols and parameter settings. It is possible that the advantages of link-directionality could be diminished due to network topologies and link packing densities, particularly when links are densely packed together. Therefore, the achievable capacity obtained by the generic approach allows one to determine whether channel allocations according to link-directionalities should be applied to a given network.

5.2. Future Work

5.2.1. Further improvements on the proposed algorithms

In Chapters 2 and 3, the link-directionality-based dual channel protocol (DCP) and signal-to-interference ratio comparison algorithm (SCA) have been proposed to increase the network capacity of carrier-sense wireless ad-hoc networks. The simulations have shown that network throughputs can be improved significantly. However, there are other algorithms and factors which can be added or fine tuned to further scale the network capacity. This sub-section outlines some of them which require further research.

a) Adaptive Physical Carrier-Sensing

References [65][66] proposed a tunable sensing threshold to avoid interference in 802.11 mesh networks without using request-to-send/clear-to-send (RTS/CTS) frames for virtual carrier-sensing. To maximize spatial reuse, the sensing threshold can be set to allow successful simultaneous transmissions while preventing transmissions that will lead to collisions. Simulations in [65][66] showed that the algorithm can increase the aggregate network throughput. This approach of adaptive physical carrier-sensing can be integrated with the proposed algorithms in Chapter 3 so that links within Region II (as shown in Fig. 3.2) can be packed even closer to link A for concurrent transmissions to increase the capacity.

b) Impacts of Data Rate and Capture Threshold

In Chapter 3, the simulations assume that the data rate is set to 12Mbps. Reference [67] reported that adjusting this value can have sufficient impacts on the network capacity. Transmission range (*TxRange*) and interference range (*InRange*) can be reduced by increasing the data rate. If the capture threshold (*CPThreshold*) remains unchanged, links within Region II (as shown in Fig. 3.2) can be packed closer to link A and thus increase the network capacity.

When data rates of links vary, Capture Threshold (*CPThreshold)* can be adjusted by an adaptive physical carrier-sensing algorithm [67] to further increase the network capacity. For example, a link with a lower data rate requires a smaller *CPThreshold*. According to equation (3.2), the interference range (*InRange*) can be reduced and thus links within Region II (as shown in Fig. 3.2) can then be packed closer to link A for simultaneous transmissions. This, again, can further improve the network capacity.

c) Using more than Two Orthogonal Channels

Since the proposed protocol requires a pair of independent channels for a link so that each channel is used to send frames in one direction, *four* channels are needed to form two pairs while 802.11b only provides three orthogonal channels. However, references [35][36] showed that the use of partially overlapped channels is not always harmful. In that case, if four channels (say channels 1, 2, 3 and 4) are available without causing interference effects, the extra pair of channels (channels 3 and 4) can be assigned to another link for simultaneous transmissions within the interference range (*InRange*). This can further improve the network capacity. Further work is required to modify the proposed protocol to allocate these additional channels. For example, if $S_{Ti->Ri} /(I_{Ti->Ri} + Power_{Tj->Ri}) \leq CPThreshold$ as derived in sub-section 3.1.1, the proposed algorithm will then assign link *j* to use the extra pair of channels for transmissions.

d) Impacts of Transmit Power and Antenna Gain

It can be observed that the network capacity can be increased by the proposed protocol even if nodes use different powers and antenna gains. For links within Region I as shown in Fig. 3.2, the protocol use availabilities of receptions of RTS/CTS frames to allocate channels for simultaneous transmissions. This algorithm is independent of the received powers and thus should work under

scenarios with various transmit powers and antenna gains. For Region II as shown in Fig. 3.2, the signal-to-interference ratio comparison algorithm (SCA) uses received powers for power comparisons which have already taken the transmit powers and antenna gains into account. Here is an example in which nodes T_A and R_A in Fig. 3.2 have smaller transmit powers and antenna gains than nodes T_B and R_B. R_A adds the received signal strength $S_{TA->RA}$ and interference level $I_{TA->RA}$ into its MAC header of the replied CTS. $S_{TA->RA}$ and $I_{TA->RA}$ have already counted the smaller transmit power and antenna gain of link A. T_B receives the CTS from R_A and records the received Power $Power_{RA->TB} \approx Power_{TB->RA}$ for power comparison. Again, $Power_{RA->TB}$ has already taken into account the smaller transmit power and antenna gain of R_A. T_B can then decide its channel for simultaneous transmission. Thus, the proposed protocol can still perform to scale the capacity even if nodes use different powers and antenna gains in the network.

5.2.2. Integrating with other enhancement schemes and applying in other wireless networks

This thesis forms the foundation for many possible research areas. They can be classified into two categories: 1) further capacity improvements by integrating with other performance enhancement schemes; and 2) applying the proposed approach in other wireless network scenarios. Moreover, real-life experiments may also help to verify the results and provide further insights.

1. Integrating with other performance enhancement schemes

   There are many potential solutions that can further improve the capacity limit achieved by the proposed scheme. Here are some examples:

   a) Power Control

   When two nodes of a link are not separated by the maximum transmission range, it is unnecessary to transmit packets with the largest transmission power. Instead, a power control

algorithm (e.g. [43][46][47]) which assigns appropriate transmission powers to links can reduce inter-link interference and extend the service life of devices in wireless sensor networks. It could be implemented on top of the signal-to-interference ratio SIR comparison algorithm (SCA) and adjust the transmit power of nodes based on the SIR information included in the MAC headers. More simultaneous transmissions could then take place to achieve even higher network capacities.

b) Multiple-input-multiple-output (MIMO)

In the original wireless local area network (WLAN) with MIMO, a base station sends independent streams simultaneously to its wireless clients to increase the link data rate [64] [62]. This can sufficiently improve the network throughput in a WLAN. However, when more base stations are deployed, the interference from nearby base stations may induce the hidden-node problem which can largely degrade the network throughput. Instead of transmitting all independent streams concurrently, nodes may choose some of the streams based on their link-directionalities to get rid of the inter-cell interference and the hidden-node problem as demonstrated in sub-section 4.4.4. The allocation of data streams for uplink and downlink traffic requires further studies, particularly under various traffic flow scenarios.

c) Directional Antennas

Smart antennas can selectively receive signals from a certain desired direction to avoid unwanted interference. This may increase the network capacity. However, they also provide higher gain for greater transmission range by beam-forming toward a desired direction [35][36][119]. In other words, they may induce larger interference distances in a specific direction. When implementing with the proposed link-directionality-based protocol, links need to be separated by larger distance for simultaneous transmissions along the desired direction of

antenna while links in other angles may be allowed to pack closer together. Further studies are required to evaluate the trade-off. The choices of antenna angle and signal gain will have significant impacts on the network performance.

d) Routing

Most of the ad-hoc routing algorithms in the literature used "the smallest hop count" (the shortest path) to select transmission routes (e.g. [120][121]). Two traffic sources may choose the same route with the smallest hop count to their destinations. In that case, they have to share some of the intermediate nodes of their routes. This may induce severe traffic congestions on these nodes. Therefore, researchers have attempted to develop methods [122][123] to scatter routes to get rid of these potential traffic congestions. With the link-directionality-based protocol, routing algorithms may not need to disperse traffic routes as far as using 802.11 MAC since the proposed scheme can allow closer packing of simultaneous transmission nodes.

2. Applying the proposed approach in other wireless network scenarios

The concept of link-directionality is not restricted for use in carrier sense wireless networks, but may also be applied to sensor networks [52][53], mesh networks [54][55], ultra-wide-band (UWB) networks [124][125] optical wireless networks [126][127]. Since most of the communications in these data networks involve bi-directional traffic, splitting the transmissions of DATA and ACK into separate channels as demonstrated in this thesis may increase the overall network throughputs.

Furthermore, supporting multimedia or voice applications [20][128] with tight quality-of-service (QoS) requirements (e.g. delay and bandwidth) in wireless networks [129][130] is challenging. Many of these applications are built on TCP (Transport Control Protocol) or UDP (User Datagram Protocol) transport-layer protocols. These protocols, however, may not perform well

in wireless networks since they were mainly designed for wired networks which have very low bit-error rates. Previous work has showed that they may trigger some performance problems such as instability or throughput degradation [76]. Extensive research (e.g. [131][132][133]) has been carried out in this area to modify transport-layer protocols for the use in wireless networks. When applying these schemes with the proposed protocols, transport-layer parameters such as congestion window size or steady state threshold may have to be fine tuned for fully exploiting the potential network capacity.

Finally, it is believed that a key step to transfer a technology into practical use is to test it through real-life experiments. Insights obtained from experiments can help further refine this research work.

Appendix A. Verification of NS-2 Simulator

To verify the accuracy of the NS-2 simulator, a real 6-node multi-hop network is set with six symmetric DELL Latitude D505 laptop PCs with 1.5GHz Celeron Mobile CPU and 512MB RAM at the Chinese University of Hong Kong. Each node has a Buffalo WLI2-CF-S11 IEEE 802.11b Wireless LAN card (as shown in Fig. A.1). All nodes run RedHat Linux 9 with HostAP [134] driver. To facilitate experimentation, the transmission power of each WLAN card is set to a small value (-38dBm), with basic and data rates set at 11Mbps. The transmission range is set to TxRange $\approx$ 2m and the carrier-sensing range CSRange $\approx$ 5m=2.5*TxRange by following similar approaches as mentioned in [135]. The routing table of each node is fixed and the distance between successive nodes is set to 2m. The data sources are UDP traffic streams with fixed packet size of 1460bytes. Figure A.2 shows the results obtained by simulations and real-life experiments. It shows that the simulation throughputs match closely with the experimental measurements, indicating that NS2 simulations do not contain major deficiencies. The system parameters assumed in the simulations are listed in Table A.I.



Figure A.1. A 6-node multi-hop wireless network

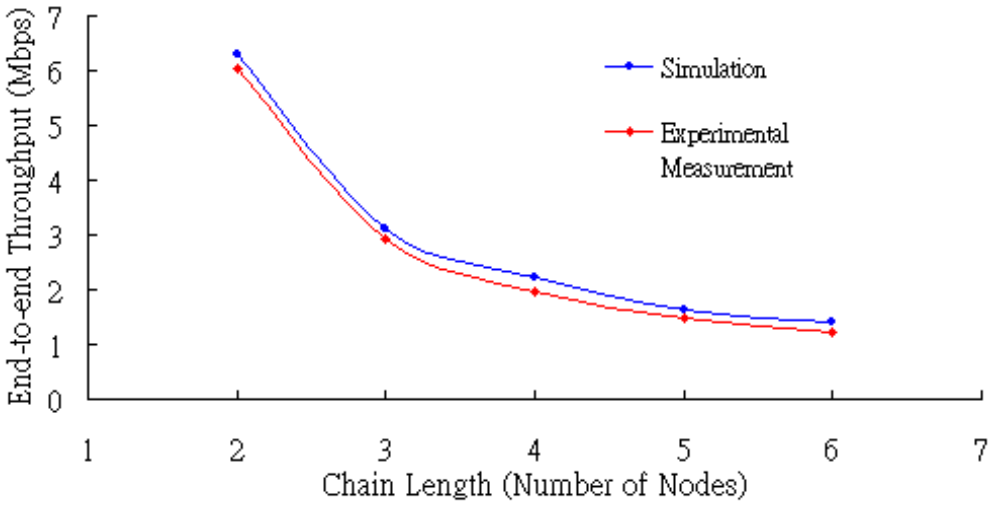


Figure A.2. End-to-end throughput versus number of nodes in a string multi-hop network with saturated traffic source

Table A.I. System Parameters Assumed in Simulations

Packet payload (*DATA*)	1460 bytes
UDP/IP header	20 bytes
MAC header	28 bytes
PHY header	24 bytes
ACK size	14 bytes
RTS size	20 bytes
CTS size	14 bytes
Data rate (DATA/ACK)	12 Mbps
Basic rate (RTS/CTS)	2 Mbps
PHY header bit rate	2 Mbps
Slot time σ	20 μs
SIFS	10 μs
DIFS	50 μs
$CW_{\min}$	31
$CW_{\max}$	1024
$CW_{average}$	310 μs
Retransmission Limit	7
Virtual Carrier-sensing Range (*VCSRange*)	550 m
Transmission Range (*TxRange*)	250 m
Capture Threshold (*CPThreshold*)	10 dB

Appendix B. Implementations of Algorithms in NS-2 Simulator

To conduct simulations for the proposed protocols in the NS-2 simulator, there are two major steps: 1) to implement the algorithms of the proposed protocols; 2) to generate the network topologies for simulations.

Step 1: To implement the algorithms of the proposed protocols

The proposed algorithms have been implemented in C/C++ language on top of the original source codes that came with the NS-2 simulator. It mainly involves mac-802_11.h, mac-802_11.cc, wireless-phy.h and wireless-phy.cc files. Here is an example for constructing the *SimTable* (Simultaneous Transmission Tables) as described in sub-section 2.1.2.i.

Codes	Descriptions

struct ProTable {
int From;
int To;
int RxRTSChannel;
int RxCTSChannel;
};
struct ProTable ProtocolTable[];
	To construct the SimTable structure with parameters representing the source, destination and transmission channels of RTS/CTS of the received packet.

int
WirelessPhy::sendUp(Packet *p)
{
……..
if
((subtype==MAC_Subtype_RTS)||(subtype==MAC_Subtype_CTS)) {
int found=0;
 	
for (int i=0;i<size;i++) {
if((ProtocolTable[i].From==p->txinfo_.getNode()->nodeid())&&(ProtocolTable[i].To==dst)) {
index=i;
found=1;
}
	To record or update the details of the received packet in the SimTable
	
	If the packet is a RTS/CTS frame,
	
	Step 1: the algorithm checks if it has previous record of this packet by comparing its source and destination.

else if ((i==size-1)&&(found==0)) {
size++;
index=i++;
ProtocolTable[index].From=-2;
ProtocolTable[index].To=-2;
ProtocolTable[index].RxRTSChannel=0;
ProtocolTable[index].RxCTSChannel=0;
}
}
	Step 2: if there is no record for this packet, a new row will be added to the *SimTable*.

if (size==0) {
size++;
index=0;
ProtocolTable[index].From=-2;
ProtocolTable[index].To=-2;
ProtocolTable[index].RxRTSChannel=0;
ProtocolTable[index].RxCTSChannel=0;
}
}
	If it is an empty table, a new row will be added to initiate the *SimTable*.

if(subtype==MAC_Subtype_CTS||subtype==MAC_Subtype_RTS) {	

if(subtype==MAC_Subtype_RTS) {
ProtocolTable[index].From=p->txinfo_.getNode()->nodeid();
ProtocolTable[index].To=dst;
ProtocolTable[index].RxRTSChannel=chl;
goto DONE;
}
	Step 3a: If the packet received is a RTS frame, the table will update the source, destination and receiving RTS-channel but leave the CTS-channel field as 0 (null).

if(subtype==MAC_Subtype_CTS) { ProtocolTable[index].From=p->txinfo_.getNode()->nodeid(); ProtocolTable[index].To=dst; ProtocolTable[index].RxCTSChannel=chl;	Step 3b: If the packet received is a CTS frame, the table will update the source, destination and receiving CTS-channel but leave the RTS-channel field as 0 (null).

if(ProtocolTable[index].RxRTSChannel==0||ProtocolTable[index].RxCTSChannel==1) {
pkt_recvd = 0;
goto DONE;
}
}
}
	Step 4: If either the CTS-channel or RTS-channel is 0 (null), the algorithm will declare the chance for simultaneous transmissions.

else if(subtype==MAC_Subtype_Data) {	If the packet is DATA or

goto DONE;
}
else if(subtype==MAC_Subtype_ACK) {
goto DONE;
}
	ACK frame, the algorithm will not update the SimTable.

Step 2: To generate the network topologies

Network topologies, traffic flows and settings are written with Tcl/Tk language in .tcl files. Usually after the simulation, NS-2 returns the result (e.g. UDP throughput). For other data (e.g. delay jitter), Perl scripts have to be written to extract information from the log file generated during the simulation. Here is an example for creating the lattice network topology described in sub-section 2.3.1.

Codes	Descriptions
Mac/802_11 set basicRate_ 2Mb Mac/802_11 set dataRate_ 12Mb Mac/802_11 set cwmin_ 31 Mac/802_11 set cwmax_ 1023	Initiate the transmission rate and contention window size settings of the 802.11 MAC (Medium Access Control) protocol
set val(rp) AODV set val(chan) Channel/WirelessChannel set val(prop) Propagation/TwoRayGround set val(netif) Phy/WirelessPhy set val(mac) Mac/802_11 set val(ifq) Queue/DropTail/PriQueue set val(ll) LL set val(ant) Antenna/OmniAntenna set val(ifqlen) 50 set val(nn) 36	Initiate the network settings, e.g., physical layer, routing protocol, channel model, propagation model, MAC protocol, antenna type. Generate 36 nodes in the network
set ns [new Simulator]	
set tracefd [open simple.tr w] $ns use-newtrace $ns trace-all $tracefd	Create the trace file
set f0 [open tput_vs_n_enhance.tr w]	
set topo [new Topography] $topo load_flatgrid 50000 50000	Set the physical size of the network area

```
create-god $val(nn)

set rng [new RNG]

set bw_past 0
set bw_now 0

$ns node-config -adhocRouting $val(rp) \
          -llType $val(ll) \
          -macType $val(mac) \
          -ifqType $val(ifq) \
          -ifqLen $val(ifqlen) \
          -antType $val(ant) \
          -propType $val(prop) \
          -phyType $val(netif) \
          -channelType $val(chan) \
          -topoInstance $topo \
          -agentTrace OFF \
          -routerTrace OFF \
          -macTrace OFF \
          -movementTrace OFF

   for {set i 1} {$i < $val(nn)+1 } {incr i} {
      set node_($i) [$ns node]
      $node_($i) random-motion 0
            set mac($i) [$node_($i) set mac_(0)]
            }

   for {set i 1} {$i < 13 } {incr i} {
      $node_($i) set Y_ [expr 1000.0+(($i-1)*250.0)]
      $node_($i) set X_ 21500.0
      $node_($i) set Z_ 0.0
       }

   for {set i 13} {$i < 25 } {incr i} {
      $node_($i) set Y_ [expr 1000.0+(($i-13)*250.0)]
      $node_($i) set X_ 20500.0
      $node_($i) set Z_ 0.0
       }

   for {set i 25} {$i < $val(nn)+1 } {incr i} {
      $node_($i) set Y_ [expr 1000.0+(($i-25)*250.0)]
      $node_($i) set X_ 21000.0
      $node_($i) set Z_ 0.0
       }
```

Assign each node with the MAC and physical settings as defined above

Assign the locations of nodes in the first row of the lattice topology

Assign the locations of nodes in the second row of the lattice topology.

Assign the locations of nodes in the third row of the lattice topology.

for {set i 1} {$i < 13 } {incr i} {
  set sink_($i) [new Agent/LossMonitor]
  $ns attach-agent $node_([expr $i*3-1]) $sink_($i)
	Create the traffic flow for 12 links

  set source($i) [new Agent/UDP]
  $ns attach-agent $node_([expr $i*3-2]) $source($i)
	Set the source and destination of each link

   $ns connect $source($i) $sink_($i)	

set rate 6.0
  set cbr($i) [new Application/Traffic/CBR]
  $cbr($i) attach-agent $source($i)
  $cbr($i) set type_ CBR
  $cbr($i) set packet_size_ 1460
	Set the data rate, traffic type and packet size of each link

set num [$rng uniform 0 1]
  $cbr($i) set rate_ [expr $rate+0.00001*$num]mb
  $cbr($i) set random_ false
  set num [$rng uniform 0 1]
  $ns at [expr 0.0001*$num+10.0] "$cbr($i) start"
  $ns at 12.0 "$cbr($i) stop"
}
	Start traffic flows with slightly time differences.

proc finish {} {
  global f0 f1 ns tracefd sink_ val
  $ns flush-trace
  close $tracefd
  set total 0
	Return simulation throughput results

  for {set i 1} {$i < 13 } {incr i} {
  set bw($i) [$sink_($i) set bytes_]
  set total [expr $total+$throughput($i)]
  puts $throughput($i)
  puts $f0 $throughput($i)
  }
  puts $total
  puts $f0 $total
  close $f0
  close $f1
  exit 0
}
$ns at 111.0 "finish"
$ns run
	Return the throughput of each flow and sum up the total network throughput
	
	Print the results

Biblography

[1] “Telephone service for St. Louis vehicles”, Bell Laboratories Record, July 1946

[2] A. Brand, H. Aghvami, “Mulitple Access Protocols for Moible Communications” John Wiley & Sons.

[3] V. K. Garg, J. E. Wilkes, “Principles & Applications of GSM”, Prentice Hall, 1999

[4] K. I. Kim, “Handbook of CDMA System Design, Engineering, and Optimization”, Prentice Hall, Upper Saddle River, NJ, USA, 2000.

[5] High Speed Packet Access, http://hspa.gsmworld.com/

[6] Tim Berners-Lee, World Wide Web, http://www.w3.org/People/Berners-Lee/WorldWideWeb

[7] C. K. Toh, “Ad-hoc mobile wireless networks: protocols and systems”, Prentice Hall, New Jersey, 2002.

[8] J. M. McQuillan, D. C. Walden, “The ARPA Network Design Decisions”, *Computer Networks*, vol. 1, pp. 243-289, August 1977.

[9] A. Leon-Garcia, I. Widjaja, “Communication Networks Fundamental Concepts and Key Architectures”, McGraw-Hill.

[10] Defense Advanced Research Project Agency, Darpa, http://www.darpa.mil/

[11] N. Pogkas, et al., “Architecture Design and Implementation of an Ad-Hoc Network for Disaster Relief Operations”, *IEEE Transactions on Industrial Informatics*, Vol. 3, No. 1, pp.63-72, Feb 2007.

[12] N. Choi et al., “Multi-channel MAC protocol for mobile ad-hoc networks”, *IEEE VTC 2003-Fall*, Vol.2, pp.1379-1382, Orlando, USA, Oct. 2003.

[13] A.Baiocchi et al., “Why a Multichannel Protocol can boost IEEE 802.11 Performance”, *ACM MSWiM’04*, pp.143-148, Venice, Italy, Oct. 2004.

[14] R. Jordan, C. T. Abdallah, “Wireless Communications and Networking: An Overview”, *IEEE Antenna’s and Propagation Magazine*, Vol. 44, No. 1, pp. 185-193, Feb 2002.

[15] E. Ferro, F. Potorti, “Bluetooth and Wi-fi Wireless Protocols: A Survey and a Comparison”, *IEEE Wireless Communications*, pp.12-26, Feb 2005.

[16] IEEE 802.11 Standard Web Site, http://ieee802.org/11/

[17] IEEE 802.11, Part 11: Wireless LAN Medium Access Control (MAC and Physical Layer (PHY) Specifications, IEEE, Aug. 1999.

[18] K. Xu, M. Gerla, S. Bae, “How Effective is the IEEE 802.11 RTS/CTS Handshake in Ad-hoc Networks?”, *IEEE GlobeCom '02*, Vol. 1 , pp. 17-21, Taiwan, Nov. 2002.

[19] G. Bianchi, “Performance Analysis of the IEEE 802.11 Distributed Coordination Function”, *IEEE Journal on Selected Areas in Communications*, Vol. 18, No. 3, pp.535-547, Mar. 2000.

[20] T. M. Trung, J. Mo, “VMcMAC: Voice Call Support over Wireless Multi-Channel MAC Protocol,” *IEEE Communications Letters*, Vol. 11, No. 5, pp.402-404, May 2007.

[21] S. Wu et al., “A New Multi-channel MAC Protocol with On Demand Channel Assignment for Multi-hop Mobile Ad-hoc Networks”, *I-SPAN’00*, pp.232, Dallas, USA, Dec. 2000.

[22] Y. Tseng, “A Multi-channel MAC Protocol with Power Control for Multi-hop Mobile Ad-hoc Networks”, *IEEE Distributed Computing Systems Workshop*, pp.419-424, April 2001.

[23] J. Chen et al., “A New Multichannel Access Protocol for IEEE 802.11 Ad-hoc Wireless LANs”, *IEEE PIMRC’03*, Vol.3, pp.2291-2296, Beijing, China, Sept. 2003.

[24] J. So, N. Vaidya, “Multi-Channel MAC for Ad-hoc Networks: Handling Multi-Channel Hidden Terminals Using a Single Transceiver”, *ACM MobiHoc’04*, pp.222-233, Tokyo, Japan, May 2004.

[25] A. Tzamaloukas, J. J. Garcia-Luna-Aceves, “A Receiver-initiated Collision-Avoidance Protocol for Multi-channel Networks”, *IEEE InfoCom’01*, Vol.1, pp.189-198, Anchorage, USA, April 2001.

[26] W. Chen, et al., “An Adaptive Multi-channel MAC protocol for Wireless Ad-hoc Networks,” *IEEE ICC’06*, Vol.8, pp.3651-3656Istanbul, Turkey, 2006.

[27] S. Lo, C. Tseng, “A Novel Multi-Channel MAC Protocol for Wireless Ad-hoc Networks,” *IEEE VTC’07-Spring*, pp.46-50, Dublin, Ireland, April 2007.

[28] C. Lin, et al., “Concurrent Multi-Channel Transmission (CMCT) MAC Protocol in Wireless Mobile Ad-hoc Networks,” *IEEE ICACT’07*, Vol.1, pp.445-449, Phoenix Park, Korea, Feb. 2007.

[29] C. Son, et al., “MAC Protocol using Asynchronous Multi-channels in Ad-hoc Networks,” *IEEE WCNC’07*, pp.401-405, Hong Kong, March 2007.

[30] C. Xu, et al., “A Novel Multi-Channel based Framework for Wireless IEEE 802.11 Ad-hoc Networks,” *IEEE WCNM’05*, Vol.2, pp.812-815, Wuhan, China, Sept. 2005.

[31] J. Gomez, A. T. Campbell, “Variable-Range Transmission Power Control in Wireless Ad-hoc Networks,” *IEEE Transactions on Mobile Computing*, Vol.6, No. 1, pp. 87-99, Jan. 2007.

[32] “IETF RFC 3561 AODV Routing”, http://www.ietf.org/rfc/rfc3561.txt

[33] K. Sundaresan, et al., “Medium Access Control in Ad-hoc Networks with MIMO Links: Optimization Considerations and Algorithms,” *IEEE Transactions on Mobile Computing*, Vol. 3, No. 4, pp. 350-365, Oct. 2004.

[34] J. H. Winters, et al., “The Impact of Antenna Diversity on the Capacity of Wireless Communication Systems,” *IEEE Transactions on Communications*, Vol. 42, No. 2, 1994.

[35] R. R. Choudhury, et al., “On Designing MAC Protocols for Wireless Networks Using Directional Antennas,” *IEEE Transactions on Mobile Computing*, Vol. 5, No. 5, pp. 477-491, May 2006.

[36] L. Bao, J. Garcia-Luna-Aceves, “Transmission Scheduling in Ad-hoc Networks with Directional Antennas,” *ACM MobiHoc*, pp.48-58, Long Beach, USA, Oct. 2001.

[37] D. E. Perkins, P. Bhagwat, “Highly Dynamic Destination-Sequenced Distance-Vectore Routing (DSDV) for Mobile Computers,” *ACM Sigcomm’94*, Vol.24, No.4, pp.234-244, London, England, 1994.

[38] P. C. Ng, S. C. Liew, "Throughput Analysis of IEEE802.11 Multi-Hop Ad-hoc Networks," *IEEE/ACM Transactions on Networking*, Vol. 15, No. 2, pp. 309-322, April 2007.

[39] J. W. Lee, R. R. Mazumdar, N. B. Shroff, "Joint Opportunistic Power Scheduling and End-to-End Rate Control for Wireless Ad-hoc Networks," *IEEE Transactions on Vehicular Technology*, Vol. 56, No. 2, pp. 801-809, March 2007.

[40] W. L. Huang, K. B. Letaief, "Cross-Layer Scheduling and Power Control Combined with Adaptive Modulation for Wireless Ad-hoc Networks," *IEEE Transactions on Communications*, Vol. 55, No. 4, pp. 728-739, April 2007.

[41] M. Zorzi, et al., "Cross-Layer Issues in MAC Protocol Design for MIMO Ad-hoc Networks," *IEEE Wireless Communications*, Vol.13, Issue 4, pp.62-76, August 2006.

[42] D.B. Johnson, D. A. Maltz, " The Dynamic Source Routing Protocol for Mobile Ad-hoc Networks," *IETF RFC in Draft*, April 2003.

[43] S. Agarwal, et al., "Distributed Power Control in Ad-hoc Wireless Networks," *IEEE PIMRC'01*, Vol.2, pp.59-55, San Diego, USA, Sept. 2001.

[44] J. P. Ebert, et al., "An Energy-Efficient Coordination Algorithm for Topology Maintenance in Ad-hoc Wireless Networks," *ACM MobiCom'01*, pp.85-96, Rome, Italy, July 2001.

[45] J. P. Ebert, et al., "Combined Tuning of RF Power and Medium Access Control for WLANs," *IEEE MoMuC'99*, pp.74-82, San Diego, USA, Nov. 1999.

[46] E. S. Jung, N. H. Vaidya, "A Power Control MAC Protocol for Ad-hoc Networks," *ACM MobiCom'02*, Atlanta, USA, Sept. 2002.

[47] J. Gomez, et al., "Conserving Transmission Power in Wireless Ad-hoc Networks," *IEEE ICNP'01*, pp.24-31, Riverside, USA, Nov. 2001.

[48] J. E. Wieselthier, et al., "On the Construction of Energy-Efficient Broadcast and Multicast Trees in Wireless Networks," *IEEE InfoCom'00*, Vol. 2, pp.585-594, Tel-Aviv, Israel, March 2000.

[49] J. Tang, et al., "Link Scheduling with Power Control for Throughput Enhancement in Multihop Wireless Networks," *IEEE Transactions on Vehicular Technology*, Vol. 55, No. 3, pp. 733-742, May 2006.

[50] T. ElBatt, A. Ephremides, "Joint Scheduling and Power Control for Wireless Ad-hoc Networks," *IEEE InfoCom'02*, Vol. 2, pp.976-984, New York, USA, June 2002.

[51] K. Wang, et al., "A Distributed Joint Scheduling and Power Control Algorithm for Multicasting in Wireless Ad-hoc Networks," *IEEE ICC'03*, Vol.1, pp.725-731, Anchorage, USA, May 2003.

[52] S. Giordano, E. Biagioni, "Topics in Ad-hoc and Sensor Networks," *IEEE Communications Magazine*, Vol. 43, pp. 92-100, April 2007.

[53] A. Wheeler, "Commercial Applications of Wireless Sensor Networks Using ZigBee," *IEEE Communications Magazine*, Vol. 45, pp. 70-77, April 2007.

[54] I. F. Akyildiz, X. Wang, "A Survey on Wireless Mesh Networks," *IEEE Radio Communications*, pp.523-530, Sept. 2005.

[55] L. Loyola, et al., "A Multi-channel Infrastructure based on DCF Access Mechanism for Wireless LAN Mesh Networks Compliant with IEEE 802.11," *Asia-Pacific Conference on Communications*, pp.497-501, Perth, Australia, Oct. 2005.

[56] J. H. Winters, et al., "Optimum Combining in Digital Mobile Radio with Cochannel Interference," *IEEE Journal on Selected Areas in Communications*, Vol. 2, pp. 528-539, July 1984.

[57] C. S. Maa, et al., "Structures of Space-Time Codes and Multipath MIMO Channels," *IEEE Signal Processing Letters*, Vol. 11, No. 4, pp. 439-442, April 2004.

[58] A. Arunachalam, et al., "Space-Time Coding for MIMO Systems With Co-Channel Interference," *IEEE Transactions on Wireless Communications*, Vol. 3, No. 6, Nov. 2004.

[59] A. J. Paulraj et al., "An Overview of MIMO Communications – A Key to Gigabit Wireless", *Proceedings of the IEEE*, Vol., 92, No. 2, pp.198-218, Feb 2004.

[60] M. Z. Siam, M. Krunz, "An Overview of MIMO-oriented Channel Access in Wireless Networks", *IEEE Wireless Communications*, pp.63-69, Feb 2008.

[61] V. Tarokh, et al., "Space-time Codes for High Data Rate Wireless Communication: Performance Criterion and Code Construction", *IEEE Trans. Information Theory*, vol. 44, pp.744-765, Mar 1998

[62] Linksys Wireless-N Gigabit Gaming Router, http://www.linksys.com

[63] Y. Xiao, J. Rosdahl, "Throughput and Delay Limits of IEEE 802.11," *IEEE Communications Letters*, Vol. 6, No.8, pp. 355-357, Aug. 2002.

[64] Y. Xiao, "Packing Mechanisms for the IEEE 802.11n Wireless LANs," *IEEE GlobeCom'04*, Vol. 5, pp.3275-3279, Dallas, USA, Nov. 2004.

[65] G. Liang, K. R. Dandekar, "Power Management in MIMO Ad-hoc Networks: A Game-Theoretic Approach," *IEEE Transactions on Wireless Communications*, Vol. 6, No. 4, pp. 1164-1170, April 2007.

[66] C. U. Saraydar, et al., "Efficient Power Control via Pricing in Wireless Data Networks," *IEEE Transactions on Communications*, Vol. 50, pp. 291-303, 2000.

[67] M. Hayaineh, C. T. Abdallah, "Distributed Joint Rate and Power Control Game-theoretic Algorithms for Wireless Data," *IEEE Communication Letters*, Vol. 8, pp.511-513, Aug. 2004.

[68] A. Spyropoulos, C. Raghavendra, "Energy Efficient Communications in Ad-hoc Networks Using Directional Antennas," *IEEE InfoCom'02*, Vol. 1, pp. 220-228, New York, USA, June 2002.

[69] K. Sudaresan, R. Sivakumar, "On the Medium Access Control Problem in Ad-Hoc Networks with Smart Antennas," *ACM MobiHoc'03*, pp.25-26, Annapolis, USA, June 2003.

[70] S. Yi, et al., "On the Capacity Improvement of Ad-hoc Wireless Networks Using Directional Antennas," *ACM MobiHoc'03*, pp.108-116, Annapolis, USA, June 2003.

[71] R. Ramanathan, et al., "Ad-hoc Networking with Directional Antennas: A Complete System Solution," *IEEE Journal on Selected Areas in Communications*, Vol. 23, No. 3, March 2005.

[72] S. Cheekiralla, et al., "Load-Sensitive Routing with Directional Antennas," *IEEE PIMRC'06*, pp.1-5, Helsinki, Finland, Sept. 2006.

[73] Y. T. Hou, et al., "Multicast Communications in Ad-hoc Networks Using Directional Antennas: A Lifetime-Centric Approach," *IEEE Transactions on Vehicular Technology*, Vol. 56, No. 3, pp. 1333-1344, May 2007.

[74] C. Y. Chang, H. C. Sun, C. C. Hsieh, "MCDA: An Efficient Multi-Channel MAC Protocol for 802.11 Wireless LAN with Directional Antenna," *IEEE AINA'05*, Vol.2, pp.64-67, Taiwan, March 2005.

[75] D. Johnson, Y. Hu, D. Maltz, "The Dynamic Source Routing Protocol (DSR) for Mobile Ad-hoc Networks for IPv4," *IETF RFC4728*, http://tools.ietf.org/html/rfc4728.

[76] P. C. Ng, S. C. Liew, "Re-routing Instability in IEEE 802.11 Multi-hop Ad-hoc Networks," *OCP Ad-hoc & Sensor Wireless Networks*, Vol.1, pp.1-25, Aug. 2005

[77] Q. Wang, J. Sun, G. Wang, "A Dual-Channel Routing Scheme in Ad-hoc Networks," *IEEE PDCAT'05*, pp.720-722, Dalian, China, Dec. 2005.

[78] D. Espes, Z. Mammeri, "Routing Algorithm to Increase Throughput in Ad-hoc Networks," *IEEE ICN'06*, pp.66, Mauritius, April 2006.

[79] G. Ferrari, O. K. Tonguz, "Performance of Ad-hoc Wireless Networks with Aloha and PR-CSMA MAC Protocols," *IEEE GlobeCom'03*, Vol.5, pp.2824-2829, San Francisco, USA, Dec. 2003.

[80] S. Panichpapiboon, et al., "Routing Reservation in Ad-hoc Wireless Networks," *IEEE Transactions on Mobile Computing*, Vol. 6, No. 1, Jan. 2007.

[81] C. Chang, et al., "MCDA: An Efficient Multi-Channel MAC Protocol for 802.11 Wireless LAN with Directional Antenna," *IEEE AINA'05*, Vol.2, pp.64-67, Tamkang University, Taiwan, Mar. 2005.

[82] Y. Zhang, et al., "Multi-Channel Smart Antennas in Wireless Networks," *ACSSC'06*, pp.305-309, Oct. 2006.

[83] X. Lin, S. Rasool, "A Distributed Joint Channel-Assignment, Scheduling and Routing Algorithm for Multi-Channel Ad-hoc Wireless Networks," *IEEE InfoCom'07*, pp.1118-1126, Anchorage, USA, May 2007.

[84] M. X. Gong, S. F. Midkiff, S. Mao, "A Combined Proactive Routing and Multi-Channel MAC Protocol for Wireless Ad-hoc Networks," *2nd International Conference on Broadband Networks*, Vol.1, pp.444-453, Oct. 2005.

[85] U. Lee, S. F. Midkiff, T. Lin, "OSPF-MCDS-MC: A Routing Protocol for Multi-Channel Wireless Ad-Hoc Networks," *IEEE CCNC'06*, Vol.1, pp.426-430, Las Vegas, USA, Jan. 2006.

[86] X. L. Huang, B. Bensaou, "On Max-min Fairness and Scheduling in Wireless Ad-Hoc Networks: Analytical Framework and Implementation", *ACM MobiHoc'01*, pp. 221-231, Long Beach, USA, Oct. 2001.

[87] J. Riihijarvi, M. Petrova, P. Mahonen, "Frequency Allocation for WLANs Using Graph Colouring Techniques", *IEEE WONS'05*, pp. 216-222, St. Moritz, Switzerland, Jan. 2005

[88] P. C. Ng, S. C. Liew, L. B. Jiang, "Achieving Scalable Performance in Large-Scale IEEE 802.11 Wireless Networks," *IEEE WCNC'05*, Vol.1, pp.69-74, New Orleands, USA, Mar. 2005

[89] L. B. Jiang, S. C. Liew, "Hidden-node Removal and Its Application in Cellular WiFi Networks," *IEEE Transactions on Vehicular Technology*, Vol. 56, No. 5, pp. 2641-2654, Sept. 2007.

[90] Y. Kim, et. Al, "A Novel Hidden Station Detection Mechanism in IEEE 802.11 WLAN," *IEEE Communications Letters*, Vol. 10, No. 8, pp. 608-610, August 2006.

[91] L. B. Jiang, S. C. Liew, "Improving Throughput and Fairness by Reducing Exposed and Hidden Nodes in 802.11 Networks," *IEEE Transactions on Mobile Computing*, Vol. 7, No. 1, pp.34-49, Jan. 2008.

[92] J. P. Monks, et al., "A Power Controlled Multiple Access Protocol for Wireless Packet Networks," *IEEE InfoCom'01*, Vol.1, pp.219-228, Anchorage, USA, April 2001.

[93] Z. J. Haas, J. Deng, "Dual Busy Tone Multiple Access (DBTMA) – a Multiple Access Control Scheme for Ad-hoc Networks," *IEEE Transactions on Communications*, Vol. 50, No. 6, pp. 975-985, June 2002.

[94] P. Gupta, P. R. Kumar, "The Capacity of Wireless Networks," *IEEE Transactions on Information Theory*, Vol. 46, No. 2, pp. 388-404, March 2000.

[95] A. Agarwal, R. R. Kumar, "Capacity Bounds for Ad-Hoc and Hybrid Wireless Networks," *ACM Sigcomm Computer Communications Review*, Vol. 34, No. 3, pp. 71-81, July 2004.

[96] T. Rappaport, "Wireless Communications: Principles and Practice", Prentice Hall, New Jersey, 2002

[97] P.C. Ng and S. C. Liew, "Throughput Analysis of IEEE802.11 Multi-Hop Ad-hoc Networks," *IEEE/ACM Trans. on Networking*, vol. 15, issue 2, pp. 309-322, April 2007.

[98] Y. Gao, D. Chiu, and J. Lui, "Determining the End-to-end Throughput Capacity in Multi-Hop Networks: Methodology and Applications," *in Proc. ACM SIGMetrics/Performance'06*, pp. 39-50, Saint Malo, France, June 2006.

[99] J. Lee et al., "An Experimental Study on the Capture Effect in 802.11a Networks", *ACM WiNTECH'07*, pp.19-26, Montreal, Canada, Sept 07.

[100] L. Jiang and S. C. Liew, "Removing Hidden Nodes in IEEE 802.11 Wireless Networks," *IEEE Vehicular Technology Conference*, Vol.2, pp.1127-1131, Dallas, USA, Sept 2005

[101] C. L. Fullmer et al., "Complete single-channel solutions to hidden terminal problems in wireless LANs", *IEEE ICC'97*, Vol.2, pp.575-579, Montreal, Canada, June 1997.

[102] "The Network Simulator – ns2", http://www.isi.edu/nsnam/ns.

[103] M. S. Gast, "802.11 Wireless Networks The Definitive Guide", O'Reilly, 2002.

[104] A. Agarwal and P. R. Kumar, "Improved capacity bounds for wireless networks", *Wireless Communications and Mobile Computing*, vol. 4, pp. 251-261, 2004.

[105] H. Zhai et al., “A dual-channel MAC protocol for mobile ad-hoc networks”, *IEEE GLOBECOM Workshop’04*, pp. 27-32, Dallas, USA, Nov. 2004.

[106] W. H. Ho and S. C. Liew, “Achieving Scalable Capacity in Wireless Networks with Adaptive Power Control”, *IEEE LCN’05*, pp. 720-728, Montreal, Canada, Nov. 2005.

[107] F. N. Ali, et al., “Distributed and Adaptive TDMA Algorithms for Multiple-Hop Mobile Networks”, *IEEE MILCOM’02*, pp. 546-551, Anaheim, USA, Oct. 2002

[108] A. Kanzaki, T. Hara, S. Nishio, “An Adaptive TDMA Slot Assignment Protocol in Ad-hoc Sensor Networks”, *ACM SAC’05*, pp.1160-1165, Santa Fe, USA, Mar. 2005.

[109] G. Kulkarni, M. Srivastava, “A channel assignement scheme for FDMA based wireless ad-hoc networks in Rayleigh fading environments”, *IEEE VTC’02*, pp.1082-1085, Vancover, Canada, Sept. 2002.

[110] Z. Cai, M. Lu, “SNDR: a new medium access control for multi-channel ad-hoc networks”, *IEEE VTC’00*, Vol.2, pp.966-971, Tokyo, Japan, May 2002.

[111] D. Brelaz, “New methods to colour the vertices of a graph”, *ACM Communications*, Vol. 22, pp. 251-256, April 1979.

[112] S. Haykin, “Communication Systems”, John Wiley & Sons. Inc.

[113] “Radio Propagation Models”, Chapter 17, *ns-Manual*, www.isi.edu/nsnam/ns/ns-documentation.html

[114] A. Mishra, et al., “Paritally Overlapped Channels Not Considered Harmful”, *ACM SIGMetrics’06*, pp.63-74, Saint Malo, France, June 2006.

[115] N. Yee, J. P. Linnartz, “Multicarrier CDMA in an Indoor Wireless Radio Channel”, Tech. Rep. 94720, University of Berkeley (CA), 1993.

[116] C. A. G. D. de Leon, et al., “MC-CDMA/VSF for the Downlink Physical Layer in Next Generation Wireless Local Area Networks”, *IEEE SIPS’04*, pp.221-226, Austin, USA, Oct. 2004.

[117] C. R. Nassar, B. Natarajan, D. Wiegandt, Z. Wu, “Multi-carrier platform for wireless communications. Part 2: OFDM and MC-CDMA systems with high-performance, high-throughput via innovations in spreading”, *Wireless Communications and Mobile Computing*, issue 2, pp. 381-403, 2002.

[118] Netgear WNR854T Wireless Router, http://www.netgear.com

[119] S. C. Swales, M. A. Beach, D. J. Edwards, J. P. McGeehan, “The Performance Enhancement of Multibeam Adaptive Base-Station Antennas for Cellular Land Mobile Radio Systems”, *IEEE Trans. On Vehicular Technology*, vol. 39, issue 1, pp. 56-67, Feb.1990.

[120] C. E. Perkins, et al., “Ad-hoc On-demand Distance Vector Routing,” *Proceedings of the 2nd IEEE Workshop on Mobile Computing Systems and Applications*, pp. 90-100, New Orleans, USA, Feb. 1999.

[121] D.B. Johnson, D. A. Maltz, “Dynamic Source Routing in Ad-hoc Wireless Networks,” *Mobile Computing*, Vol. 353, pp.153-181, August 1996.

[122] W. Krause, J. Scholz, M. Greiner, "Optimized Network Structure and Routing Metric in Wireless Multihop Ad-hoc Communication," *Physica A*, Volume 361, Issue 2, p. 707-723, 2005.

[123] K. Nakano, R. K. Panta, M. Sengoku, S. Shinoda, "On performance of a charging/rewarding scheme in mobile ad-hoc networks," *IEEE International Symposium on Circuits and Systems*, 2005 (ISCAS 2005), pp. 2962 - 2966 Vol. 3, Kobe, Japan, May 2005

[124] L. D. Nardis, et al., "UWB Ad-Hoc Networks," *IEEE Conference on Ultra Wideband Systems and Technologies*, pp.219-223, Baltimore, USA, May 2002.

[125] P. Kong, M. R. Shajan, "A Medium Access Control Protocol for Ultra-Wideband Wireless Ad-hoc Networks," *IEEE VTC'05-Spring*, Vol.3, pp.1993-1997, Stockholm, Sweden, May 2005.

[126] C. C. Davis, et al., "Flexible Optical Wireless Links and Networks," *IEEE Communications Magazine*, pp. 51-57, March 2003.

[127] D. Kedar, S. Arnon, "Urban Optical Wireless Communication Networks: The Main Challenges and Possible Solutions," *IEEE Optical Communications*, pp. 52-57, May 2004.

[128] P. C. Ng, S. C. Liew, W. Wang, "Voice over WLAN via Wireless Distribution System," *IEEE Vehicular Technology Conference (VTC'04 Fall)*, Vol.4, pp.2564-2567, Los Angeles, U.S.A., Sept. 2004.

[129] C. Bravo, S. Aissa, A. Girard, "Providing Quality of Service for Critical Nodes in Ad-Hoc Networks," *IEEE VTC'05-Spring*, Vol.4, pp.2478-2482, Stockholm, Sweden, May 2005.

[130] J. Kim, H. Tode, K. Murakami, "Friendly Coexistence of Voice and Data Traffic in IEEE 802.11 WLANs," *IEEE Transactions on Customer Electronics*, Vol. 52, No. 2, pp. 347-354, May 2006.

[131] Yang R. Yang, M. S. Kim, Simon S. Lam, "Transient Behaviors of TCP-friendly Congestion Control Protocols", *IEEE InfoCom'01*, pp.1716-1725, Anchorage, USA, April 2001.

[132] Cheng Peng Fu, Soung C. Liew, "TCP Veno: TCP Enhancement for Transmission Over Wireless Access Networks", *IEEE Journal on Selected Areas in Communications*, Vol. 21, No. 2, pp. 216-228, Feb. 2003

[133] GeorgeXylomenos, George C. Polyzos, "TCP and UDP Performance over a Wireless LAN", *IEEE InfoCom'99*, pp. 439-446, New York, USA, Mar. 1999.

[134] "HostAP" driver, http://hostap.epitest.fi/

[135] G. Anastasi, E. Borgia et al., "Wi-Fi in Ad-hoc Mode: A Measurement Study", *IEEE PERCOM'04*, pp.145-154, Orlando, USA, March 2004.

[136] P.C. Ng, D. Edwards, S. C. Liew, "A Link-directionality-based Dual Channel MAC Protocol for IEEE 802.11 Ad-hoc Networks", *IEEE INFOCOM'06 Student Workshop*, Barcelona, Spain, April 2006.

[137] J. S. Pathmasuntharam, A. Das, A. K. Gupta, "Primary Channel Assigment based MAC (PCAM) – A Multi-Channel MAC Protocol for Multi-Hop Wireless Networks", *IEEE WCNC'04*, pp.1110-1115, Atlanta, USA, March 2004.

[138] P.C. Ng, D. Edwards, and S. C. Liew, “Doubling Capacity by a Link-directionality-based Dual Channel MAC Protocol for IEEE 802.11 Ad-hoc Networks”, *in Proc. IEEE GLOBECOM’06*, pp.1-5, San Fransico, USA, Nov. 2006.

[139] P. Bahi et al., “SSCH: Slotted Seeded Channel Hopping for Capacity Improvement in IEEE 802.11 Ad-hoc Wireless Networks”, *ACM MobiCom’04*, pp.216-230, Tokyo, Japan, Sept. 2004.

[140] A. Muqattash and M. Krunz, “Power controlled dual channel (PCDC) medium access protocol for wireless ad-hoc networks”, *IEEE INFOCOM’03*, pp. 470-480, San Francisco, USA, Mar. 2003.